The measurement of velocity profiles in anomalous fluids

Robert Marmaduke Underwood

T H E S I S

Presented in candidature for the degree of

DOCTOR OF PHILOSOPHY

of the University of Durham

By

ROBERT MARMADUKE UNDERWOOD

Entitled

THE MEASUREMENT OF VELOCITY PROFILES IN ANOMALOUS FLUIDS

The work was carried out at the Science Laboratories of the Durham Colleges in the University of Durham, under the supervision of J.E. Caffyn, B.Sc.,F.Inst.P.

CONTENTS

THE MEASUREMENT OF THE VELOCITY OF ANOMALOUS FLUIDS IN LAMINAR FLOW.

INTRODUCTION

The theoretical investigation of the flow of anomalous fluids is complex. To simplify the treatment an ideal equation of state is postulated and the appropriate equations of motion obtained. These can then be solved in some simple cases (Reiner,[1] Scott-Blair,[2] and Oldroyd[3]) provided some a priori assumption has been made as to the nature of the flow; e.g., the flow of a visco-elastic liquid through a straight tube of circular section the stress distribution can be found if it is assumed that the motion* is rectilinear.

The theoretical solution will, of course, involve a stress and rate of strain distribution; it is important, therefore, as was recognised by Lawrence[4] and has been again emphasised by Eirich[5] to measure the velocity distribution when studying the flow of anomalous fluids. It was felt desirable, therefore, to develop an accurate method of fluid velocity measurement so that the velocity distribution of an anomalous fluid flowing in a circular pipe could be determined (it was not until this work was completed that the paper of Lawrence was found).

Methods of Velocity Measurement.

Goldstein[6] and Richardson[7] have reviewed the methods of fluid velocity measurement and they can conveniently be classified as follows:-

* (Oldroyd provided communication)

(1) Hot wire anemometer methods.

(2) Pitot tube methods

(3) Streamer methods*.

(4) Miscellaneous methods.

(1) Hot wire anemometers have been used for the measurement of velocity in liquids by Richardson and Tyler[8] but suffer from the disadvantages that they depend on introducing an obstruction into the fluid stream and may affect the fluid properties in the vicinity of the wire, thus giving spurious velocity measurements. In addition the size of the probe is a limiting factor particularly for experiments in straight circular section tubes.

(2) Pitot tubes. These have been used for the measurement of fluid velocity distributions in pipes but there are two disadvantages to be surmounted.

In the first place the kinetic pressure which a pitot tube measures, $K.\frac{1}{2}.\rho v^2$ would be very small under these experimental conditions and would require elaborate means of measuring: ρ and v are the density and velocity of flow of the fluid respectively and K a constant which is very nearly equal to unity (Bramwell et.al.[9]) provided that va/ν exceeds 30 (Barker[10]) where 'a' is the radius of the mouth of the pitot

*(The term "streamer" is used quite loosely to indicate any substances, solid, liquid or gaseous, which when borne by the flowing fluid, will indicate visually by their movement the nature of the flow).

tube and ν the kinematic viscosity of the fluid. Secondly the response time of small diameter pitot tubes feeding into any ordinary pressure measuring device is large owing to the limited rate of flow through it to the pressure device.

If the maximum head to be registered by the pitot tube manometer is P cms. water, say, and if the fluid flow is regulated to reach its maximum value after T seconds, then at any time t ($< T$) the kinetic pressure is $\frac{P.t}{T}$ cms. At the same time, if the manometer is registering a head 'h' cms. water, then the net value of the head across the pitot tube is $(\frac{P.t}{T} - h)$ cms., water and the flow rate through the pitot tube to the manometer will be $K.(\frac{P.t}{T} - h)$ c.c. per sec. K is $\frac{\pi.\rho.g.a^4}{8.\eta\, L}$ and arises from the Poiseuille-Hagen formula, $Q = \frac{\pi.h.\rho.g.a^4}{8.\eta.L}$ = rate of flow of fluid of viscosity through a pipe of radius 'a' and length L with a manometric pressure $h.\rho.g$ across the tube. Hence at any instant the rate of change of head as recorded by the manometer will be

$$\frac{dh}{dt} = \frac{K}{A}.(\frac{P.t}{T} - h) \text{ cms. per sec.} \quad \ldots\ldots\ldots\ldots\ldots (1)$$

where A is the cross sectional area of the manometer tube. The integrating factor for this equation is $e^{\frac{K\,t}{A}}$ and hence

$$he^{\frac{K\,t}{A}} = \frac{KP}{AT}\int te^{\frac{K.t}{A}}.dt$$

$$= \frac{KP}{AT}\left[\frac{A}{K}.t.e^{\frac{K.t}{A}} - \frac{A^2}{K^2}\,e^{\frac{K\,t}{A}}\right] + C \quad \ldots\ldots (2)$$

and when $t = 0$ $h = 0$ and hence $C = \frac{A.P}{K.T}$

and therefore from equation (2)

$$h = \frac{P.t}{T} - \frac{AP}{KT}.\left(1 - e^{\frac{-K.t}{A}}\right) \quad \text{cm. water} \quad \ldots\ldots (3)$$

let $h = h_o$ when $t = T_o$

After T seconds the flow becomes steady and the manometer continues to rise under a head of $P - h_o$. The rate of change at the manometer reading is thus similarly

$$\frac{dh}{dt} = \frac{K}{A}\left(P - h\right) \text{ cm. per sec.} \quad \ldots\ldots\ldots\ldots\ldots\ldots \quad (4)$$

or,

$$-\ln(P - h) = \frac{K\,t}{A} + C \quad \ldots\ldots\ldots\ldots\ldots\ldots\ldots \quad (5)$$

At $t = 0$, the head $= P - h_o$ cm.

$$\therefore\ t = \frac{A}{K} \ln\left(\frac{P - h_o}{P - h}\right) \text{ sec.} \quad \ldots\ldots\ldots\ldots \quad (6)$$

which will give the time after the end of T seconds before the manometer will register a head to within any chosen limits of P.

If for example L = 5 cms. and a = 0.0325 cms. (= approximately 1/20th radius of the flow tube) and T is taken as 10 sec. then, from (3) with a manometer diameter of 1 cm.

$$h_{10} = P\left\{\left(1 - \frac{10}{5.967}\left(1 - \frac{1}{1.8164}\right)\right)\right\} \text{ cm.}$$

$$= P(1 - 0.736) = .264\ P \text{ cms.}$$

i.e. only a little over 25% of the correct pressure head is recorded. From (6) allowing owing to premature reading, the final recorded pressure a 2% error then, $P - h$ will be $P - \frac{49\ P}{50}$ and

$$t = \frac{100}{5.967} \ln\left(\frac{0.736}{1 - 0.98}\right)$$

$$= 60.38 \text{ seconds delay.}$$

This could be reduced by the use of a wider bore pitot tube though this would give an average velocity over too great

a range of radii. Other reductions could be made by reducing the bore of the manometer though surface tension affects could become serious, particularly with open ended manometer tubes. The above estimate of a typical delay takes no account of the reduction of static head which would further complicate matters.

Further it is not possible to obtain all components of the fluid velocity if it should happen that the movement is not parallel to the length of the tube.

(3) The streamer methods. Various methods are applicable to reveal details of fluid motion and to enable such details to be photographed and analysed. The observed or recorded feature depends upon the method of observation and also the experimental arrangement. Thus a photographic record may show stream lines, filament lines or particle paths. A filament line is the line joining the instantaneous positions of all particles which have passed through a given point in the fluid, while a particle path is the track of any particle in the fluid. In steady motion a stream line is at the same time a filament line and a particle path but this not so in unsteady motion. Hence in steady motion filament lines will not yield information regarding the velocities at points in a fluid unless the filaments are in some way discontinuous or regularly sinuous, so the requirement of instantaneous velocities dictates that the streamers be either oscillatory at the source with a known frequency or regularly discontinuous. In the latter case the method is essentially that of observing particle paths,

and the choice between a finite exposure time or a stroboscopic type of illumination to enable a photographic record to be made depends upon the particular experimental arrangement. Methods relying upon the use of such streamers require their injection into the fluid in such a way that the motion will not be disturbed.

Townend[11] has used periodic sparks in air. Relf[12] and Jones, Farren and Lockyer,[13] used oil droplets suspended in a fluid and obtained the particle velocity photographically from a known time exposure.

Pichot and Dupin[14] and Andrade and Tsien[15] used suspended particles; the latter using aluminium powder and from photographs of short exposure (0.008 to 0.005 secs) obtained a velocity distribution in a liquid-liquid jet.

Favre[16] used the ingenious technique depending on the injection of a coloured filament (nigrocene dye) ejected from an oscillating jet. From measurement of peak to peak distances two dimensional velocity fields were explored.

Birkhoff and Cagwood[17] have used a slightly different method in which a vertical sheet of air bubbles rises in the fluid into which a projectile is fired. From a double flash photograph, each air bubble gives rise to two images, thus the velocity of each air bubble can be computed if its velocity of rise under gravity is known. Hence they have obtained the velocity field in the neighbourhood of a projectile entering the fluid.

Most of these methods suffer from disadvantages, particularly if it is necessary to obtain all velocity components accurately, without seriously interfering with the flow distribution which is to be measured. All suffer the same disadvantage previously mentioned in that they only measure the velocity components in one particular plane.

(4) Miscellaneous methods. The only other two methods which might have been of value in determining the velocity distribution in the cross section of a pipe were that of Kolin[18] [19] [20] and Alcock and Sadron[21]. The former method depends on the introduction of a potential gradient in the flowing medium as it traverses a magnetic field perpendicular to its direction. This, however, involves a probe and does not give the direction of the velocity measured. Alcock and Sadron[21] have shown how a flow bi-refringent liquid can be used to obtain the velocity when the fluid is flowing past a solid boundary. The accuracy, however, of the method is not very great and it is limited to flow distributions which have two dimensional symmetry.

From a consideration of all these methods it was decided to modify that of Birkhoff and Cagwood replacing the air bubbles with oil droplets but still using the double flash technique for photography as it was felt that this gave the most promise of an accurate method. This decision was, however, not taken until some experimental work had been carried out in attempting to modify the method of Favre. It is proposed, therefore, to

describe the latter experimental work next and to follow it with a description of the final technique employed.

Consultation of Durham University theses.

In using the undermentioned thesis

.....THE MEASURMENT OF VELOCITY PROFILES.....
.....IN ANOMALOUS FLUIDS. by R.M. Underwood...
.....

I undertake

(1) to handle it with great care and not to add to, alter, or diminish it in any way, or interfere with its structure and arrangement.

(2) to acknowledge any use made of it, or any quotation from it, in any work of my own.

(3) not to publish (or in the case of a Music thesis perform) any part of the work without obtaining the consent of the author (or his representatives after his death) during the period of copyright.

X (4) to keep it under lock and key when not in use, in a place to be agreed upon when it is borrowed.

X (5) to observe strictly any conditions for the method of transport agreed on with the Library.

Signature .....L. Edwards.....

Address .....Physics Dept.....

Place of deposit of the thesis .....

X Removal of a thesis from the University Library will only be permitted in exceptional circumstances, by agreement with the Librarian.

CHAPTER 1

PRELIMINARY EXPERIMENTS.

1. Dye Streamers.

Having reviewed the methods of measuring the velocity distributions in flowing fluids it was decided to adopt the method of Favre[16] as a first attempt to measure the velocity profile of fluids flowing in a glass tube of circular section.

Very briefly the apparatus consisted of a reservoir into which protruded a flow tube fitted with a flared entry, a stroboscopic illumination system and a flow gauge. The latter recorded a measure of the flow rate by means of a rotating drum camera and a hot wire anemometer arrangement which was attendant upon the air displaced from a large receptacle by the fluid flowing from the flow tube.

In the first instance a dye streamer was used which issued from a drawn out glass capillary tube fitted with a steel nut and caused to oscillate by means of an electro-magnet. The frequency of oscillations was governed by a vibrating contact maker which at the same time regulated the rotation of a sector disc thus allowing for stroboscopic observation. The dye used was nigrocene black. At a distance downstream beyond which the flow ceased to show any entry-initiated fluctuations, the arrangement served to show the nature of the flow, i.e., whether it was turbulent or laminar (viewing the streamers as a whole rather than the sinuosities), but as means of velocity measurement these streamers were discarded for the following reasons.

(a) The filaments needed to be very thin in order that they retained their definition and approached a single filament line as opposed to a conglomeration of filament lines. This requirement reduced their visibility and made photographic recording very difficult.

(b) The velocity gradients existing in the flow tube were large in the proximity of the wall of the tube and thus the relative velocities at neighbouring radii were quite large.

The velocity of flow v at a distance r from the axis of a pipe of radius a through which a fluid is flowing under laminar conditions is given by

$$v = K(a^2 - r^2) \quad \ldots\ldots\ldots\ldots\ldots\ldots\ldots\ldots\ldots\ldots (1.1)$$

where $K = P/4.\eta.L$. P is the pressure drop across the tube of length L and η the viscosity of the fluid. The difference in velocity corresponding to two radii r_1, r_2 is thus

$$\Delta v = K.\ (r_1^2 - r_2^2). \quad (r_1 > r_2) \quad \ldots\ldots\ldots\ldots\ldots (1.2)$$

Considering the wave form of the streamers to be sinusoidal of frequency n cycles per second and L to be the wave length in the flowing fluid, then Δv can also be given by

$$\Delta v = \frac{1}{T}.\ \Delta L \quad \ldots\ldots\ldots\ldots\ldots\ldots\ldots\ldots\ldots\ldots (1.3)$$

where ΔL is the difference in the peak to peak distances at the two radii and T is 1/n sec. Thus,

$$\Delta L = T.K.\ (r_1^2 - r_2^2) \quad \ldots\ldots\ldots\ldots\ldots\ldots\ldots\ldots\ldots (1.4)$$

From the form of the Reynolds' number, $R_n = 2.u.a.\rho/\eta$ the average velocity of flow is $u = R_n.\eta/2.a.\rho$ cm. per sec., and the mean flow is therefore $Q = \pi.a^2.u$ cc. per sec., which

by the Poiseuille-Hagen equation is

$$Q = \frac{\pi . P . a^4}{8 . \eta . L} \quad \ldots\ldots\ldots\ldots\ldots\ldots\ldots\ldots \quad (1.5)$$

and thus,

$$\frac{P}{4 . \eta . L} = \frac{R_n . \eta}{a^3} \text{ for water taking } \rho = 1 \quad \ldots\ldots\ldots \quad (1.6)$$

(It was anticipated that any other fluid which might be used would have a density very nearly equal to unity).

$$\therefore \Delta L = \frac{T . R_n . \eta .}{a^3} (r_1^2 - r_2^2) \text{ cm. per wave length} \quad (1.7)$$

For the flow tube $a^3 = 0.244$ cm^3 and if $T = 0.05$ sec., $r_1, r_2 = 0.5$ cm., 0.4cm., respectively then for $R_n = 2000$ and and with $\eta = 0.01$ poise

$$\Delta L = \frac{0.05 \times 2000 \times 0.09 \text{ cm.}}{0.244 \times 100}$$

$$= 0.369 \text{ cm. (per wave length)}$$

For a circular section tube with a rapidly convergent flared entry there exists for a distance down the tube known as the 'inlet length' a central solid cone-shaped plug of flowing fluid in which at any section the flow is of uniform velocity. From the published curves of Schiller et.al.[22] the flow at a radius of 0.4 cm. for this flow tube, is outside the central plug at a value of x/aR_n of 0.05 with $R_n = 2000$, whence $x = 62$ cm., which is the distance downstream from the entrance to the tube. Thus from this point onwards the streamers at the 0.4 cm., radius will suffer distortions due to the velocity gradient. (In fact for the peaks of the oscillations at the 0.5 cm. radius, the distortion begins earlier than at 62cm. from the entry: this fact is neglected

in this illustration. The actual effect of this is to increase the distortions further than is shown below). From here to the observation section of the pipe, 105 cms. downstream the distortion increases by an amount 0.369 cms. per wave length traverse. The distance covered is 43 cms., and taking the peaks at the inner radius as the datum line at which, over this distance, u/u_m has a value of approximately 1.2, the velocity of flow is then $\frac{1.2.2000.7}{2a.\rho}$ cm/sec. (Using the equation for R_n).

$$= 19.2 \text{ cm/sec.}$$

At a frequency of 20 c.p.s., this distance contains 20 wave lengths and so 43 cms. contains

$$\frac{43.20}{19.2} = 44.8 \text{ wave lengths.}$$

The peaks, then, at the 0.5 cm. radius will thus lag by an amount 44.8 x 0.369 cms. = 16.5 cms. by the time the observation section is reached. By this time the streamer is so distorted as to be indistinguishable from a solid streamer 0.1 cm. wide.

It was an advantage to have the frequency small in order to distinguish the form of the streamers, but it was found in view of their thinness that they could not be photographed. No advantage was to be gained by reducing the amplitude as this made it harder to distinguish their form and at the same time the largest amplitudes precipitated turbulence and threw the dye off the injecting jets in a spikey fashion with consequent blurring.

(c) Owing to very slow moving disturbances in the reservoir and to those set up by the jets vibrating, the streamers almost invariably moved from the position of injection so that with a system of several oscillating jets giving multiple streamers, rarely did they remain in the same diametral plane into which they were injected. * They could therefore only be localised by observing them from two directions at right angles and even then it was the exception rather than the rule for the plane of any of the streamers to be at right angles to either of the viewing directions: their form was therefore rarely distinguishable.

2. Interrupted Dye Streamers.

Having discontinued work on oscillating streamers it was decided to inject the dye in short threads using several jets and to view from two orthogonal directions normal to the flow tube.

Two methods of injection were attempted. The first employed an electro-magnetic valve to pulse the rubber tubing feeding the dye to the jets at a regular frequency and so produced the required interruptions. (The current to the valve operated at the same time a sector disc for stroboscopic viewing.)

* Glass jets were dispensed with for the multiple streamers and 0.006" diameter drawn copper tubing of wall thickness 0.002" was used.

The second employed a similar principle [redacted] the difference being in that magnetic pulses were applied to a thin metal diaphragm which formed one wall of a metal box through which the dye was fed. (By introducing a sufficient length of jet tubing at the inflow end of the box the diaphragm pulses were transmitted to the jets which [redacted] formed the path of least resistance).

Both methods were not very successful because the ends of the dye pulses inevitably tailed off to fine points and their beginnings were hazy due to the fact that at relaxation of the pressure a small amount of water was drawn into the jets and consequent mixing with the dye solution in the jets took place.

Owing to the many disadvantages which became apparent when using dye streamers they were abandoned.

3. Particle Streamers.

Several methods have been used in the study of fluid flow which readily give the fluid velocities at one and the same time at several positions in the field of view which do not depend upon dye streamers. Particles of aluminium or mica dispersed in the fluid appear as pin points of light when illuminated in the appropriate direction, but such methods involve in general a large number of particles in suspension. They also rely on 'thin sheet' illumination and the focussing of the observing instruments upon a single plane, the number of particles present being sufficient to ensure that there will be several in the viewing plane. As it was desired to observe the whole of the pipe's cross section and not just a diametral

plane, too many particles would be visible at one time using such suspensions; in any case the relatively large depth of focus of the recording camera would not permit of focussing on one plane and the stroboscope which was constructed could not give sufficient light, in a narrow enough sheet for a diametral illumination, to produce a sufficient scatter from the type of particles used to render them susceptible to photographic recording.

Relf[12] used illuminated oil droplets which consisted of a mixture of olive oil and nitro-benzene in such proportions as to make the density equal to that of the water which he was observing. The refractive index was such as to give an emergent ray of light at right angles to an incident ray, a condition of great advantage in eliminating direct light to the camera. Under such conditions, provided the illuminating sheet of light was sufficiently thin, all the illuminated droplets could be brought to a focus at the same time upon a photographic plate.

In place of nitro-benzene and olive oil a mixture of carbon tetrachloride and benzene was used with a density equal to that of the fluid under investigation and the mixture was injected into the flow tube at the throat of the flared entry from the previously mentioned 0.006" diameter jets. Since the mixture had a lower viscosity than the nitro-benzene/olive oil mixture lower pressures could be used in the jet assembly to exude the mixture. With the lower viscosity oil, small

droplets were more readily drawn by the fluid from the ends of the jet. In view of this it was not necessary to vibrate the jet in order to break off small droplets. The pressure in the jet assembly was adjusted until droplets were produced which, when they reached the viewing section, were about one centimeter apart. The oil was drawn off by the fluid flowing past the copper jets giving droplets of regular size and spacing. With increasing fluid flow rate both the size and spacing of the droplets decreased. For the maximum flow rate for which the flow remained laminar the droplets had a minimum size of about 0.2 mm. The size of the droplets was measured with a long focus travelling microscope and was found to be very regular with any given set of conditions, but in turbulent flow a large variation of size resulted with a minimum of about 0.1 mm.

Difficulty was met with, however, in obtaining equal flow of oil from all the jets; very small irregularities caused widely differing rates of discharge, so that while one jet was giving droplets of the required size, the discharge from the others, when excessive, gave too many drops of widely different sizes, and when too little, too few drops to be effective. In the latter case the chances were that there was no certainty of a droplet being in the field of view of the recording camera (a matter of 2.25 cms), and in the former case vitiation of results ensued owing to the impossibility of deciding whether two adjacent images of the droplets at the same radius were the

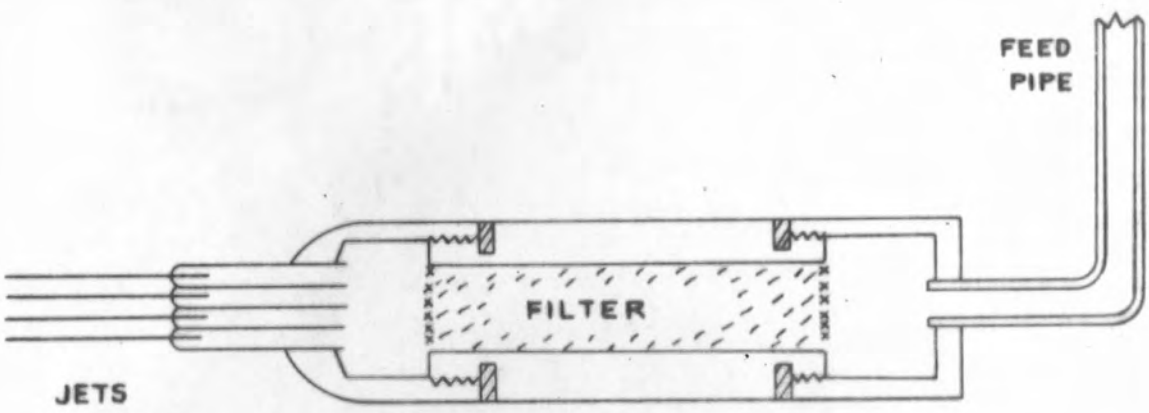

FIG. 1.1. JET ASSEMBLY.

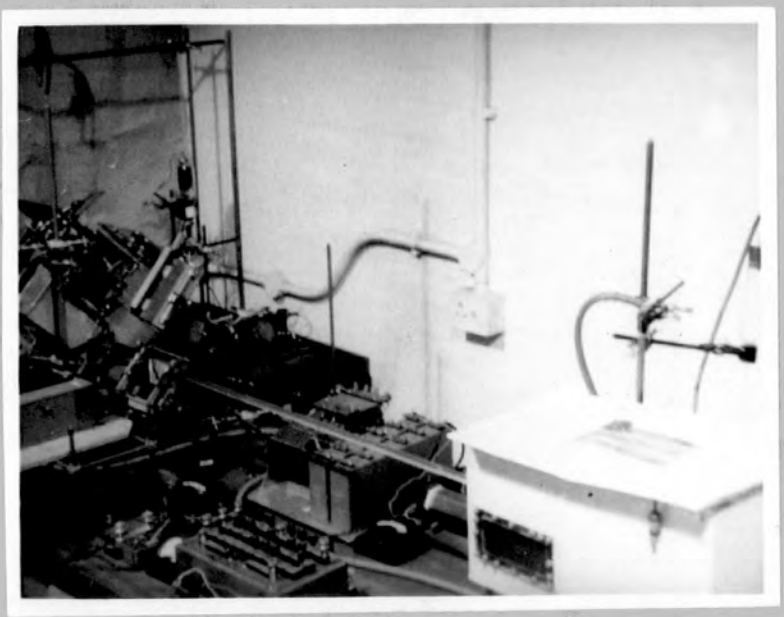

PLATE 2.1

images of the same drop in the light of the dual stroboscopic flashing or whether one drop had, as it were, "caught up" its nearest neighbour's last image. As with previous streamers, here again there was migration from the position of injection of the droplets due to initial disturbances, particularly at low rates of flow, which were attributed to the jet holder. At higher flow rates the efflux of droplets precipitated turbulence. It was observed that with Reynolds' numbers somewhat greater than 2000, turbulent flow could be created, with one jet operative, by increasing the rate of oil discharge and that laminar flow was again restored by a further increase in oil discharge. On decreasing the rate the reverse was seen to apply, turbulence appearing and then dying out. It was thought that there must be some critical frequency of oscillation set up by the break off of the oil droplets, at one particular discharge rate, for which the flow ceased to be stable. Varying the fluid flow rate while maintaining a fixed though excessive oil discharge rate was observed to produce the same effect, as was to be expected.

Fig.1.1 shows, enlarged, the construction of the jet assembly, which was made of brass with a copper feed pipe. It was fixed by means of the feed pipe to a small horizontal carriage on two sets of rails at right angles to each other on the top of the reservoir by which means two-dimensional horizontal motions of the jets were made possible by worm drives. The vertical adjustment was made with a rack and pinion. No

position of the jets could be found which reduced the migration of the droplets, though very nearly even discharge was achieved by scrupulous cleaning of the jets and careful attention to the jet mouths. It was decided then, to have the droplets distributed at random in the reservoir and thus overcome the precipitation of turbulence and at the same time eliminate the difficulties attendant with the use of several jets.

To this end, all but one of the jets were removed. Prior to a run the jet feed pressure was made high and the jet moved in a rapid spiral through the reservoir, hence dispersing the droplets and at the same time ensuring their small size by forcing their detachment from the jet by the rapid motion and fluid friction. With this technique there was no need for the carriage and rails and they were consequently discarded. It soon became possible with practice to distribute the droplets very similarly on successive occasions with almost identical droplet size each time. Only when a sudden change of direction of the jet was made did the uniformity of the droplet size alter; at such places there were large droplets. By slightly squeezing the jet mouth with a micrometer screw gauge even smaller droplets were obtained. A number of measurements gave the droplet size to be about 0.1 mm to 0.15 mm.

The droplets having been dispersed, remained in suspension while the liquid in the reservoir was allowed to settle down, though only very little disturbance had been caused owing to the fineness of the jet.

CHAPTER 2.

THE APPARATUS.

4. General.

An apparatus was required which would give by a photographic record the nature of the flow existing in a circular section flow tube at a number of points on the diameter so that in a time of somewhat less than a second a complete record of the velocity profile could be obtained.

A series of investigations were carried out upon the necessary components of such an apparatus and finally a satisfactory apparatus was obtained. The apparatus was then tested with water and yielded excellent results. Finally the velocity profiles at various rates of flow were measured using a visco-elastic ammonia soap solution.

An initial survey was made of apparatus which might be needed and in view of this, preliminary experiments were carried out on the following items.

1. Types of streamers which would be susceptible to photographic observation and which would not, to any great extent, interrupt the nature of the flow through the flow tube and which could be easily injected into the fluid under observation.

2. Methods of recording the flow pattern which would record quickly a complete picture of the velocity profile for the flow. Photographic recording was immediately decided upon and this restricted the types of streamers which could be employed, though it was not apparent, until after a lengthy

series of experiments with streamers and methods of illuminating them, that a direct method of photographic observation was not possible so that eventually a two-dimensional system of viewing was adopted.

3. Optical systems which would permit of photographic recording and a system of mirrors whereby two views of the flow tube from two directions at right angles could be observed simultaneously in such a way that the two views were superimposed and of the same size giving the appearance of a single section of the flow tube.

4. (a) Stroboscopes which could give variable (though constant at any one time) short periods of intense illumination with a sharp start and cut off and whose frequency could be governed by the recording camera.

(b) Flash tube stroboscopes which could give short duration light flashes, at a frequency locked to that of the recording camera and faithfully following any speed variations, in such a way that two flashes separated by a short time interval should occur during the stationary periods of the film.

This investigation proved to be exceedingly profitable and interesting. It involved an examination of a number of types of flash tubes as regards methods of triggering them to initiate their discharge and particularly the effect on their triggering characteristics of the time for which they had been continuously running, on the voltage applied across the tubes and on their age and condition.

Also in connection with the flash tube stroboscope, a series of experiments and a theoretical investigation was carried out on various types of chokes, with pulse sharpening spark gaps across them, capable of producing high voltage pulses by stopping the current flow in them, sufficiently great to trigger the flash tube discharge.

5. The electronic circuit, controlled by the camera, which would produce the above mentioned high voltage pulses.

6. A flow gauge which would record the rate of flow through the flow tube so that theoretical or established experimental profiles for such a rate of flow could be compared with the measured profiles.

5. The Final Apparatus.

With the results of the above investigations a final apparatus was assembled, Plate 2.1 which consisted essentially of four distinct sections:

(a) The flow tube, reservoir and associated streamer injectors.

(b) The stroboscope, including auxilliary electronic equipment.

(c) The optical system.

(d) The flow gauge.

(a) The reservoir, a rectangular section tank 9" x 10" x 18", was charged with 26 litres of fluid and this served for several short runs as the position of the flow tube entry in the tank allowed for the outflow of about 12 litres before the flow

tube entrance affected the inflow owing to the proximity of the entry to the fluid surface. The flow tube had an internal diameter of 12.5 mm. and was chosen as a compromise between a large bore tube which would have necessitated the use of large quantities of fluid and a small bore tube in which the velocity gradients would have been excessively high.

The velocity of flow at a distance r from the axis of a pipe of radius a in which there exists laminar flow of a Newtonian fluid is given by Eq. (1.1). Neglecting the negative sign, the velocity gradient at the radius r is given by

$$\frac{dv}{dr} = 2\,k.r \quad \ldots\ldots\ldots\ldots\ldots\ldots\ldots\ldots\ldots\ldots \quad (2.1)$$

and for algebraically similar distances from the axes of two pipes of different radii ($r = c.a$) the ratio of the respective gradients is $2.k_1.c.a_1/2.k_2.c.a_2$. The constants $k_i (i = 1,2)$ are given by Eq. (1.7). Thus for similar values of the Reynolds' numbers, R_n, the ratio of the two velocity gradients for the two pipes under dynamically similar conditions is

$$(dv/dr)_1/(dv/dr)_2 = a_2^2/a_1^2 \quad \ldots\ldots\ldots\ldots\ldots\ldots \quad (2.2)$$

$\therefore$ the smaller the radius of the pipe the greater the corresponding gradients for similar radial positions. As a result of considerations set out below in the next paragraph, a relatively large flow tube of internal diameter 12.49 mm. was used. Even so, the velocity gradients were prohibitively high, as is indicated in Chapter 2, and denied the use of oscillating dye filament types of streamers.

Originally it was thought that oscillating dye streamers (16) would be used as flow indicators with which the velocities could be obtained by the variations in peak to peak distances of the sinuosities with radius, their distances however, became prohibitive with high gradients as was quantitatively discussed in Chapter 1. It was found that the colouration brought about by the nigrocene dye streamers prevented further use of the fluid and so for low gradients a large radius flow tube was indicated while wastage of fluid dictated a smaller bore tube. The flow tube adopted was the most convenient size to hand and at R_n = 2000 the flow rate per minute was 1.18 litres which was considered to be sufficiently economical as runs of this length were not anticipated. The flow tube was fitted with a detachable flared entry which was turned from perspex. In fact dye streamers were abandoned for reasons which are set out later but the flow tube was not altered.

The streamers finally adopted consisted of small oil droplets whose density, by a suitable admixture of constituents, was made equal to that of the fluid and they were obtained by means of a 0.006 inch internal diameter drawn copper tubing jet.

(b) Briefly the operation of the stroboscope was as follows. A switch, mechanically operated by the recording cine camera, upon closure, caused a saw-tooth relaxation-oscillator to fire and thereby control the frequency of oscillation of an asymmetrical multivibrator; negative going voltages from which

(either from the grids or anodes) suddenly backed beyond cut-off two pentodes with inductive anode loading. The resulting high voltages developed in the loads due to the cessation of current flow, after sharpening by means of spark gaps, were employed as trigger pulses for two Siemens S.F.6 flash tubes which were built into a screened 0-4000 volt d.c., power pack. The normal operating voltage of the flash tubes was 2000 volts. Associated with the flash tubes were cylindrical lenses and plane mirrors whereby the light could be focussed and brought to bear on the observation section of the flow tube.

(c) The feature of the optical system was that by means of two plane mirrors placed symmetrically one on either side of the flow tube, with a semi-reflecting mirror between them the flow tube could be viewed at one and the same time from two directions at right angles with the two views superimposed. This arrangement allowed for the localisation of events in the flow tube in three dimensions.

(d) The flow gauge which included a recording drum camera was simple but good in operation and recorded a measure of the flow rate by a hot wire anemometer principle working on the air displaced by the fluid upon entering a large air vessel. Electrically, the anemometer circuit was a Wheatstone Bridge network.

Operational Procedure.

Prior to a run small oil droplets were dispersed in the fluid in the reservoir and time allowed for any disturbances

which had thus been created to die out. This was easily observed as the oil droplets remained in suspension. One end of the flow tube, the other end of which was fitted with a removable flared entry protruding into the reservoir, was connected by means of rubber tubing, fitted with a stop cock, to the air vessel of the flow gauge (section 8, Chapter 3) and flow was started by opening this valve. The suspended oil droplets carried into the flow tube were illuminated at the observation section with light from the stroboscope, which had been rendered slightly convergent by large cylindrical lenses, from two directions at right angles with the aid of auxilliary plane mirrors to give symmetrical illumination. At this section the flow tube was surrounded by the optical system (e) and here the recording camera was focussed on to the two superimposed images of the flow tube. The camera, when running, operated the mechanical switch whenever the film was stationary and thereby governed the stroboscope as already indicated and two distinct flashes occurred whose time separation was controllable by means of the multivibrator auxilliary to the stroboscope. The time interval was equal to the time for which one of the valves of the multivibrator was conducting. The triggering pulses for the flash tubes were derived from the negative grid swings (or the sudden falls in anode voltages) of the multivibrator valves, and the flashing interval, which was the conducting time of that valve which was conducting for the least time

during one complete cycle, was easily variable through the grid leak, which was a variable resistor, of the other valve.

Knowing the time interval between the two flashes which occurred during each exposure, the velocities of the individual droplets could be computed from the distances between their photographed images. As will be described later in the optical system section, the radial positions of the droplets could be computed and a velocity profile obtained from a single exposure as there were in general several droplets in the observation section at any time. Thus from a run at a slowly varying flow rate profiles could be obtained at a number of different Reynolds' numbers. Alternatively, a constant flow rate could be employed and frames chosen at random thus yielding a large number of droplet velocities with a consequent greater variance of radii. This latter method was preferred and it was often possible to follow the path of a droplet through several consecutive frames which proved the existence of rectilinear motion and also gave a check on the reliability of the stroboscopic flashing.

The flow gauge, essentially a hot wire anemometer, recorded, through a Wheatstone Bridge and galvanometer, a continuous measure of the flow rate throughout the run on a rotating drum camera which was driven at a constant speed by a series-series/parallel twelfth horsepower motor. A calibration yielded the true flow rate from the recorded deflection.

An auxilliary lantern recorded a straight line datum trace on the drum camera recording paper: its power supply was switched on at the same time as that for the trigger pulse pentodes of the stroboscope by means of ganged switches, hence, in carrying out a run the order of events was as follows.

1. A photographic record of the pipe alone was taken for the determination of the centre of the photographed image of the flow tube.

2. The drum camera was switched on to record a zero trace for the flow gauge.

3. After a few seconds the flow was started, followed shortly by

4. The switching on of the recording cine-camera which quickly settled down, the first few frames suffering no exposure

5. When the camera was steady, the datum galvanometer lantern and pulse generators were switched on, starting the flash tubes and datum trace on the drum camera paper.

6. Any desired variations of flow rate were made by means of the stop cock while observing the flow whose nature could be seen (i.e. laminar or turbulent) as the droplets appeared as pin points of light.

7. Power supplies to pulse generators and datum lantern switched off.

8. 7 terminated the run and the sequence of events was repeated, generally, in the reverse order. The repeating of operations 2 and 1 gave a final zero trace for the flow gauge

and a second determination of the pipe centre thus ascertaining whether any relative movement had taken place between the camera and the flow tube.

The speed of the camera was generally constant (though variations did not matter with constant rate of flow runs), and any irregularities could usually be traced to dirt in the mechanism or to the mechanical switch or to lack of lubrication, any of which was easily remedied. If the total number of frames in a record was counted the appropriate point along the datum trace of the drum camera record could be easily obtained for any particular frame and hence the corresponding flow rate for the frame obtained.

The method of obtaining data from the records and a fuller account of the individual components of the apparatus, their construction, operation and calibration where necessary, follows in the ensuing chapters.

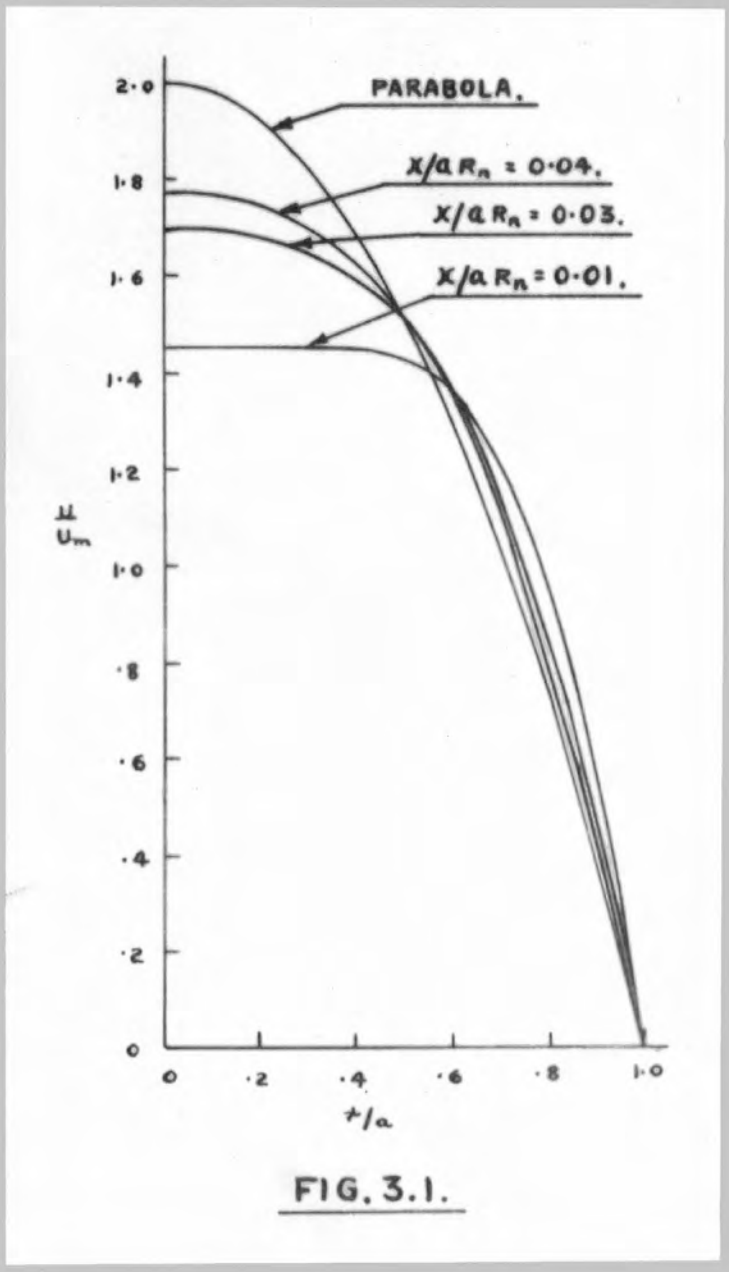
PARABOLA.
X/a Rn = 0·04.
X/a Rn = 0·03.
X/a Rn = 0·01.
2·0
1·8
1·6
1·4
1·2
1·0
·8
·6
·4
·2
0
u/Um
0
·2
·4
·6
·8
1·0
r/a

FIG. 3.1.

CHAPTER 3

THE FLOW GAUGE

6. General.

In order to ascertain the performance of the observing and recording techniques it would be necessary to calibrate the apparatus by measuring the known flow patterns found with simple fluids of which water was the obvious choice. A flow gauge was thus required which would give the instantaneous average rate of flow (within reasonable limits) of the calibrating water and the experimental fluids.

The length and diameter of the flow tube (Chapter 2) were 120 cms and 1.249 cms respectively and the observation section, somewhat over 2 cms long was centred 105 cms downstream from the throat of the flared entry to the flow tube. With such geometrical conditions and with a Reynolds number of flow of 2000 the Schiller criterion (22) x/aR where $x = 105$ cms, and $a = 0.6246$ cms has a value of only 0.084 so that the velocity profiles in general could be expected to be other than parabolic (22). In these cases the velocities at any distance from the axis of the flow tube could only be calculated approximately from Schiller's theoretical results and not at all from the usual Poiseuille Hagen formulae $Q = \frac{\pi P a^4}{8.\eta.L}$ and $v = \frac{P}{4.\eta.L}(a^2 - r^2)$. The established experimental determinations of the velocity profiles of Schiller and Nikuradze (22) were accepted. These are shown reproduced in a slightly different form with a theoretical parabola in fig.3.1 for a range of values of

x/aR from 0.01 to 0.13. At the latter value the curve is a parabola.

For obvious convenience, experimental results were plotted dimensionlessly in the form of U/Um against r/a where U was the measured velocity at the radius r from the axis of the flow tube of radius 'a' and where Um was the mean velocity of flow. It was only neeessary then to know the rate of flow of fluid Q cc/sec in order to determine the mean velocity and hence the Reynolds number of flow and consequently to determine the theoretical, or more correctly, the experimentally established velocity profile for any set of conditions.

Obvious requirements of the flow gauge were that it should be capable of self recording or capable of continuous photographic recording of a measure of the flow rate and that in any case it should have a rapid response to changes of flow rate.

In view of the fact that the 'inlet length' for the flow tube for Reynolds numbers of flow greater than about 2000 was greater than the 105 cms, between inlet and observation section, it was not permissible to determine the rate of flow by measuring the pressure gradient along a length of the pipe by means of pressure tapping points in the flow tube wall and applying Poiseuille's equation; because, in the inlet length there is an accelerating conical plug of flowing fluid and hence the pressure gradient is greater in this region being greatest at the entry (23)(24) and decreases until it reaches

a steady value in regions of fully developed flow. Any such measured pressure gradients would thus give a greater flow rate than the actual. Should the pressure points be restricted to two positions astride the observation section and the flow rates restricted to low values to allow fully developed flow to be established, the pressure gradient with water, with this flow tube, at a Reynolds number of 2000 being about 3.3 dynes per cm^2 /cm, only about 0.5 mm water head would be developed over 20 cms of the flow tube. Several gauges have been designed which could measure quite easily such small differential pressures. Hindley (25) employed two balanced inverted bells with their mouths below the liquid levels in the limbs of a manometer. However the falling static head complicates matters and the necessity of wide manometer limbs involves a delay in response due to the finite time required for the liquid to flow into the manometer limbs. Mathessen and Eden[26] and A.G. Keenan and R.L. MacIntosh[27] used differential bellows, the latter employing a strain sensitive wire; these were essentially for steady small differential pressures. Such sensitive gauges in general suffered from finite delay times for reasons of the flow time of the fluid into the systems. With visco-elastic fluids the viscosity depends upon the rate of shear of the fluid (28) so that pressure gauge measurements for the determination of the flow rate only lend themselves to such systems if a knowledge of the viscosity is known in relation to water from a series of

determinations of the viscosity from measured flow rates and pressure gradients. In any event the viscosity during the flow in the flow tube will vary from the wall where the rate of shear is greatest to the centre of the tube where it is zero. Such matters add complications and increase errors. There being insufficient length of flow tube beyond the observation section it was not possible to insert a hot wire anemometer into the tube which in any case has no steady true zero owing to local heating of the fluid. Methods therefore of measuring the flow rate using the actual flow tube were not suitable. It was decided to employ a method of measuring the flow rate after the fluid had left the flow tube, in fact to measure the air it displaced upon entering a thirty litre bottle.

A differential water manometer with narrow limbs operated by air flowing through a tube having two pressure tapping points responds fairly rapidly to changes of flow rate and offered a possible means of flow measurement. However in order that the photographed manometer could be measured up accurately with at best a 3 to 1 reduction in photography, a difference in levels of about one centimetre per thousand change in Reynolds number was necessary with the vernier microscope reading to .01 mm. This necessitated a narrow bore air tube and consequent delay in pressure build up in the air reservoir before the steady state was reached. At the same time flow variations were not reliably reproduced. It was decided to use an electrical gauge of the anemometer type.

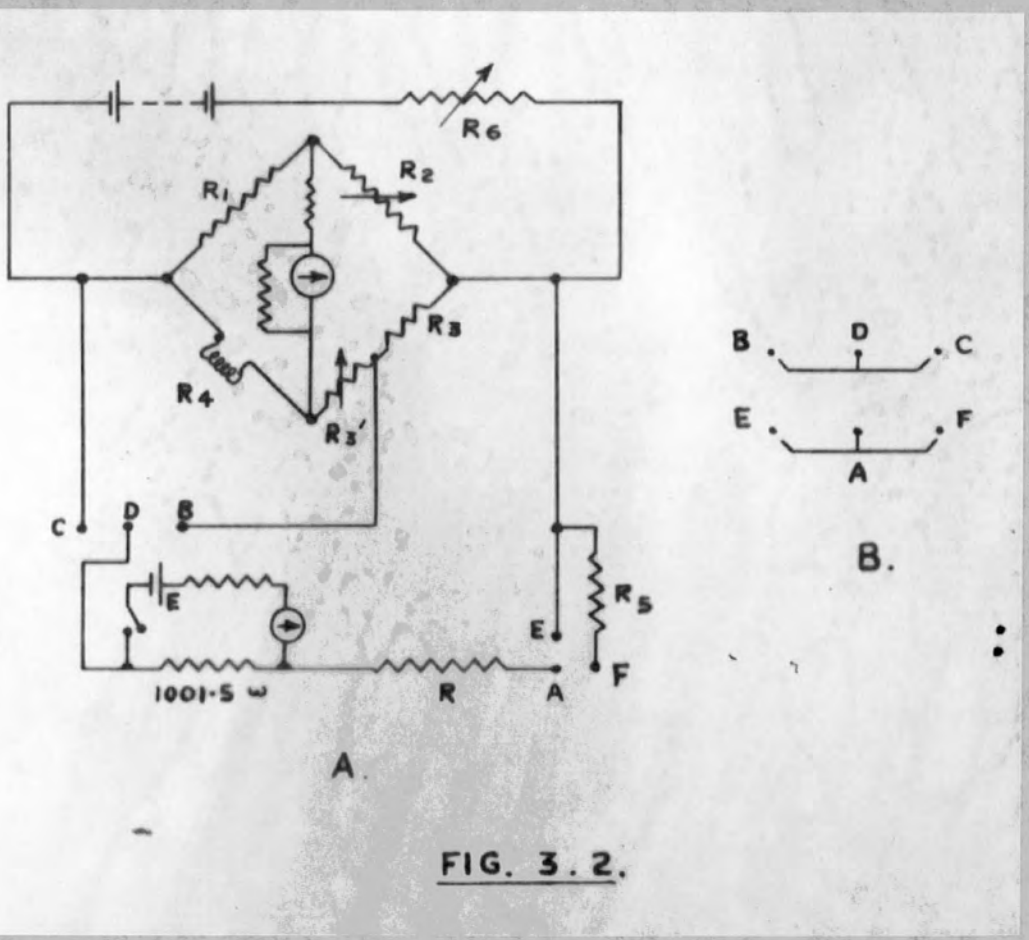

FIG. 3.2.

J.H. Lamb (29), used an electrically heated coil with differential thermocouples up and down stream which had the advantage of being unaffected by zero drift, but to be capable of rapid response to variations of flow rate, the thermocouples had necessarily to be of small gauge wire and in consequence the gauge was sensitive to large scale eddies in the turbulent air stream at the lower flow rates. It was necessary then to measure the cooling effect upon the heated system over a fair section of the air tube containing the gauge element in order to get a more integrated effect and thus be independent of localised regions of high or low flow rate.

7. Construction of Gauge.

A simple electrically heated coil was finally decided upon where change of resistance due to cooling by the air displaced from the 15 litre bottle could be measured as the unbalance current in a Wheatstone network and recorded by means of a rotating drum camera through the agency of a galvanometer and a deflected light spot. The circuit diagram of the Wheatstone network is shown in fig.3.2.

L.V. King(30) showed that the heat loss from an electrically heated wire in an air stream flowing with a velocity V was given by a relationship of the form

$H = A\sqrt{V} + B$ where A & B are constants involving the temperature difference between the heated wire and the air. This formula applies however to a wire whose temperature is maintained constant by varying the heating current. At

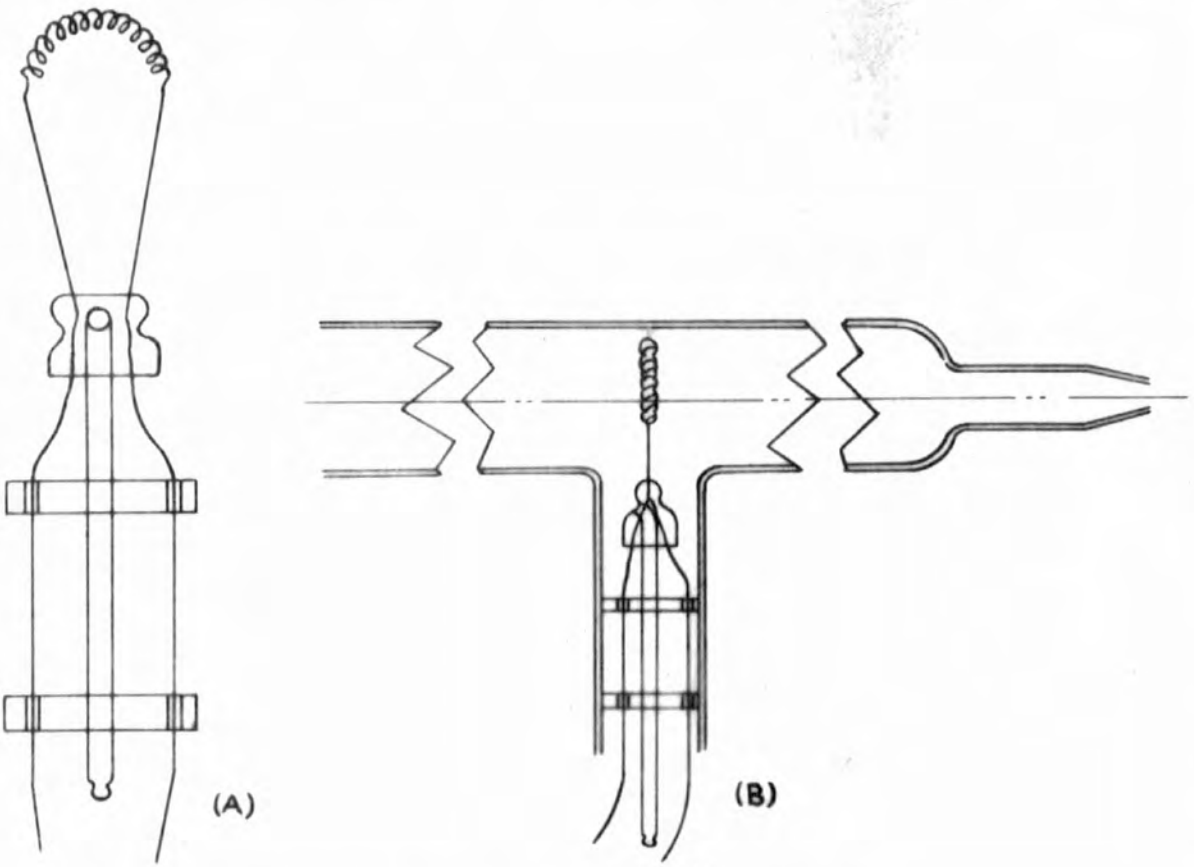

FIG. 3. 3. NICKEL GAUGE FILAMENT.

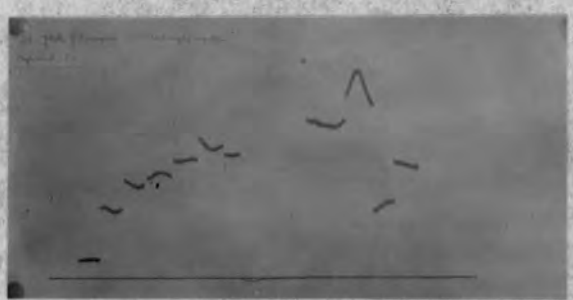

PLATE 3.1

lower velocities the form of the relationship is

$$H = \frac{C}{\log\left(\frac{D}{V}\right)}$$ where C & D are constants.

For the gauge employed the current was not maintained constant but it was assumed that the graphical relationship between the unbalance current of the bridge, due to the change of resistance, and the air flow would be of the form of a sigmoid curve passing through the origin, the abscissæ being the rate of flow. It was further assumed that by variations of heating current the inflection region could be made almost linear over quite a range of air flow rates and that thereby except at low rates of flow a sensibly linear relationship could be found for the required range of velocities.

The filament was made of 0.01 cm diameter nickel wire in the shape of a semi-circular coiled coil, silver soldered to the pinch leads of an electric light bulb fig. 3.3 (a) mounted in a side arm of a 3 cm bore glass tube fig.3.3(b) one end of which was open to atmosphere and the other end sealed to a standard B.19 cone for ease of assembly to the air lead from the 15 litre bottle which was a wide bore rubber tube fitted with a B.19 socket. The lead was kept wide to prevent delays due to pressure build up in the reservoir.

For two fluids flowing in pipes of different radii, Reynolds' No. is inversely proportion to the product of the radius and the kinematic viscosity. So that in the 3 cm gauge tube the air might be expected to be flowing in a laminar

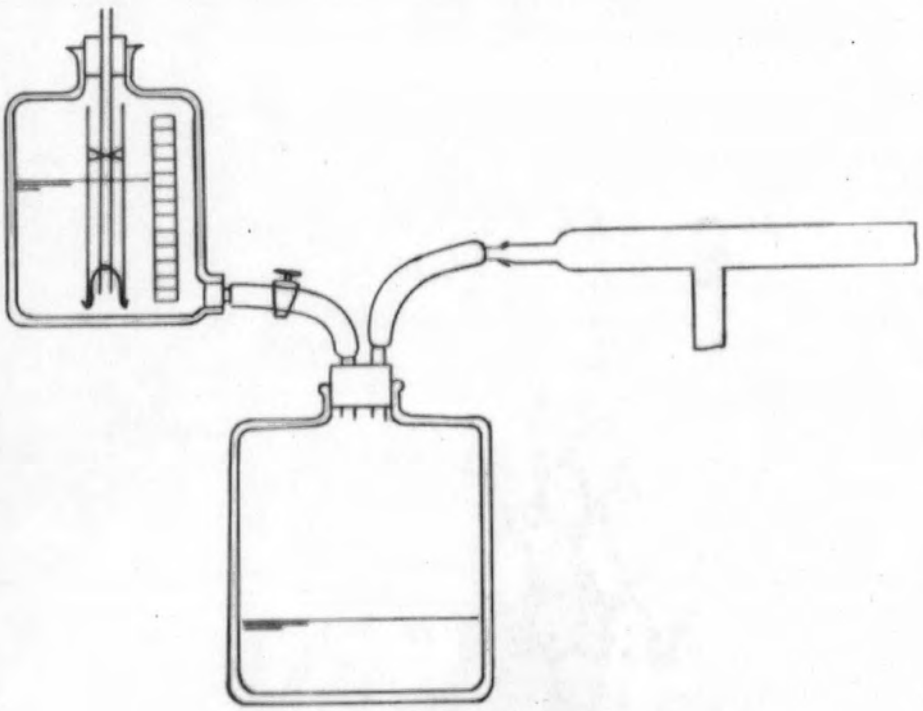

FIG. 3.4.

condition, but the irregular divergent entry to the gauge tube undoubtedly caused some large scale turbulence as will be seen later. It was for this reason that a coiled coil was used to cover a section of the air flow and obtain a more representative cooling than is obtainable with a single strand. The unsteadiness in response of a single strand mounted on a similar pinch is shown in plate 3.1 which was obtained as the drum camera record for a series of constant rates of flow, the heating current being 0.4 amp. The coil was made by winding 30 turns of the nickel wire on a 4 B.A. bolt heating the wire all the time with a tiny gas flame. In this way the coil did not spring loose upon release and accurately reproducible coils could be made.

8. Calibration of Flow Gauge.

For calibration of the gauge a ten litre Mariot Bottle was used with a variable head of water, the discharge being fed into a 30 litre air reservoir and the displaced air to the flow gauge fig. 3.4, and the unbalance current of the Wheatstone network of which the heated coil formed one arm was recorded by means of the usual galvanometer and lantern on a rotating drum camera. The Mariot Bottle was fitted with a scale and the meniscus was timed over a number of divisions, each of which represented 202 ccs, dependent upon the particular rate of flow being used. To prevent rippling of the water surface in the bottle the air inlet tube was surrounded(fig.3.4) by a wide bore glass tube so that the disturbances caused by

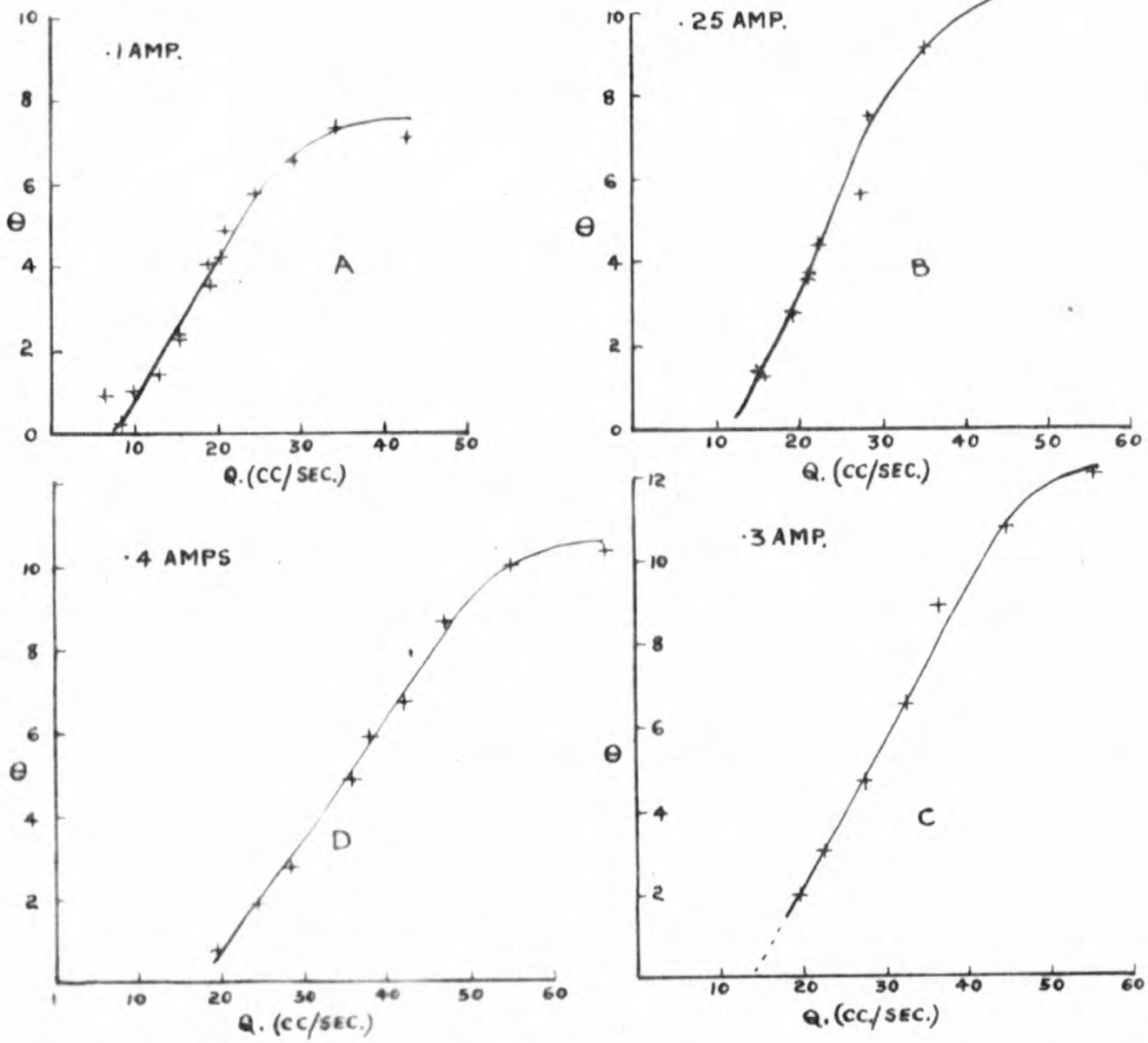
·1 AMP.
A
θ
Q. (CC/SEC.)
·25 AMP.
B
θ
Q. (CC/SEC.)
·4 AMPS
D
θ
Q. (CC/SEC.)
·3 AMP.
C
θ
Q. (CC/SEC.)

FIG. 3.5.

the inflowing air were confined to within this jacket. The galvanometer lantern and drum camera were switched on for a few seconds during the time of each calibration flow as near the middle of the time as could be estimated.

In the first instance the response curves were plotted at heater currents of 0.1, 0.25, 0.35 and 0.4 amps to ascertain the validity of the first of the assumptions indicated above and the four resulting curves are shown in Fig.3.5, A.B.C.D. The curves are shown separately as the ordinates bear no relation to each other as the bridge components were varied, while maintaining 16 volts across the bridge, to obtain the required heating currents, and also the galvanometer series resistance was altered to ensure a reasonable deflection.

In the case of flow gauges consisting of two wires in close proximity, one of which is heated relatively to the other, and which two form two arms of a bridge network, the shape of the initial region of the response curve is determined largely by the particular array used; whether the wires are horizontal or vertical, parallel or at right angles to the mean flow and whether the hot or cold wire is uppermost or upstream. In the horizontal position with the cold wire above the hot one with either orientation with respect to the mean flow a slow rate of flow has little cooling effect but merely removes from the colder wire the slip stream from the hot, the relative temperature difference is consequently increased and a negative deflection is obtained. It was thought that arguments on these

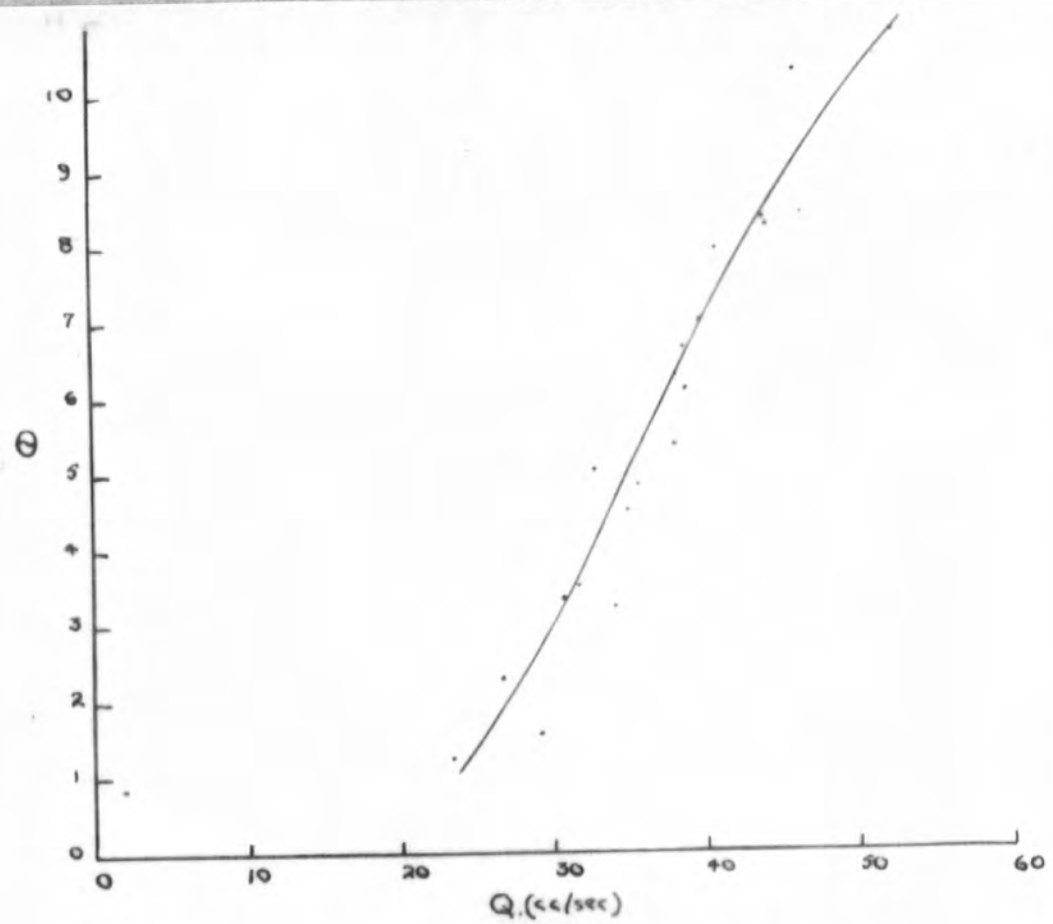

FIG. 3.6

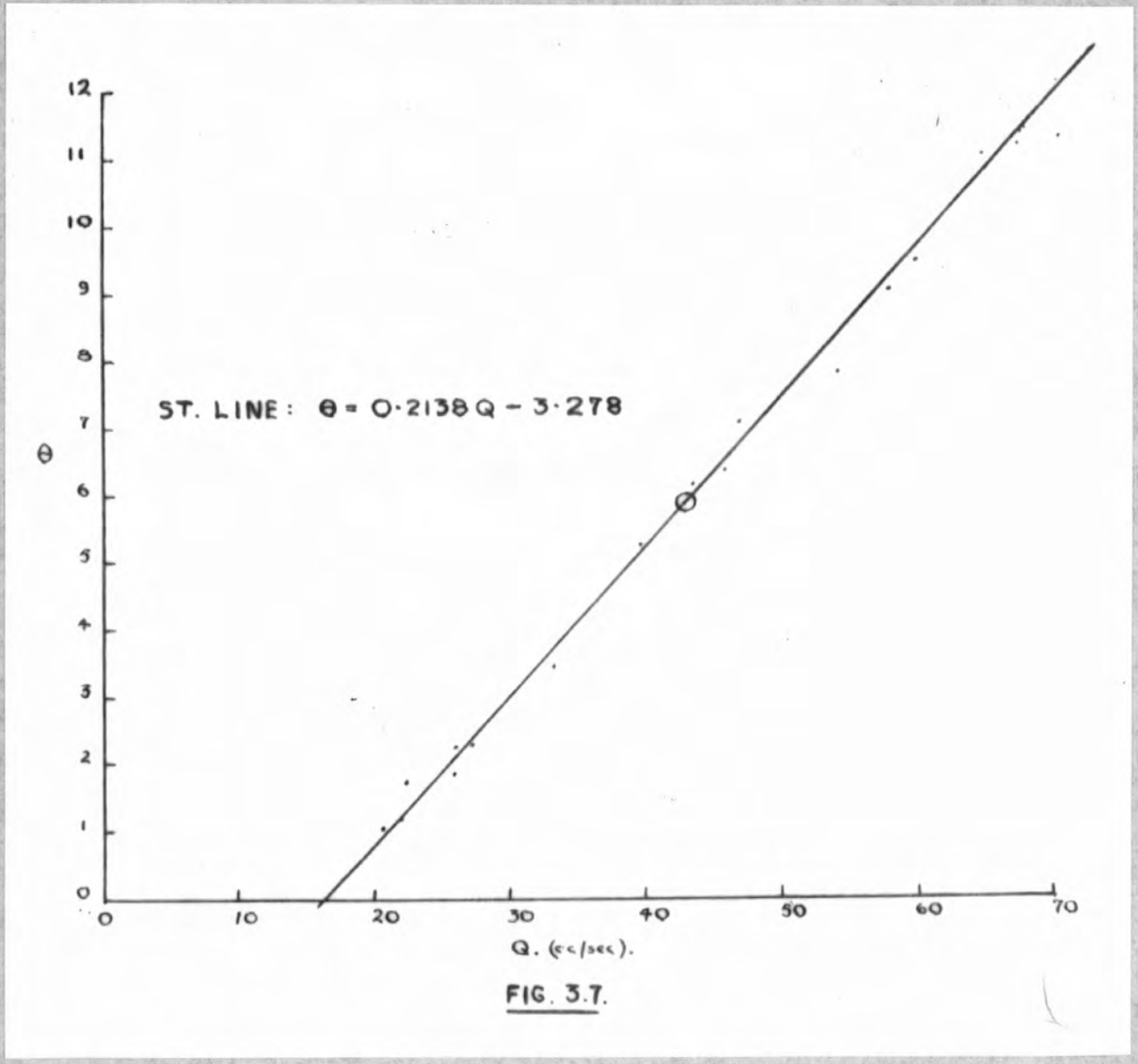
ST. LINE : θ = 0·2138 Q − 3·278
θ
Q. (c.c/sec).
0
1
2
3
4
5
6
7
8
9
10
11
12
0
10
20
30
40
50
60
70

FIG. 3.7.

lines could explain the negative trend of the above curves which was most noticeable with the curve obtained with a 0.4 amp heating current. It was apparent from the calibration curves that the curves had the estimated shape and that a linear portion could be obtained particularly with currents of over 0.4 amp.

A further calibration was carried out at 0.4 amp to obtain a best fit straight line to the centre section of the curve but the result fig. 3.6 was very poor. The filament was examined and it was found to be collapsed, probably due to overheating at some time while adjusting the current. A new similar coil was made and the calibration continued, after several unrecorded dummy runs to age the coil, and the result is shown in fig. 3.7. There was a certain amount of scatter and the same tendency to have an initial negative characteristic. The best fit straight line was calculated for the points between $Q = 20$ and $Q = 70$ in the usual manner from the formula $m = \frac{\Sigma XY}{\Sigma X^2}$ where m is the slope of the best straight line and X, Y are $Q - \bar{Q}$; $\theta - \bar{\theta}$; $\bar{Q}$ and $\bar{\theta}$ being the arithmetic means of Q and θ the flow rates and deflections respectively. The resulting equation was

$$\theta = 0.2138Q - 3.278 \quad \ldots\ldots\ldots\ldots\ldots\ldots\ldots\ldots (3.1)$$

To test the validity or otherwise of this empirical result a second galvanometer lantern whose circuit included an on/off switch was arranged to project on to the drum camera in the same plane as that of the galvanometer deflected beam to

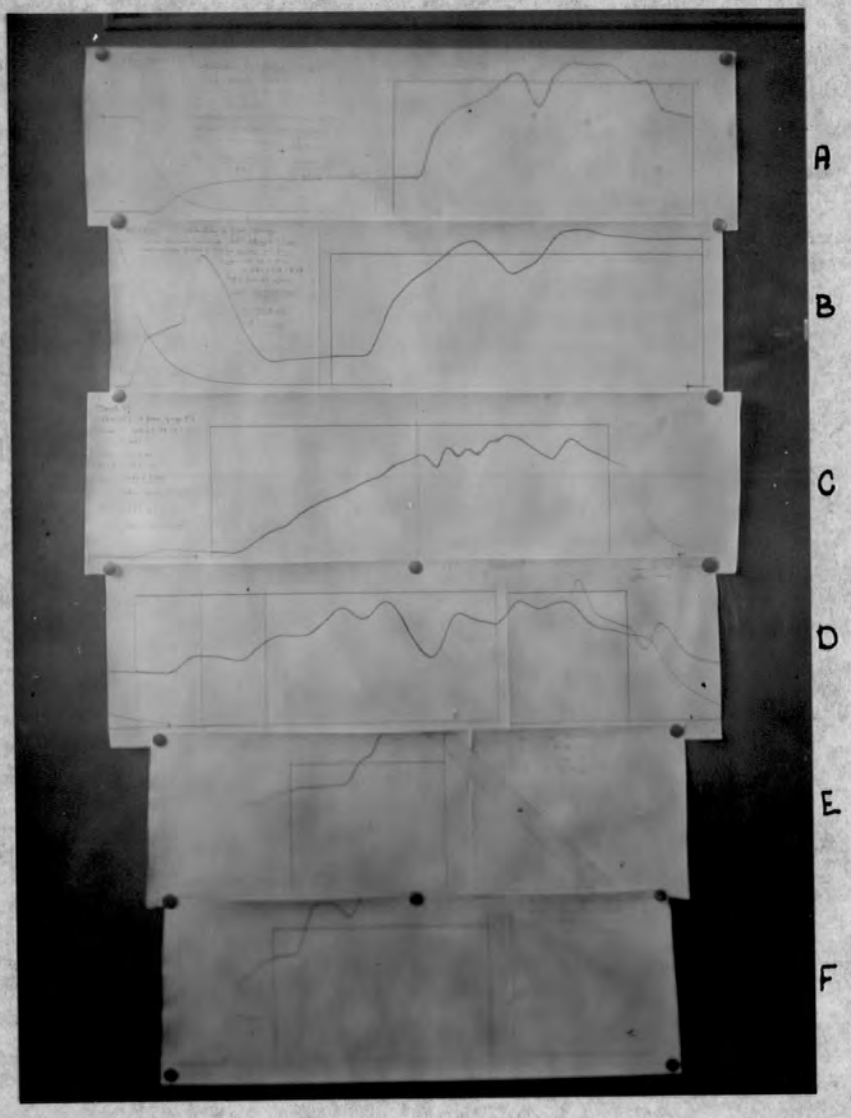

PLATE 3.2

give a datum line. If the second lantern was switched on for a known length of time during a continually varying flow rate and if during this time the total flow was measured, then the quantity of fluid as computed from the area under the drum camera photographic trace should correspond to the actual collected and measured quantity, provided due allowance is made for the negative intercept of the mean line on the deflection axis. Thus, if the length of the datum trace is L cm, the area between the curve and the zero line A, the time of flow T seconds, the computed slope and intercept parameters m and c respectively and the mean ordinate and abscissa of the calibration graph θ and Q respectively, then the computation is carried out from axes with origin (0, - C) and the area A must be increased by an amount $L \times c$. A steady deflection $\theta + c$ with respect to the new axes for one second i.e. a length on the datum trace of L/T involves an area $\frac{L}{T}(\theta + c)$ and represents a flow of Q ccs. So, the area $A + L \times c$ represents a flow of

$$\frac{(A + L.c).QT}{(\theta + c).L} \text{ ccs.}$$

$$= \frac{A'T}{m.L} \text{ ccs. where } A' = (A + Lc) \text{ \& } m = \frac{\theta + c.}{Q}$$

Six such calibrations were carried out in two groups, two then four, the heating current being left on overnight between the two sets. The relevant data is tabulated in table 3.1 while plate 3.2 a,b,c,d,e,f, shows the actual records in miniature.

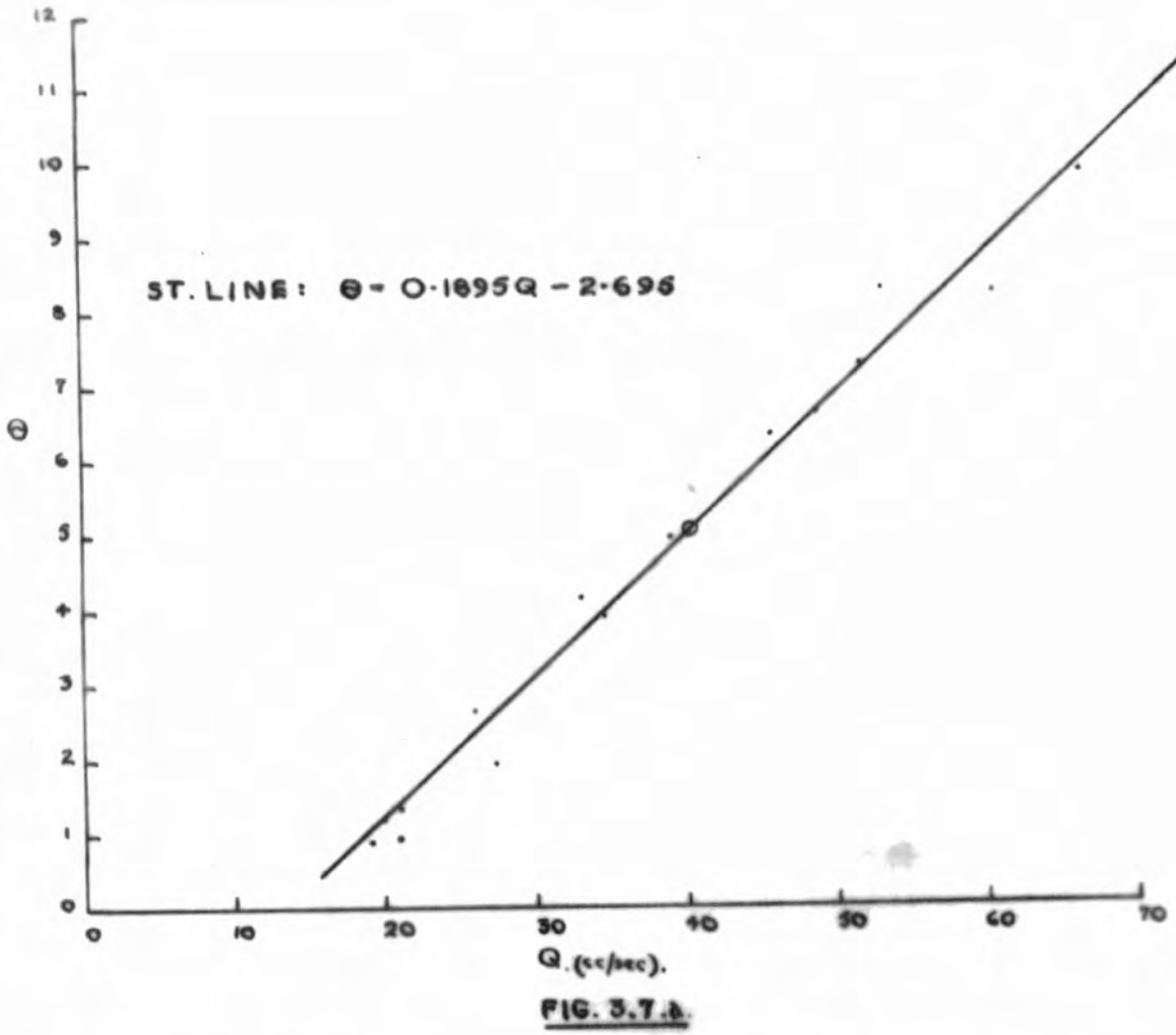
ST. LINE: θ = 0·1895Q − 2·696
θ
Q (cc/sec).
0
1
2
3
4
5
6
7
8
9
10
11
12
0
10
20
30
40
50
60
70

FIG. 3.7.b.

TABLE 3.1

Cal.No	L cms.	A' sq. cm.	T (sec)	m	c	A' T / m.L	Actual Q	%Error	
a	23.5	279.35	36.5	0.2138	3.278	2,051	2,022	+ 1.5	
b	28	356.46	35	"	"	2,084	2,022	+ 3	
c	30.7	287.75	51.3	"	"	2,249	2,424	- 7.9	
d	36.9	372.28	39.5	"	"	1,770	2,020	- 12.4	
e	11.85	160.12*	17.6	"	"	1,113	1,213	- 8.2*	- 8.1
f	16.55	243.65*	20.6	"	"	1,419	1,617	- 12.2*	-11.8

It was immediately obvious from an inspection of the results of table 3.1 that either the gauge technique as a whole was at fault or else the gauge had incurred a major change in its response to the flow as a result of leaving it switched on overnight. To check the correctness of either of these statements a recalibration of the gauge was carried out under precisely similar conditions as the previous calibration with constant rates of flow and a second graph - rate of flow v deflection - obtained. From this graph a new best fit straight line was obtained in the usual manner and the result was

$$\theta = .1895\ Q - 2.695$$

Fig.3.7a shows the result including the best fit straight line.

In the light of this new curve, the results c,d,e,f, of table 3.1 were recalculated with m = .1895 & C = -2.695 and table 3.2 shows the results obtained with the old ones for comparison.

TABLE 3.2

Cal.No	A'	m'	A'.T / m'.L	c'	Actual Q	%Error	Previous % Error
c	269.89	0.1895	2,379	2.695	2,424	-1.9	- 7.9
d	350.73	"	1,981	"	2,020	-2	- 12.4
e	153.21	"	1,194	"	1,213	-0.85*	- 8.1
f	234.15	"	1,530	"	1,617	-3.5*	- 11.8

* These percentage errors are the corrected values.

The results for e and f (asterisked) could be seen (plate 3.2 e,f) to be a little doubtful owing to the fact that the drum camera trace had left the recording paper due to the flow rate being too large. The doubtful regions were one and six centimetres long respectively and though in case 'f' the trace left the paper steeply only six square centimetres were added as a correction, that for 'e' being taken as one square centimetre. The figures in the appendage to the table are the percentage errors for these two cases with the correction included.

It was concluded from the above that the nickel filament underwent serious aging with prolonged heating, though the wire at 0.4 amp was not even at dull red heat. It was nevertheless believed that in principle the gauge was satisfactory and therefore platinum wire of the same diameter was obtained to obviate this aging. The heat capacity of platinum compares favourably with that of nickel, the products of specific heat and specific gravity being 0.715 and 0.879 respectively, so that heating currents of the same order as those used for the nickel filament should yield similar results.

9. Platinum Filament Gauge.

Upon the change to platinum, as a first step, a single strand filament of 0.005 cm diameter wire was constructed on the usual pinch and it behaved in a similar erratic fashion as the single strand nickel gauge (see plate 3.1). Hence a spiral filament was immediately constructed using the same number of turns and technique as described above. A rapid check on the shape of the response curve at a series of constant, though different flow rates, showed that a current of 0.45 amp, which maintained the wire at just below red heat, would be a suitable value.

It appeared from the results so far that the gauge technique was satisfactory. In order to ensure accuracy and repeatability of gauge conditions the Wheatstone network was amended to incorporate a permanent potentiometer and a high current capacity 10 ohm coil, specially constructed for the

purpose, of 18 S.W.G. manganin wire, fig. 3.2(a). Previously the current had been adjusted by altering R_3 which had been a simple resistance box and R_2 had served to ensure balance while an ammeter had been included in series with the anemometer R_4 in order to measure the heating current. A voltmeter had sufficed to check the overall voltage across the bridge. The potentiometer included a standard cell, 1.018 volts at 20° C (-0.000046 volts per °C) and using a Pohl commutator fig. 3.2(b) whose connections were in accordance with the lettering on the diagrams the switching was easily accomplished and the potential difference across the 10 ohm coil, which at balance gave the heating current and that across the bridge as a whole could quickly be measured and adjusted. The overall voltage was fixed at 16 volts and was regulated by R_6 which consisted of a low resistance with a high resistance in parallel for fine adjustment. Knowing the e.m.f. of the standard cell the appropriate value of R was simply calculated to give the correct potential across the fixed 1001.5 ohm resistor for balance against the bridge voltage or that of the 10 ohm coil.

For balance across the bridge (connections A - F, C - D) the condition is

$$E = \frac{1001.5}{1001.5 + R + R_5} \times 16 \text{ volts}$$

$$\text{i.e. } R = \left(\frac{16 \times 1001.5}{E} - 1001.5 - R_5 \right) \text{ ohms}$$

R_5 was included (a nominal 4.7 KΩ carbon resistor, value

4615 ohm) because the single plug resistance box R had not sufficient range. E was taken as its value at 16°C as the ambient temperature varied insufficiently from this to cause appreciable errors, and the values on the resistance box R were taken as correct, as repeatability was the essential factor. In this case R was 10,126 ohms. R_5 was by-passed when the potential across the 10 ohm resistor was being measured (connections A - E; D - B) and here, if the current to the heated wire is equal to C amps then

$$10C = \left(\frac{E\,(R + 1001.5)}{1001.5} \right) \text{ volts}$$

and $$R = \frac{10.1001.5\,C}{E} - 1001.5 \text{ ohm.}$$

The values of R for C varying from .3 to .5 amps are tabulated in Table 3.3.

TABLE 3.3

C (amp)	R (ohms)
0.3	1945
0.35	2436
0.4	2927
0.45	3418
0.5	3909

The values of R were preset according to the measurement required and one or two alternate repeat balances were required as adjustments to the main voltage control resistor

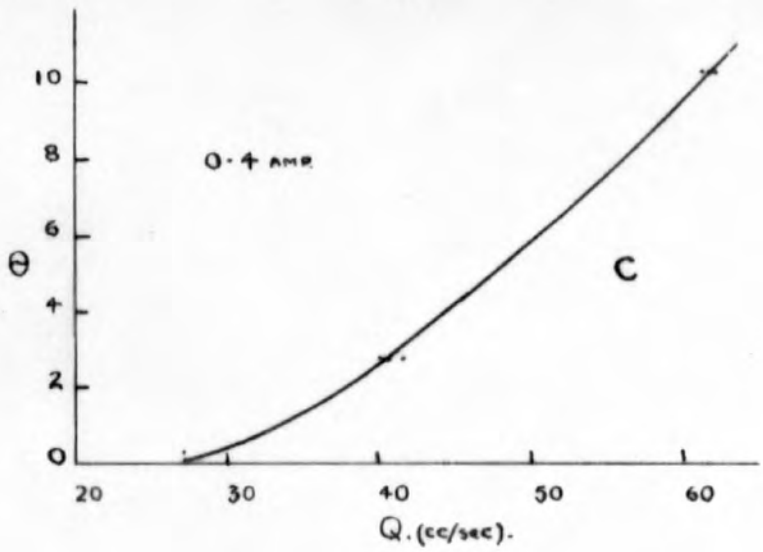
0·4 AMP.
C
θ
0
2
4
6
8
10
20
30
40
50
60
Q. (cc/sec).

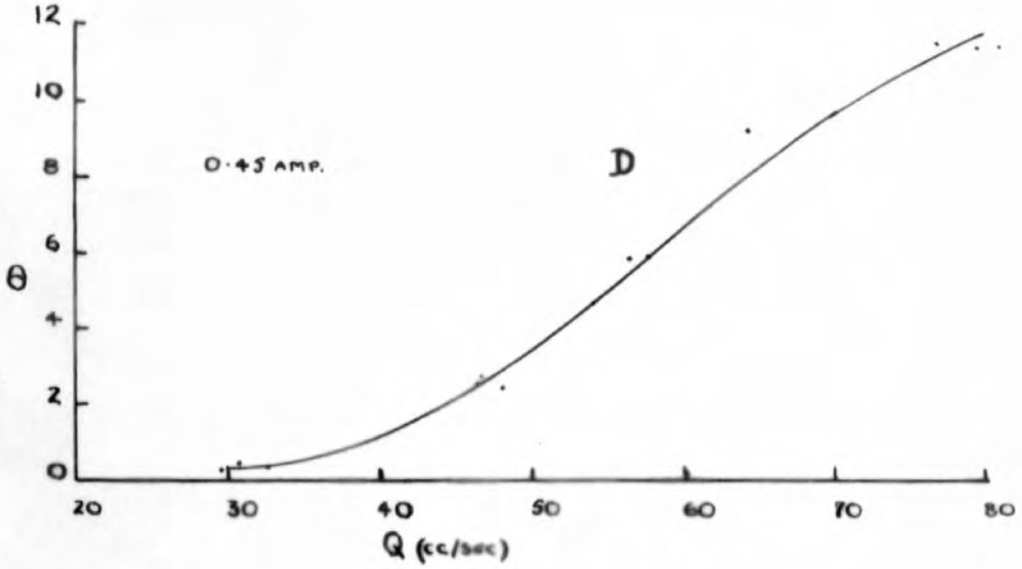
0·45 AMP.
D
θ
0
2
4
6
8
10
12
20
30
40
50
60
70
80
Q (cc/sec)

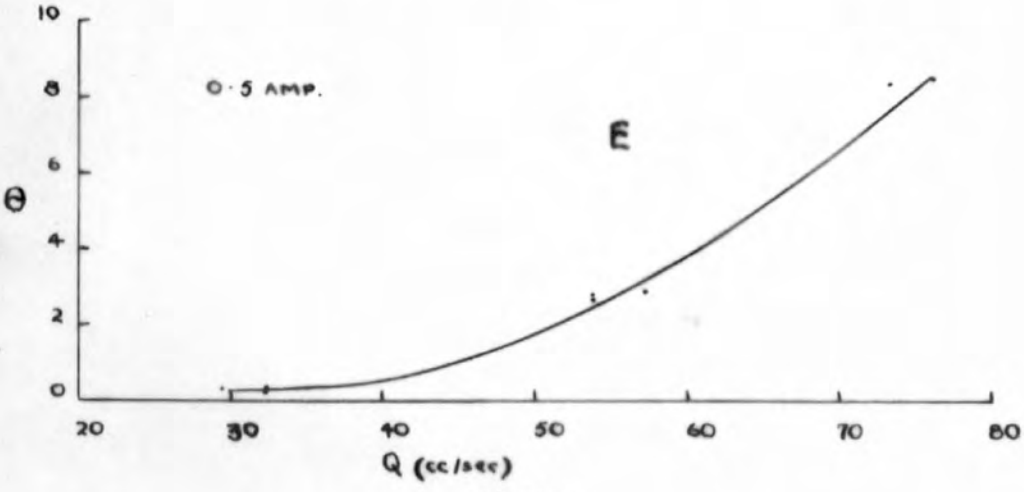
0·5 AMP.
E
θ
0
2
4
6
8
10
20
30
40
50
60
70
80
Q (cc/sec)

FIG. 3.8

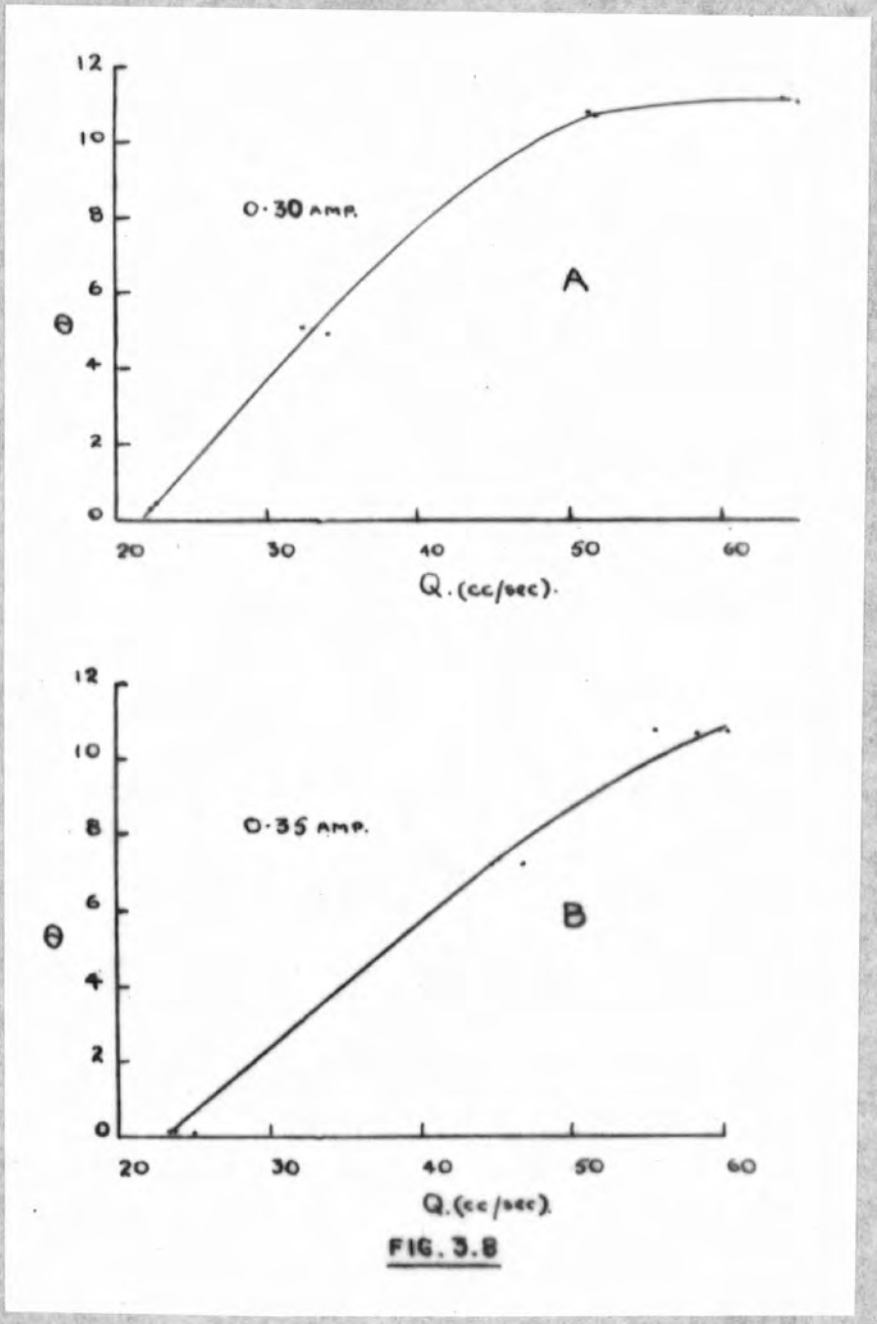
12
10
8
6
4
2
0
θ
0·30 AMP.
A
20
30
40
50
60
Q. (cc/sec).
12
10
8
6
4
2
0
θ
0·35 AMP.
B
20
30
40
50
60
Q. (cc/sec).

FIG. 3.8

in series with the supply voltage and R_3' (which was the main agency for controlling the heating current) affected the previous balance (adjustable through R_2). R_1 was fixed at 1000 ohms and the galvanometer shunt and series resistors were set to give critical damping and reasonable full scale deflection for maximum flow rate respectively.

When the potentiometer was connected, the bridge resistance as a whole or the current adjusting arm R_3 had its resistance slightly altered with a consequent slight change in current values upon disconnecting the potentiometer, but it was not necessary to make any allowance for this as the prime concern was repeatability and a check on the battery supply not a knowledge of actual accurate values of the heating current.

10. Calibration of Platinum filament Flow Gauge.

Preliminary curves for this platinum coil anemometer showed the usual shape at 0.3, 0.35, 0.4, 0.45, 0.5 amp (fig. 3.8 a,b,c,d,e) and are smoothed curves through experimental points which show a certain amount of scatter. The anomalies at the low flow rates are still present. The curves had the desired characteristics though the response to steady flow as shown by the drum camera records was rather inclined to be erratic in a similar manner to the single stranded filaments. Examination of the coil showed that while it was still fairly even there were two regions of rather more closely crowded turns. If local overheating occurred

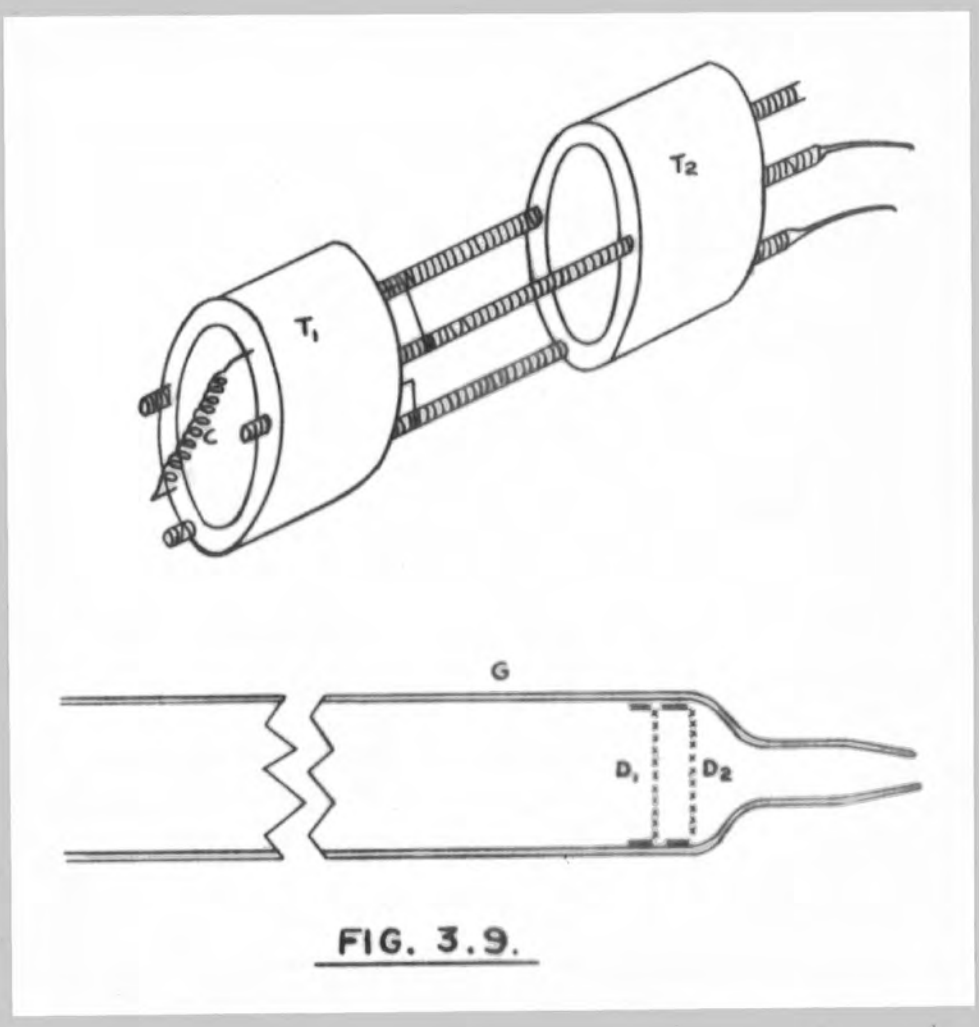

FIG. 3.9.

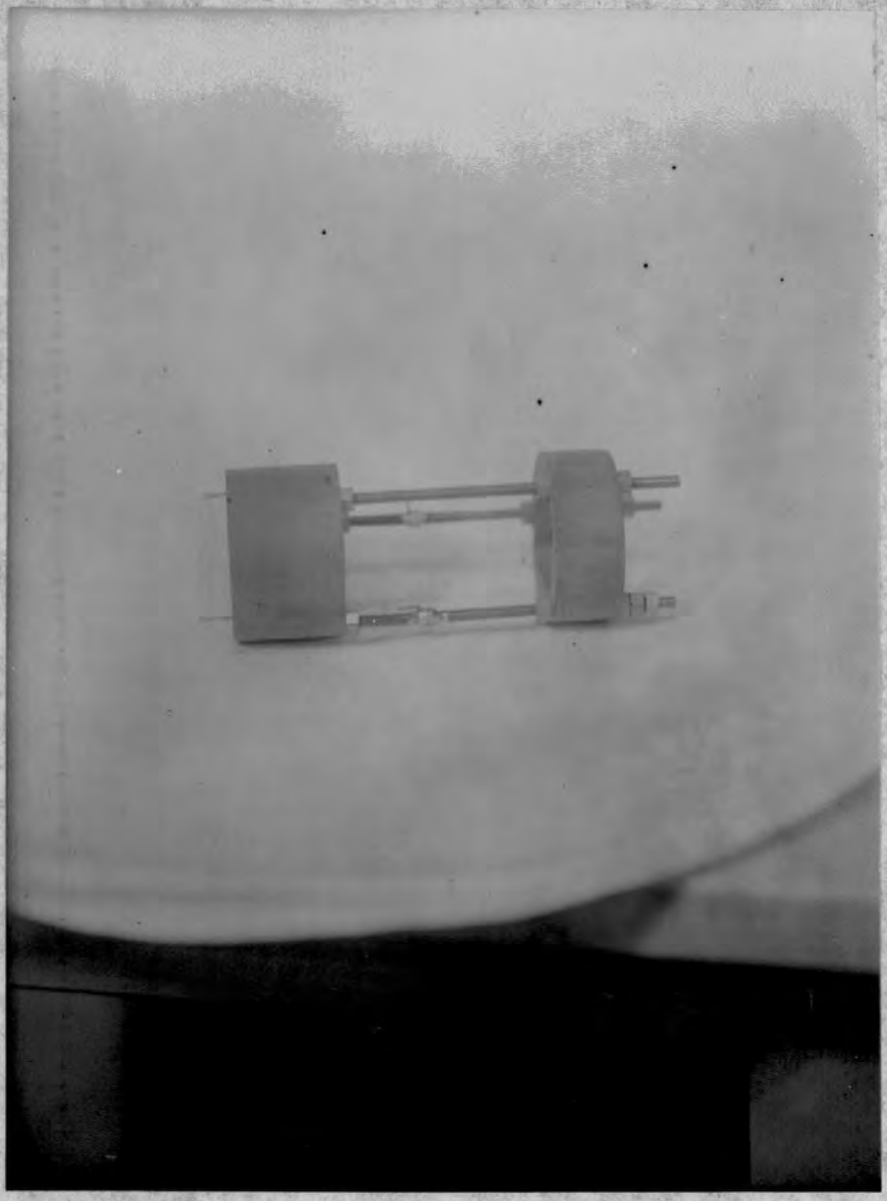

PLATE 3.3

here these 'hotspots' would, it was thought, tend to cause the unsteady response by more than average cooling in the face of the unsteady air flow. Mounted in this fashion on the pinch it was quite liable to damage due to shock while it was being inserted through the side arm of the gauge tube fig.3.4. In addition, sagging whether mounted with the coil concave upwards or downwards would cause overcrowding of the turns in the centre region of the coil. Hence the design of the mounting was changed in an effort to overcome these weaknesses. The coil C, fig. 3.9 (plate 3.3) was straight and under a slight tension. It was silver soldered to two leads passing tightly through one of two 'Tufnol' annuli T_1 T_2 spaced on three lengths of 4 B.A. studding two of which served as current leads. The whole assembly was a sliding fit in the open end of the glass gauge tube G of three cm. bore and thirty cm. long with a B19 standard cone at one end. To reduce the scale of turbulence in the gauge tube two 70 mesh gauze discs D_1D_2 were inserted in the gauge tube at the inlet end.

When the gauge tube was mounted vertically (inlet end down) the filament being horizontal and perpendicular to the mean flow there existed zero fluctuations which were due to uninterrupted convection currents from the wire. When horizontal with the filament again horizontal the gauge took an appreciable time to settle down to a steady zero but this was not a true zero owing to local heating of the surrounds, convection being effectively nil. Keeping the filament

horizontal, a position for the gauge tube was found, approximately 40° to the vertical, in which there was no erratic behaviour and no zero drift other things being constant. It was henceforth used at this inclination and it was found that no discernible difference in behaviour or response was present after taking down and reassembly. There was a distinct difference in the character of the response curves in the neighbourhood of the origin for the vertical and horizontal positions of the filament. Slight changes from the horizontal had little if any effect. Changes from the vertical however had, particularly if the filament was sloping backwards to the flow. This was probably due to the fact that at low rates of flow the upper regions of the coil came under the influence of the slip-stream of the lower turns and this counteracted the effect of the actual air cooling: the net result was a rise in temperature with resultant negative deflection until the cooling due to the latter exceeded the heating due to the former. Response curves for the truly vertical arrangement had a steeper rise from the origin of the response curve (for slip-stream removal reasons) but took a little longer to settle down to a straight mid-section. It was obvious from consideration of the responses for the filament arrangements that it was an advantage to have it horizontal and henceforth this arrangement was adopted.

With the gauge tube inclined, what convection currents remained were additive to the main flow so that the deflections

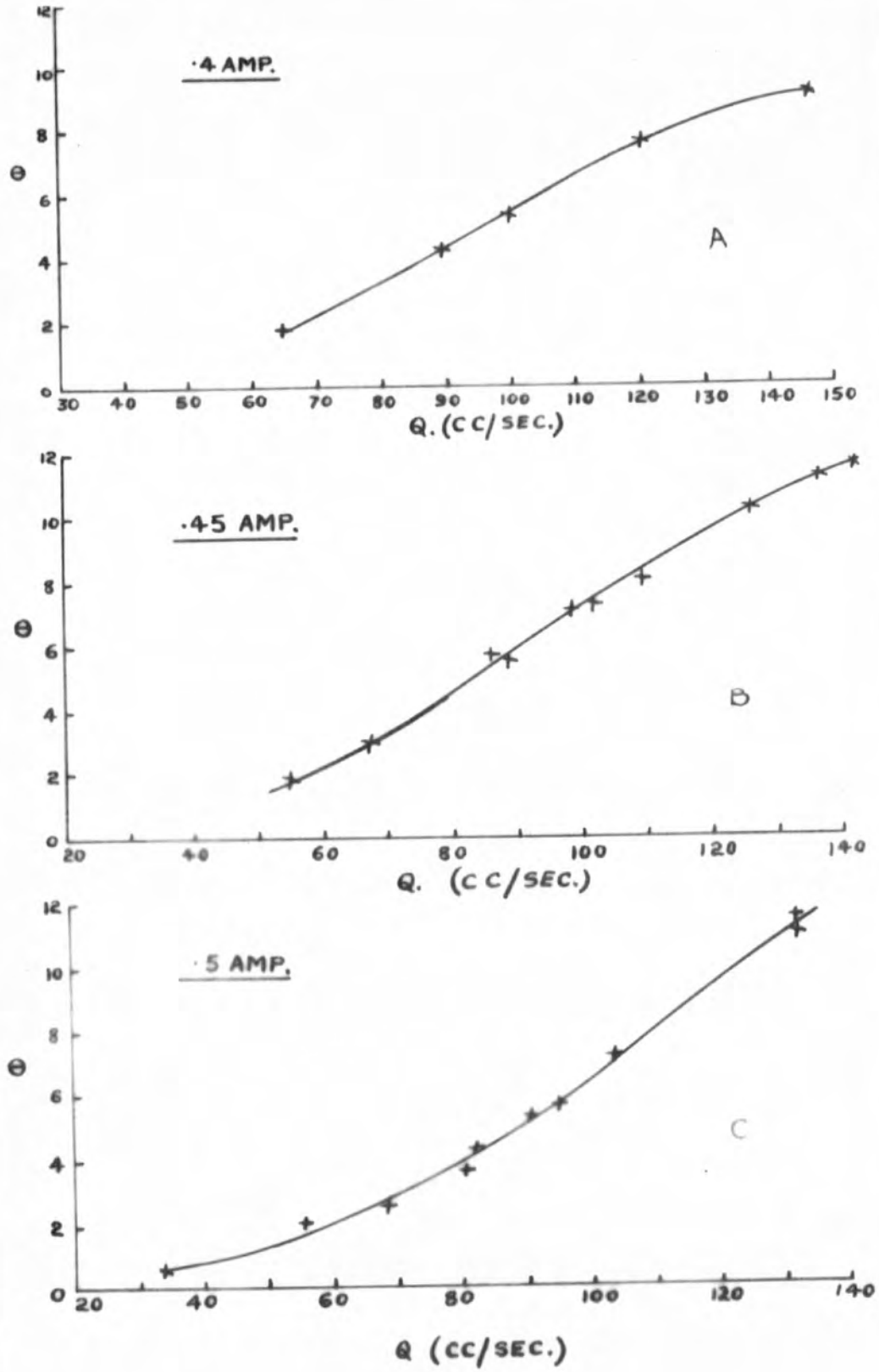

FIG. 3.10

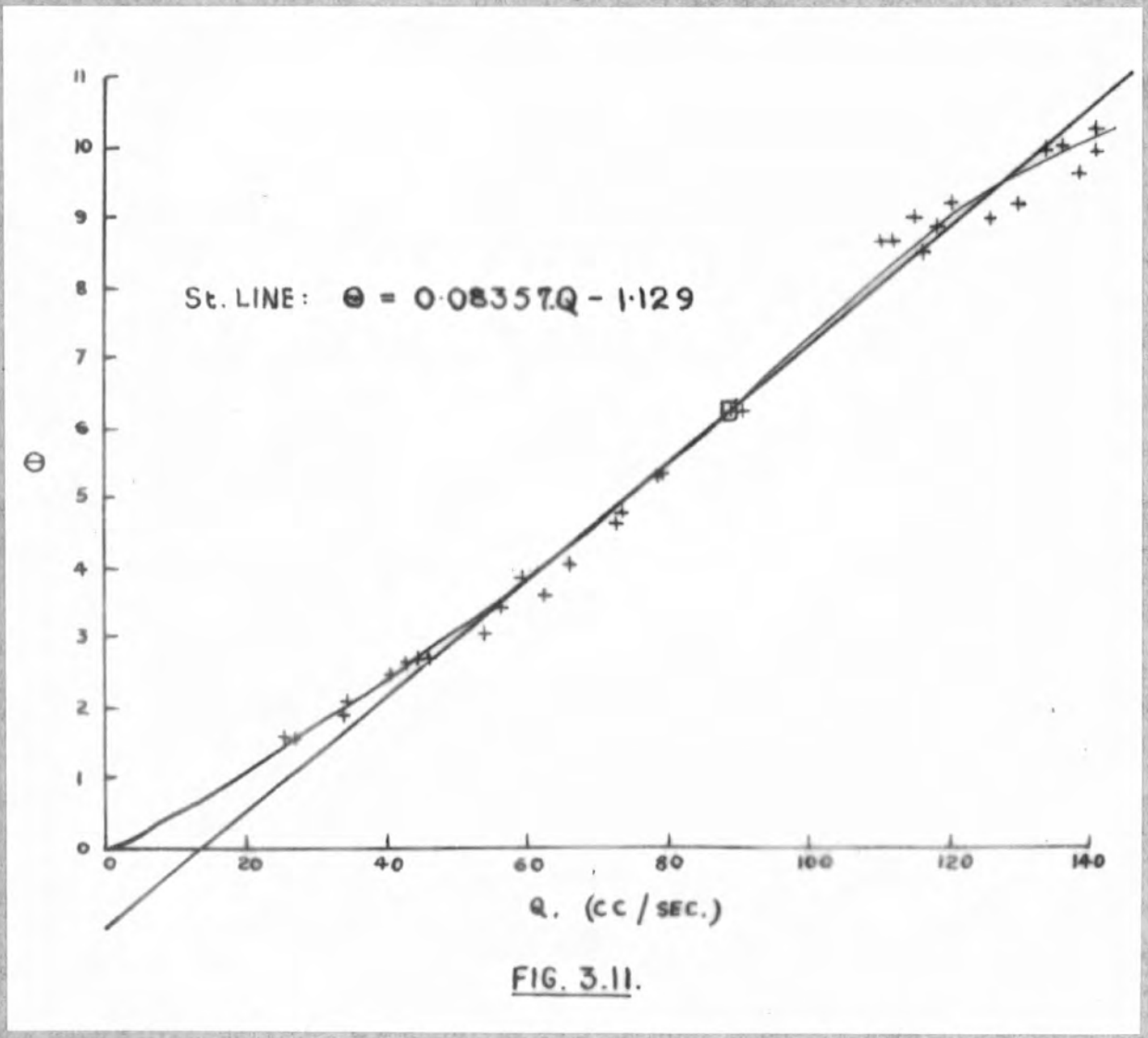
St. LINE: Θ = 0·08357Q - 1·129
Θ
Q. (CC / SEC.)
0
1
2
3
4
5
6
7
8
9
10
11
0
20
40
60
80
100
120
140

FIG. 3.11.

for given flow rates were increased with the result that the curve as a whole was moved towards the origin; a reduction in length of the low flow rate region of the response curve was the outcome. A comparison of the curves of fig. 3.10 a,b,c which were obtained with the gauge tube horizontal at 0.3, 0.45 and 0.5 amps, and that of fig.3.11 at 0.45 amps with the tube inclined at 40° to the vertical brings out this point.

For the curve of fig.3.11 the best straight line was computed for the mid-section by the method of least squares, assuming the values of Q to be known accurately, giving the line

$$\theta = 0.08357\ Q - 1.129$$

A series of quantitative flow calibrations was carried out, in a manner similar to that employed with other gauges, over a period of six days; the heating current was not switched off during this period. The relevant data is tabulated in Table 3.4.

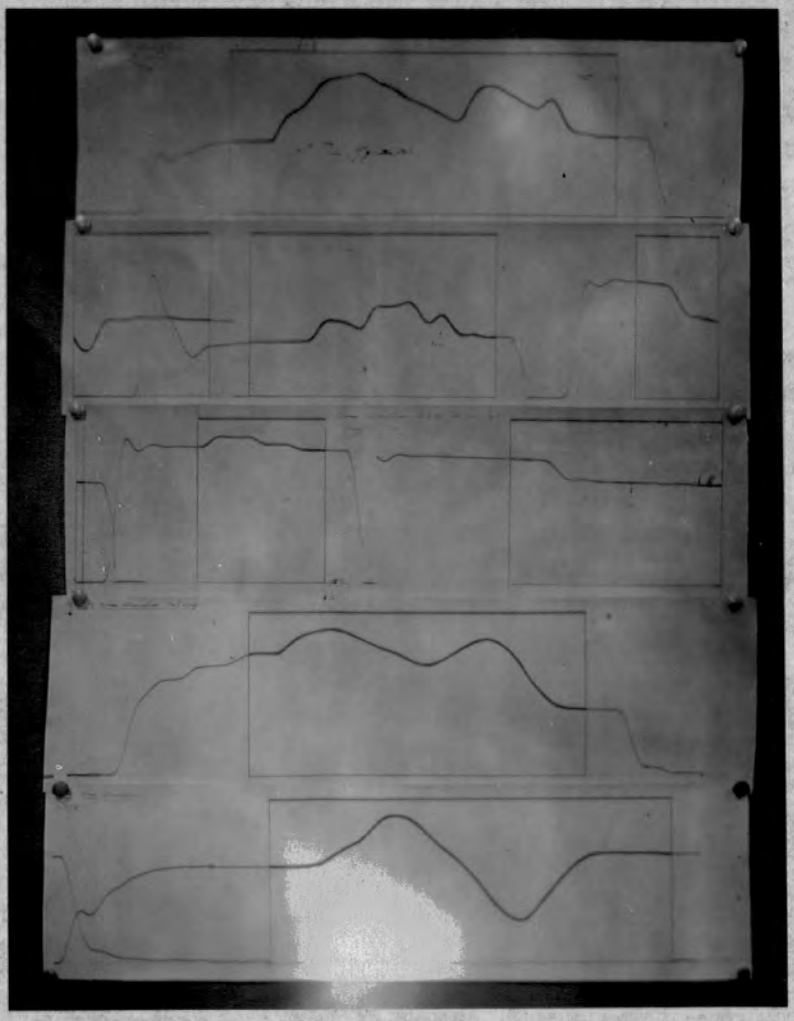

PLATE 3.4

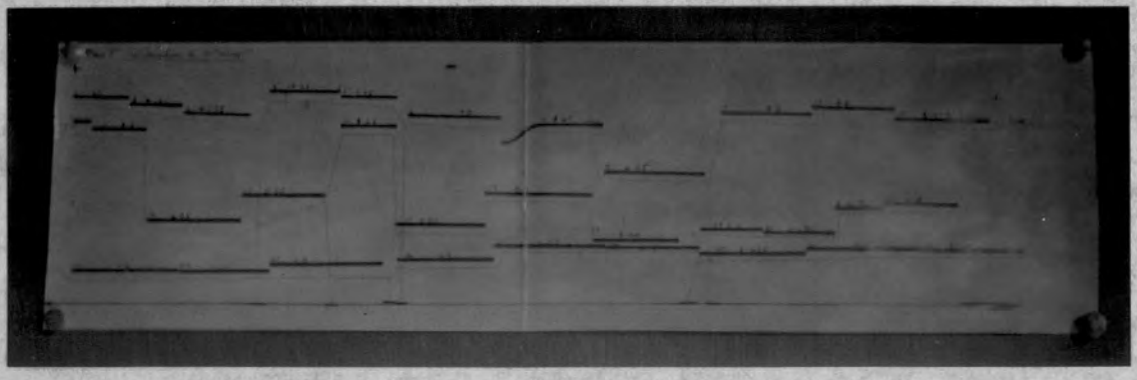

PLATE 3.5

TABLE 3.4

Cal.No.	L (cms)	A (sq.cms)	T (sec)	m	c	$\frac{A'.T}{m.L}$	Actual Q	%Error
a	28.55	236.56	32.2	0.08357	1.129	3,220	3,234	-0.43
b	23.95	224.88	28	"	"	3,154	"	-2.5
c	27.64	244.87	39.4	"	"	4,155	4,043	+2.8
* d	18.7	112.66	23.6	"	"	1,701	1,617	+5.2
e	16.7	114.44	20	"	"	1,617	"	0.0
* f	9.13	100.82	11.8	"	"	1,560	"	-3.5
g	16.6	145.04	19.2	"	"	2,008	2,022	-0.7

* (with these pairs of calibration runs the individuals of the pair were carried out in immediate succession on the same recording paper).

The records of the runs are shown on plate 3.4. In obtaining the calibration curves the drum camera and bridge galvanometer lanterns were switched on and off simultaneously. The low gearing of the motor and an incorporated electromagnetic clutch gave almost instantaneous stop and start. In this way the records traced for the various flow rates had the appearance of an irregularly battlemented line and a large number of short duration traces could be obtained on one sheet of recording paper for any calibration. These traces were easily separated into chronological order when the drum

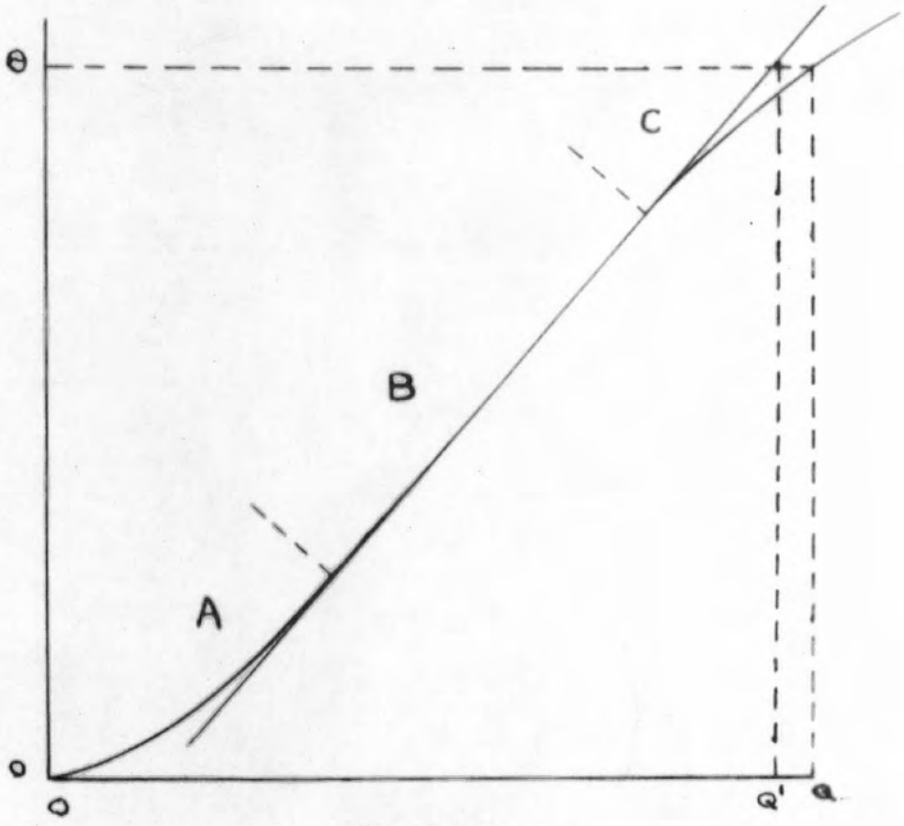

FIG. 3.12.

made more than one completed revolution provided the commencement of the calibration was indicated. This could be done by having a galvanometer lantern or datum lantern on without the drum camera motor and thereby producing an intense star at the start of or above the initial zero. The calibration of fig.3.11 was sorted out in this way and plate 3.5 shows the actual record in miniature, the faint lines were drawn on after development for convenience to indicate at a glance the order of the traces.

A typical θ/Q curve (a sloping letter S) with the computed straight line is shown diagramatically in fig.3.12 and it can be divided into three regions A,B, and C. For a quantitative calibration in which the rate of flow is predominantly in the 'B' region agreement between computed and actual total flow can reasonably be expected. In the upper portion 'C' a deflection θ corresponds to an actual flow rate Q, but according to the best straight line to Q' where $Q' < Q$. With Q constant for a time 't' seconds the calculated quantity of flow would be $Q't$, hence for comparatively large average flows computation can be expected to yield low results. Conversely, in region 'A', computation should yield high total flow, while a varying flow covering the whole region might be expected to have a measure of automatic compensation. In general, the results obtained were in accordance with this reasoning.

In all events such drastic changes of flow rate would not

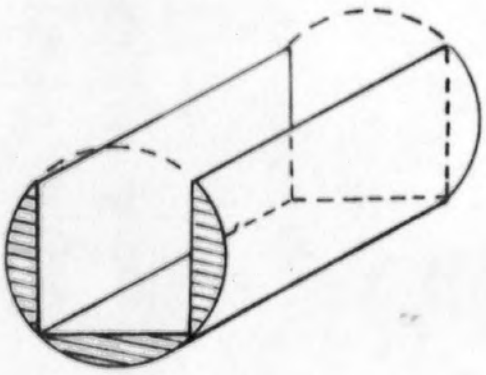

FIG. 3.13.

normally be employed, a fair representation of the actual flow could then be expected. Using the sequence of operations as given in the general apparatus chapter a cine record of, say, 'x' frames would be obtained. For the y^{th} frame from start, if the datum trace of the drum camera record be L cm long along the drum camera record, the flow rate corresponds to a point $\frac{x.L}{y}$ cms along L.

11. The Drum Camera.

The drum camera was constructed with a 6" diameter drum to take up to 18 cm wide bromide paper and was driven at constant though variable speed by means of a pully drive from a 1/10 hp series/series-parallel motor fitted with an electro-magnetic clutch.

The 7" length cylindrical lens of focal length approximately 3/4" was made of perspex from a 3/4" diameter perspex rod by cutting away the centre section of the rod along its length on a milling machine with a 1/2" side and face cutter as shown in fig.3.13. Three lenses were produced at the same time. Polishing was accomplished with metal polish and cotton wool after a preliminary rubbing with 00 wet or dry emery cloth to remove coarse machine marks.

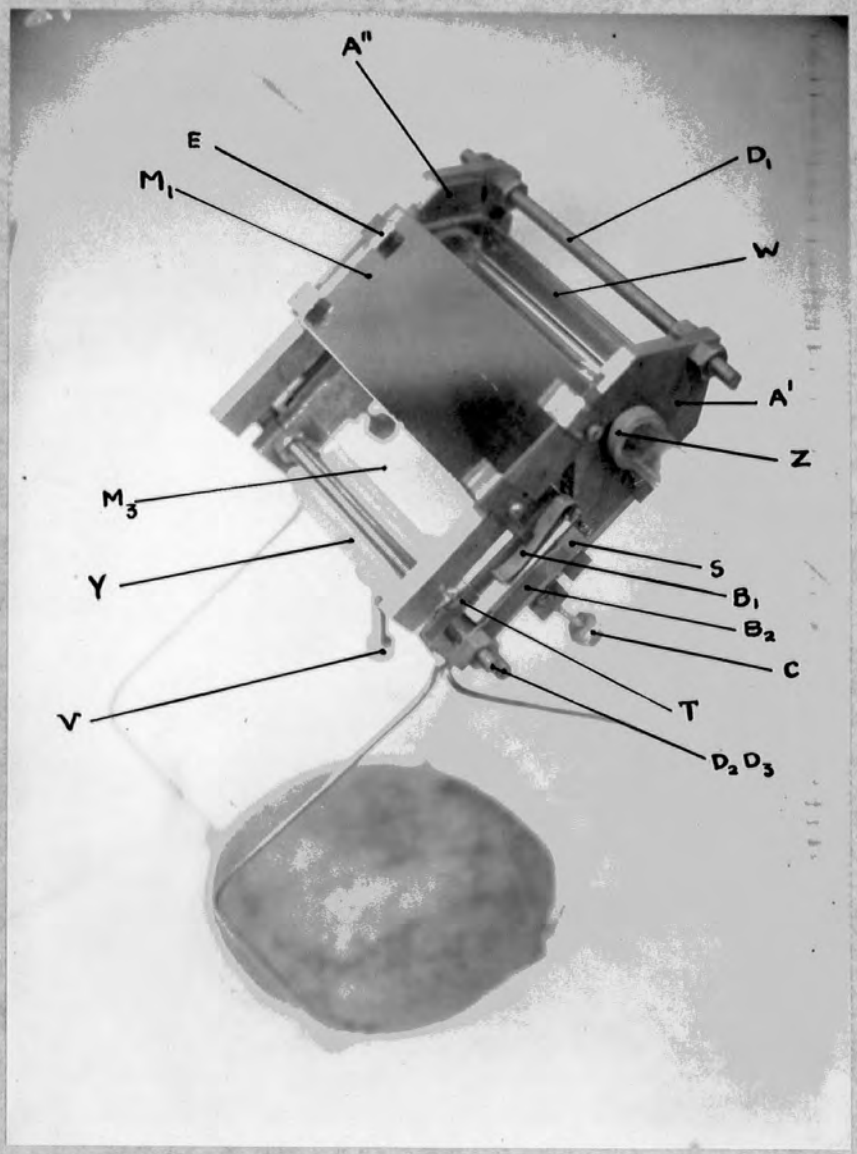

PLATE 4.1

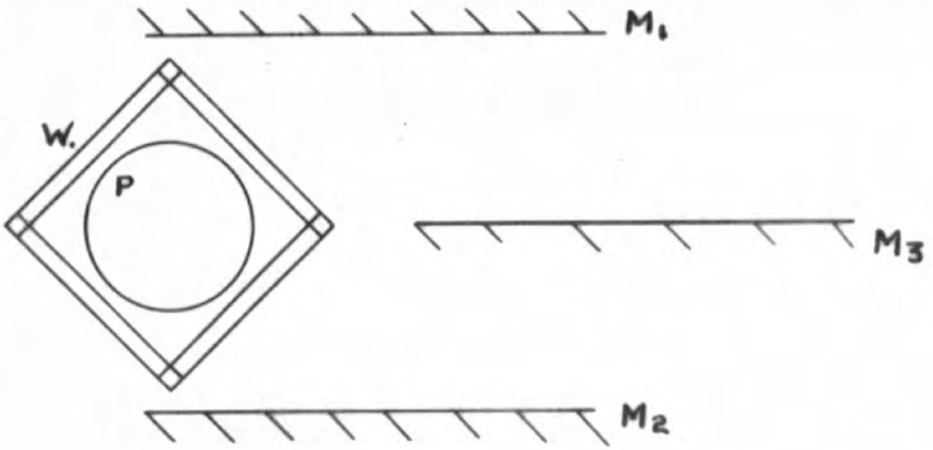

FIG. 4.1. THE MIRROR SYSTEM.

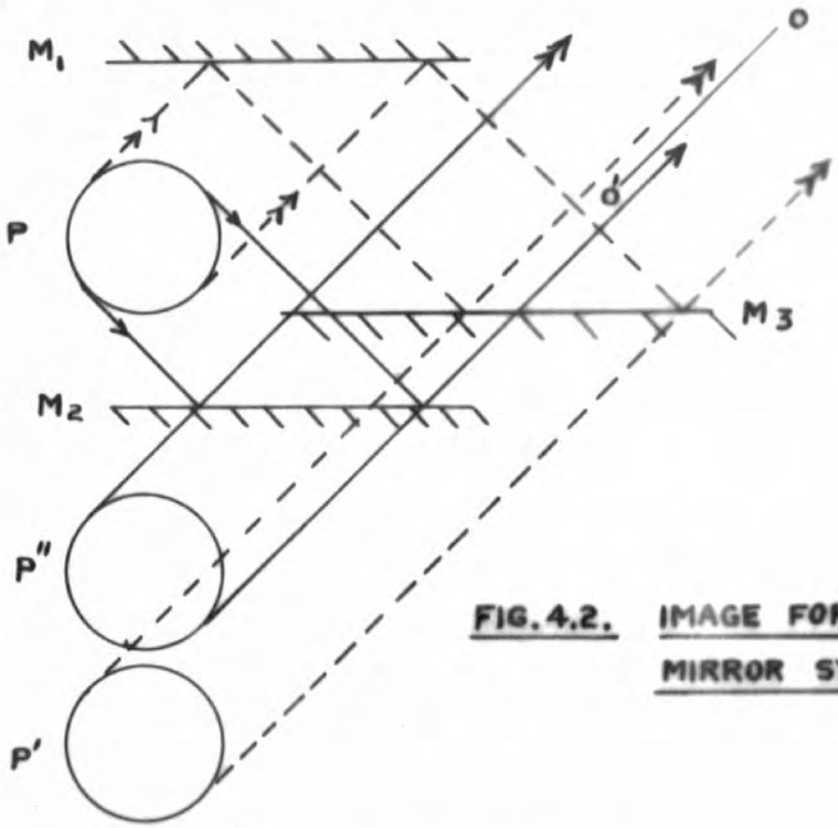

FIG. 4.2. IMAGE FORMATION BY MIRROR SYSTEM.

CHAPTER 4

THE OPTICAL SYSTEM

12. General.

The optical viewing system was designed in order that two views of the flow tube, from two directions mutually at right angles, could be seen simultaneously so that all components of velocity of the oil droplets could be computed from measurements on the images of the droplets as photographed from these two directions. The actual arrangement was such that the two images were parallel to each other, of the same size and superimposed; they thus appeared as a single image. A complete three-dimensional picture of events inside the flow tube was by these means obtainable. It was of no consequence that throat-injected streamers migrated from the position of injection; it was in fact desirable that dispersed streamers be used and the method of obtaining them is indicated above (Chapter 1, Section 3). From a single frame of the photographic record, then, provided that there were several droplets in the field of view on exposure, information could be obtained about the flow at several points, each at a different radius in the cross section of the pipe.

13. Mirror System.

A photograph of the mirror system is shown in plate 4.1 Figs. 4.1, 4.2 show the system diagramatically in cross section while in position surrounding the flow tube.

M_1 M_2 are fully aluminised surface reflecting mirrors

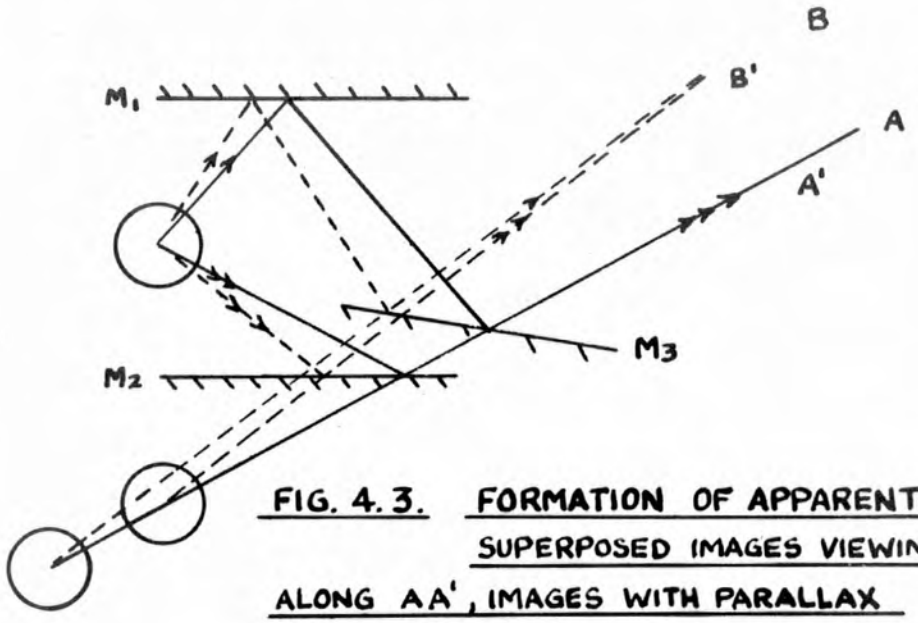

FIG. 4.3. FORMATION OF APPARENTLY SUPERPOSED IMAGES VIEWING ALONG AA', IMAGES WITH PARALLAX VIEWING ALONG BB'

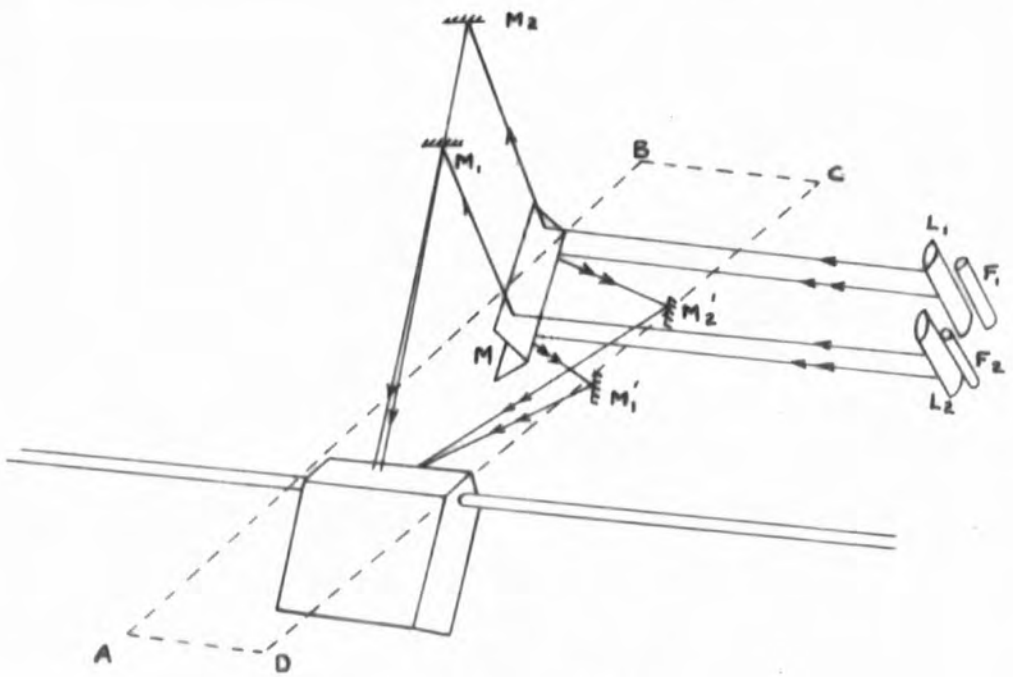

FIG. 4.3.a.

while M_3 is a partially reflecting mirror with approximately equal reflection and transmission coefficients at 45° incidence. P is a cross section of the pipe.

Two images of the pipe can be seen by observation along a direction OO', say, which appear in cross section as P'P". The construction lines for the edges of the pipe only are indicated.

In practice the three mirrors are parallel to each other and to the axis of the pipe in directions perpendicular to and in the plane of the paper. The movement of M_3 while maintaining these conditions alters the position of the image P', so that when the position of M_3 is such that the images P'P" are superimposed and when OO' is at 45° to M_3 the two images are two views of the pipe from two directions at right angles. With a fixed setting of M_1 and M_2 with the images superimposed, the geometry of the system readily shows that the light paths to M_3 from equivalent points of the pipe (mirror images of each other about M_3) are of equal length so that the two images are of equal size. This size is constant and is dependent on the positions of P and M_3 between M_1 and M_2 provided they are such as to superimpose P' and P", as the final images are always at the same distance from M_3.

Apparently superimposed images can be obtained when there is an assymetrical arrangement of M_3 (not parallel to M_1 M_2 in the plane of the paper), fig. 4.3. However, variation of the direction of viewing shows parallax to exist between them;

the images are also of different sizes. This property in particular was used when the system was being aligned, as there exists no parallax between the images when true alignment is achieved. With M_1 and/or M_2 partially blacked out the image of the pipe shows regions of approximately half intensity with sharp demarcation lines. At these lines relative visibility is good and consequently this blacking out greatly assists in the process of adjustment.

14. Construction.

The flow tube passes through A' and A", (Plate 4.1) these also carry the mirrors M_1 M_2 M_3. From considerations of symmetry of the system as a whole and for convenience in machining A' and A" the flow tube was arranged centrally between M_1 M_2.

The partially reflecting mirror M_3 rests upon two slides S, one on each end plate, which run in milled slots T and are held thereon by means of phosphor bronze spring strips B. Vertical adjustment of M_3 is achieved by manipulation of the spring loaded adjusting screws C. Further spring strips B_2 maintain the slides in the guiding slots T. D_1 D_2 D_3 are three mild steel rods of O.B.A. studding passing through the end plates and bolted tightly in position in accurately reamed holes thereby holding the system rigid, M_1 and M_2 being clipped on to the end plates by the clips E and being held parallel to each other. The two end plates were gang milled while pinned rigidly together through the studding holes. W is a square

section water jacket of perspex which fits into milled slots in the end plates and sealed therein by rubber gaskets. The walls of the jacket were at 45° to the mirrors and one pair normal to the direction of viewing. The jacket when full of water served to reduce the optical distortions inherent with viewing events inside an unjacketed fluid filled pipe and also to eliminate glare arising from the flow tube walls. The subject of the residual optical distortions is dealt with later.

In use the mirror system was inclined at an angle of 45° to the horizontal allowing the cine camera to be horizontal and resulting in greater simplicity of adjustment of the stroboscopic illumination, the beams from which were then in vertical and horizontal planes respectively, fig. 4.3a. (ABCD is the horizontal plane). To achieve this alignment the mirror system was supported on a stiff wire framework (plate 4.1) having a vertical adjusting screw V which fitted into a recess in a wooden block Y, in a slot in which rested the lower of the three O.B.A. spacing rods. The mirrors could thus be pivoted about the flow pipe in the rubber sealing washers Z until the 45° alignment was attained.

Partially reflecting mirrors were made in a vacuum evaporation apparatus, which was constructed in a large glass belljar. A trial and error method was used to obtain the desired 50% reflectivity and this was determined by measuring the intensity of the light reflected at 45° and that transmitted

with a simple selenium cell photometer. Owing to the simplicity of the vacuum system it was not possible to obtain similar mirrors by evaporating equal amounts of aluminium wire, as repeatable vacuum conditions could not be guaranteed. Aluminium was used in preference to silver as such mirrors were less subject to change with age due to tarnishing and oxidation. A very thin film of passive oxide forms on the aluminium which increases its durability without affecting the reflecting powers of the mirror.

Good quality glass was used for the mirrors which, before the deposition process had to be scrupulously cleaned. Prolonged washing with a detergent and rinsing, using glass distilled water throughout, ensured a fair degree of cleanliness. For the chemically deposited silver films the glass was not dried before immersion in the silvering solution and mirrors, though difficult to obtain correctly silvered, were achieved tenacious enough to allow gentle dusting with cotton wool. It was not long, however, before these mirrors became useless owing to tarnishing. Glass to be aluminised was cleaned as above, dried with degreased linen and just prior to placing in the bell jar beaten and wiped with clean silk which electrostatically removed any dust etc. A final cleaning was carried out in the bell jar during evacuation by bombardment with ions produced by a glow discharge.

15. Principle of Observation.

The principle employed in the observation of the streamers

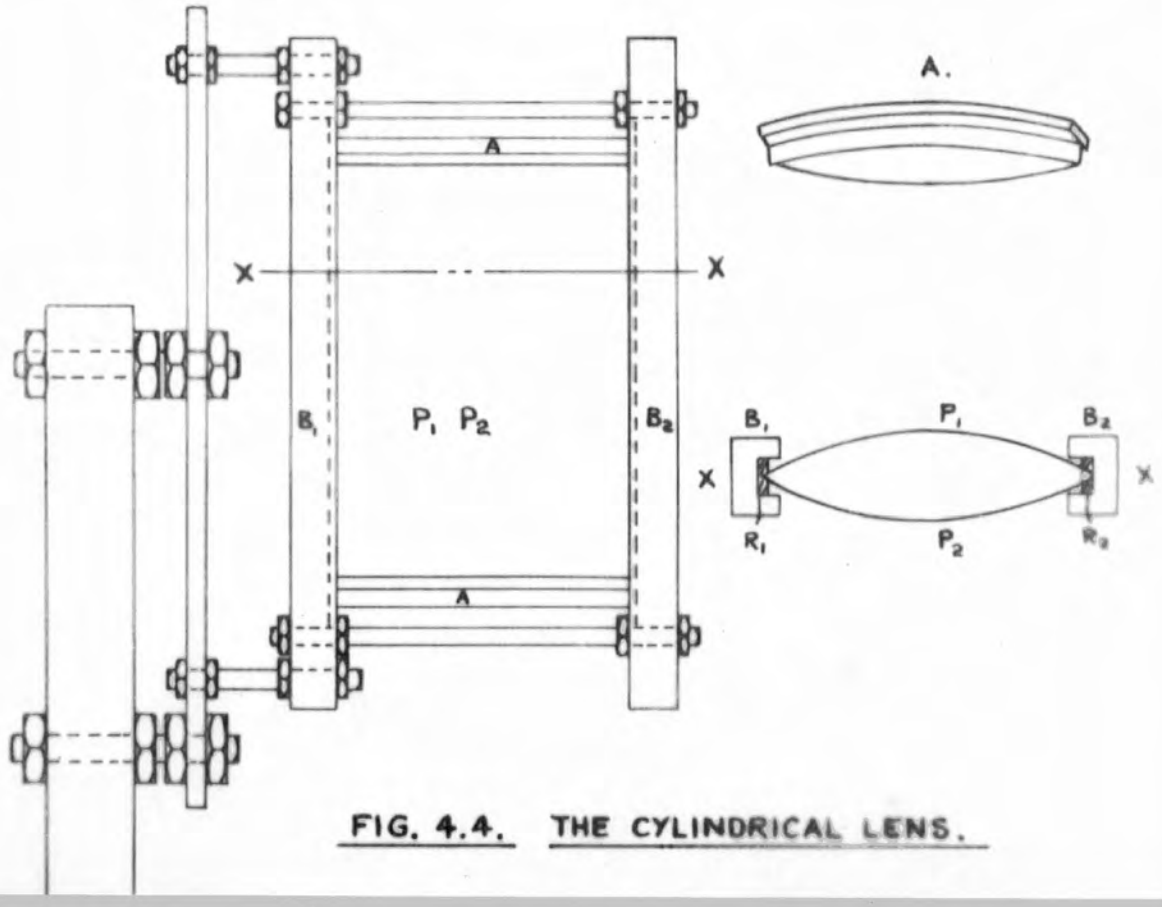

FIG. 4.4. THE CYLINDRICAL LENS.

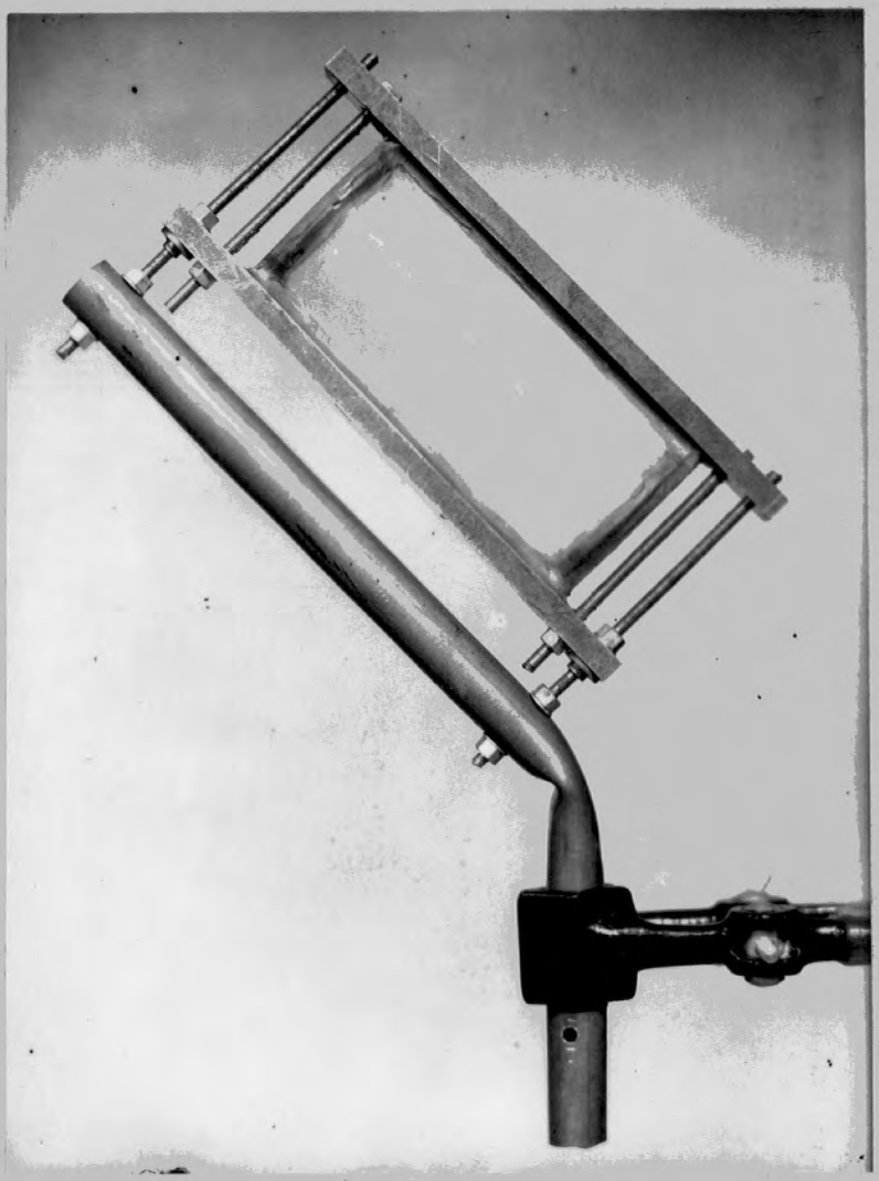

PLATE 4.2

was that of the ultra-microscope, though the droplets were in fact large enough for direct observation.

The light from the flash tubes F_1 F_2 fig 4.3a was rendered slightly convergent by means of large cylindrical lenses L_1 L_2 so that it could be concentrated on to the flow tube. The two beams were split by inclined mirrors M and thence suffered further reflections from M_1 M_1' M_2 M_2' and finally illuminated the tube. The beams from M_1 M_2 were at right angles to the plane containing the beams from M_1' M_2', this gave symmetrical vertical and horizontal illumination which was in fact slightly oblique to the line of viewing hence prevented direct reflection of light into the recording camera. M_1 M_1' M_2 M_2' could be rotated about three orthogonal axes thus facilitating adjustment.

The droplets appeared as pin points of light and the system viewed them from two directions at right angles to the incident illumination. Sufficient light was reflected from the surfaces of the droplets to produce an image that could be photographed, so that a benzene/carbontetrachloride mixture could be used in place of olive oil and nitro-benzene.

16. Cylindrical Lenses.

The lenses fig.4.4, plate 4.2, were constructed from two sheets of perspex $2\frac{1}{8}$" x 4" x 1/32", P_1 P_2, clamped between two rectangular section brass rods B_1 B_2 on rubber strips R_1 R_2 inlet into the rods. The ends were sealed by shaped end pieces A and plasticine, the inner space being filled with water.

For any desired focal length, the necessary radii of curvature followed immediately knowing the refractive index of water and the end pieces were constructed accordingly, in this instance of perspex. B_1 and B_2 were spaced on two lengths of 4 B.A. brass studding which also served the purpose of varying the perspex curvature and hence focal length.

Unfortunately the perspex sheets acquired after some time a curvature greater than that into which they were originally bent, the sealing pressure on the rubber strips was thus reduced and leaks ensued. This was, however, anticipated and as an added precaution plasticine was added to the seals which adhered rather tenaciously to the perspex and flowed with it, automatically sealing leaks to a large extent. This warping was attributed to two causes:

(a) an uneven absorption of water by the perspex which undoubtedly reduced its rigidity and

(b) a slow plastic or viscous flow.

The deformation was found difficult to remove other than by prolonged pressure or the application of a reverse curvature.

Crazing on the surface of the perspex due to the water was largely eliminated by carefully finishing the surfaces with prolonged polishing using metal polish and cotton wool.

The lenses were periodically dismantled and the perspex sheets reversed upon assembly rather than attempting to flatten them.

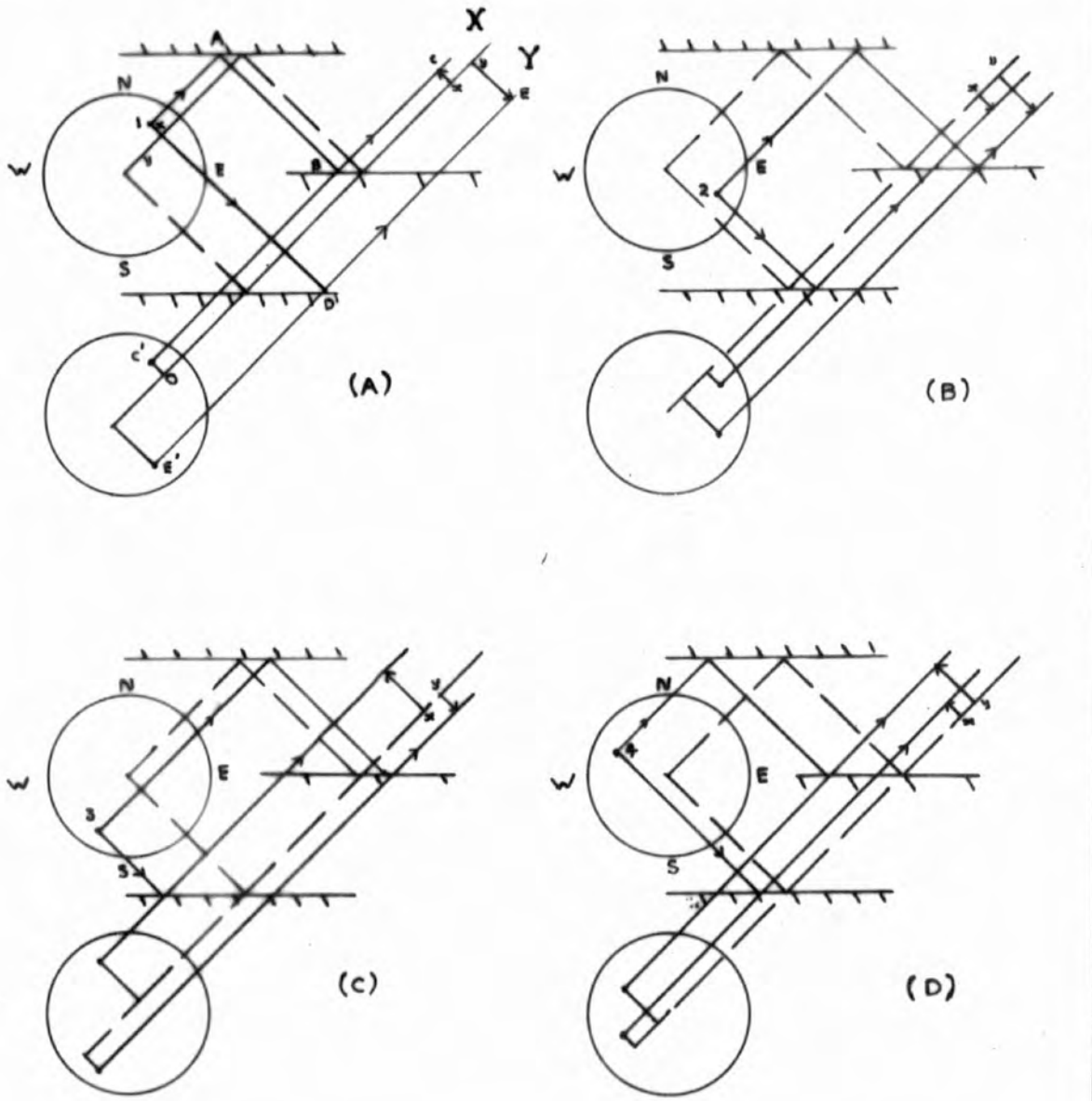

FIG.4.5. IMAGE POSITIONS FOR DROPLETS IN ALL QUADRANTS OF TUBE SECTION.

17. Operation of the Optical System.

Fig.4.5 A.B.C.D shows schematically the arrangement of the mirrors of the optical system about the flow tube section, wherein the cross section of the pipe is divided into four quadrants labelled N,E,S and W. It is assumed that the mirrors have been adjusted for parallelism and that the direction of viewing is at 45^{o} to the mirrors as indicated by the arrows. Thus two images of the flow pipe are superposed. These images are two views from two directions at right angles to each other.

Consider the droplet No.1 in the N quadrant, fig.4.5 A. The images C' and E' associated with the droplet are observed one vertically above the other after the light scattered from the droplet has traversed paths for the upper and lower images respectively of 1-A-B-C and 1-D-E, and appear to have come from C' and E' in the image pipe. The distances C'O, E'O of the images from the axis of the photographed image of the pipe can be seen to be the 'x' and 'y' coordinates of the original drop (except for a scale factor and corrections) with respect to axes parallel and perpendicular to either light path and with a z-axis along the axis of the pipe. From the measured values of C'O and E'O the radial distance of the droplet, r say, from the axis of the flow tube can, after corrections have been applied, be calculated simply from

$r = (C'O_1'^2 + E'O_1'^2)^{\frac{1}{2}}$ the subscript dash denoting corrected values.

PLATE 4.3a

PLATE 4.3 b

PLATE 4.4

The droplet 2 in the east quadrant can be seen from the construction lines to have an x and y both on the same side of the axis of the image pipe. Droplet 3 in the S quadrant (C) has again images one on either side of the axis similar to droplet 1. Droplet 4 in the W quadrant (D) results again in a pair of images on the same side of the axis but in this case they are on the opposite side from that in which the images associated with droplet 2 (B) lie. A droplet in the pipe on the same plane as that of the partially aluminised mirror has equal and coincident x and y images and thus they appear to be but one image.

Plate 4.3 is an enlarged photograph of superposed images of the flow tube through which water containing suspended droplets was flowing. The droplets appear as stationary dots since the photograph was taken with stroboscopic illumination consisting of two short light flashes a known time interval apart. Twenty dot images can be seen which can be segregated into five groups of four, each set of four corresponds to one original droplet and the four images of each set lie on the corners of different sized rectangles. Knowing the time interval between the two flashes the longitudinal and radial velocities can be obtained from the longitudinal measurements of the rectangles and the radial positions which can be computed as indicated above. Plate 4.3,a is a negative of plate 4.3.b The droplets are clearly visible but the tube walls are no longer distinguishable.

It can be seen that there exists in some cases a small amount of parallelogram or trapezium distortion associated with a set of four images. From fig.4.5 A,B,C,D, it is apparent that the images can be at slightly different distances from the recording camera. A plan view containing the direction of viewing would show that a certain amount of parallax may exist between the images with respect to the camera. The effect is small and the lengths of the sides of the parallelograms are effectively the same so that in analysing the photographs the lengths of one side only was measured the side being chosen which had the best definition. A difference of intensity assisted in fixing exactly, as will be shown later, in which quadrants the droplets were for the ambiguous case of the N S quadrants.

The existence of any divergence from parallelism between the pipe centre and the line joining the images is indicative of either the flow being other than laminar or of interference between nearby droplets. To determine which of these causes resulted in any deformation from true rectangles it was only necessary to examine the preceding and succeeding frames of the record for a persistance of the same condition. To reduce interference between droplets, the number in suspension was reduced at the reservoir.

The parallelogram distortion can occur in either sense, i.e. the parallelogram can lean either way dependent upon whether the upper or lower images are nearer the camera.

In the case of truly turbulent flow, in order to ensure that it should be possible to differentiate between images of different droplets, as in this case they lie in general upon the corners of trapezia, it is necessary to restrict the interval between the two exposures to a small value. Corresponding images can thus be distinguished and hence average components of velocity u,v,w (axial, radial and circumferential respectively) of the flow can be computed. Thus from an experiment at either constant or varying flow rate both temporal and spacial correlations between each or all of u,v,w can be obtained. It was hoped to carry out such an investigation though time restriction prevented it.

To determine the datum line (the position of the centre of the flow tube image), the tube was photographed just before a run against an illuminated white background which had the effect of intensifying the definition of the tube walls which appeared as black lines. The distances of these lines from one edge of the negative (the reference edge) were measured, and the everage of the two measurements positioned the flow tube axis. Plate 4.4 is an enlargement of one such photograph though a large amount of definition has been lost in the process of reproduction. Thus, in determining the co-ordinates of the images their positions relative to the reference edge of the negative were measured; the differences between these measurements and the distance of the tube axis from the reference edge gave the required x's and y's. It was essential in order

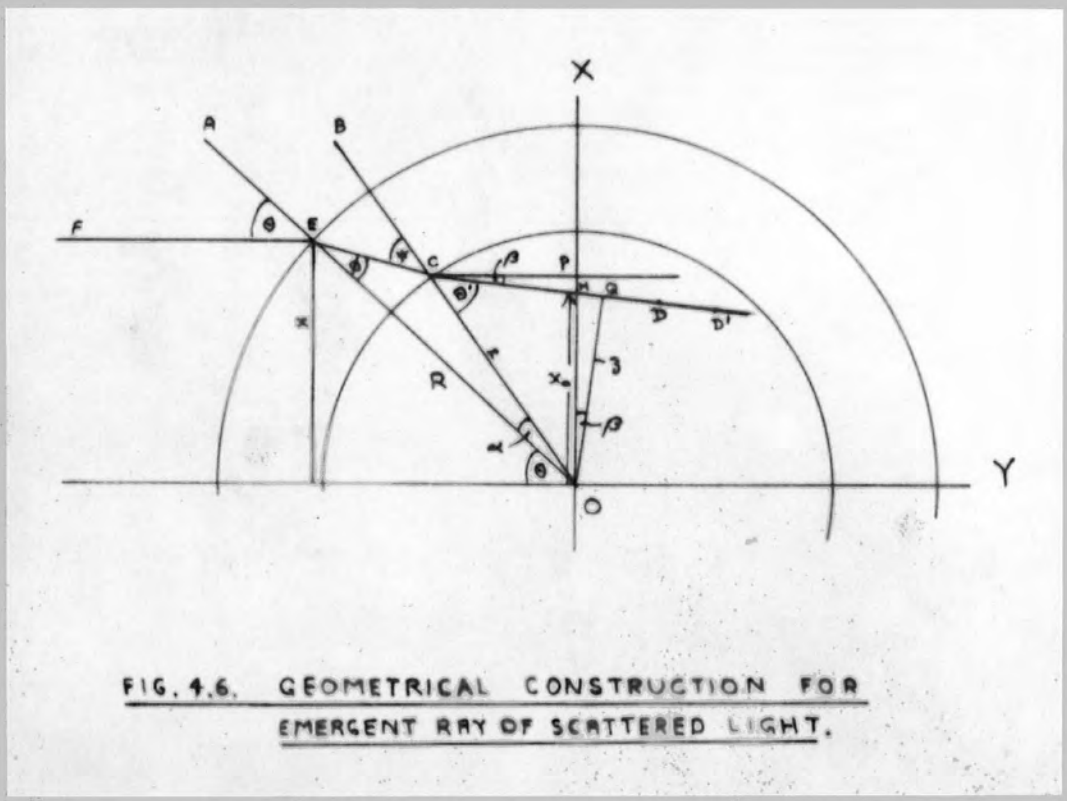

FIG. 4.6. GEOMETRICAL CONSTRUCTION FOR EMERGENT RAY OF SCATTERED LIGHT.

to maintain focus and the same scale factor for each frame of the record that there was no movement of the flow tube relative to the camera during a run. To ascertain whether or not there had been any such movement the determination of the tube centre was repeated at the end of the record.

18. Residual Corrections for Refraction at the Flow Tube Walls.

The droplets scatter light in all directions and among the pencil of rays incident upon the camera which together produce the final image upon the film, there will be one, which, after refraction at the two water/glass surfaces, emerges and is incident normally upon the perspex water jacket and thence passes undeviated through to the camera. Another similar ray from the same droplet will, after undergoing similar refractions emerge from the water jacket at 90° to the first ray and in the same plane, i.e., that of the flow tube cross section containing the droplet. From the principal of reversibility of light, then two rays originating at the camera and in identical positions to the above two rays would intersect inside the flow tube in a position which, if it were a light source, would produce the two postulated rays. Hence it is a sufficient condition in determining the true positions of the droplets from the measured co-ordinates that only two such rays need be considered.

Fig. 4.6 represents a cross section of the pipe and the construction of a ray, from a droplet at D, which after refractions emerges parallel to the direction of viewing.

The angles at O, P and Q are 90°; OA, OB are the

normals for the outer and inner surfaces of the pipe respectively at the points of incidence; x is the measured co-ordinate on the negative, corrected for the scale factor which is obtained as the ratio of the actual to photographic external diameter of the flow tube. R and r are the outer and inner radii of the flow tube respectively; θ and ϕ respectively the angles of incidence and refraction at the outer water/glass surface and ψ and θ' those for the inner surface.

It is convenient to calculate the intercept on the vertical axis OX made by the line CD' for any position from which a droplet could produce the emergent ray EF. This intercept is called x_o, the subscript zero being used to indicate that value of the real x in the flow tube for which the droplet has a value of zero for its corresponding y co-ordinate. (For this particular droplet at D there would be a similar y_o on the horizontal OY axis if the emergent ray perpendicular to EF were considered).

In the triangle OHQ (OQ = z)

$$x_o = \frac{z}{\cos\beta}$$

and from triangle OCQ

$$z = r.\sin\theta'$$

$$\therefore \quad x_o = \frac{r.\sin\theta'}{\cos\beta} \qquad \ldots\ldots\ldots\ldots\ldots\ldots\ldots\ldots (4.1)$$

At the inner surface $\sin\theta' = \mu.\sin\psi$ where $\mu = \frac{\mu(\text{glass})}{\mu(\text{water})}$

$$\therefore \quad x_o = \frac{r.\mu.\sin\psi}{\cos\beta} \qquad \ldots\ldots\ldots\ldots\ldots\ldots\ldots\ldots (4.2)$$

In triangle OEC

$$\frac{r}{\sin\phi} = \frac{R}{\sin(180 - \psi)} = \frac{R}{\sin\psi}$$

$$\therefore \quad \sin\psi = \frac{R.\sin\phi}{r} \qquad \ldots\ldots\ldots\ldots\ldots\ldots\ldots\ldots\ldots\ldots (4.3)$$

$$\therefore \quad x_o = \frac{r.\mu.\ R.\sin\phi}{r.\cos\beta} \qquad \ldots\ldots\ldots\ldots\ldots\ldots\ldots\ldots\ldots\ldots (4.4)$$

and at the outer surface $\sin\theta = \frac{x}{R} = \mu.\sin\phi$

i.e. $\sin\phi = \frac{x}{\mu.R}$

$$\therefore \quad x_o = \frac{\mu.R.x.r}{r.\mu.R.\cos\beta}$$

$$x_o = \frac{x}{\cos\beta} \qquad \ldots\ldots\ldots\ldots\ldots\ldots\ldots\ldots\ldots\ldots (4.5)$$

(i.e. $x = z$)

<u>The value of β.</u>

For every x ($0 \leqslant x \leqslant R$) there exists a θ and a $\sin\theta = \mu.\sin\phi$ i.e. $\theta = \sin^{-1}(\mu.\sin\phi) = \sin^{-1}\frac{x}{R}$ and working back from θ all the angles ϕ, ψ and θ' can be determined in terms of μ, x, r and R.

Thus,

$$\phi = \sin^{-1}\left(\frac{x}{R.\mu}\right)$$

and from (4.3)

$$\psi = \sin^{-1}\frac{(R.\sin\phi)}{r} = \sin^{-1}\left(\frac{R.\ x}{r.\mu.R}\right)$$

i.e. $\psi = \sin^{-1}\left(\frac{x}{\mu.r}\right)$.

and $\sin\theta' = \mu.\sin\psi$

$$\therefore \quad \theta' = \sin^{-1}\left(\frac{x}{r}\right) \qquad \ldots\ldots\ldots\ldots\ldots\ldots\ldots\ldots\ldots\ldots (4.6)$$

Alternatively, using the result of (4.5) i.e. $x = z$, θ' and ψ can be simply found.

TABLE 4.1

'x'	θ o,',,"	ϕ o,',,"	θ' o,',,"	ψ o,',,"
0. 1	7.46.28	6.54.29	9.12.48	8.11.9
0.2	15.42.08	13.55.10	18.40.31	16.32.14
0.3	23.57.00	21.09.15	28.42.23	25.16.34
0.4	32.46.12	28.45.43	39.49.28	34.41.57
0.5	42.34.43	36.58.14	53.11.00	45.21.55
0.53	45.49.30	39.36.24	58.03.30	48.57.44
0.57	50.28.18	43.17.05	65.52.00	54.12.53
0.6	54.17.07	46.11.50	73.52.15	58.38.15
0.6246	57.41.30	48.42.06	90,00,00	62.44.09

TABLE 4.2

'x'	α o,',,"	β o,',,"	Cos β	Tan β	$\theta-\theta'$ (negative)
0.0	0. 00.00	0.00.00	1.00000	0	0
0.1	1. 16.40	0.09.40	1.00000	0.00281	1.26.20
0.2	2.37.04	0.21.19	0.99999	0.00621	2.58.23
0.3	4.07.18	0.38.05	0.99995	0.01105	4.45.23
0.4	5.56.24	1.06.52	0.99982	0.01946	7.03.16
0.5	8.23.14	2.12.36	0.99925	0.03857	10.36.17
0.53	9.21.20	2.52.40	0.99875	0.05028	12.14.00
0.57	10.55.48	4.27.54	0.99696	0.07810	15.23.42
0.6	12.26.25	7.08.43	0.99223	0.12537	19.35.08
0.6246	14.02.03	18.16.27	0.94956	0.33021	32.18.30

TABLE 4.3

'x'	$x_o = \frac{x}{\cos\beta}$	$x_o - x$
0.0	0.0	0.0.
0.1	0.1	0.0.
0.2	0.2	0.0
0.3	0.3	0.0
0.4	0.40006	0.00006
0.5	0.50037	0.00037
0.53	0.53065	0.00065
0.57	0.57173	0.00173
0.6	0.6047	0.0047
0.6246	0.6578	0.0332

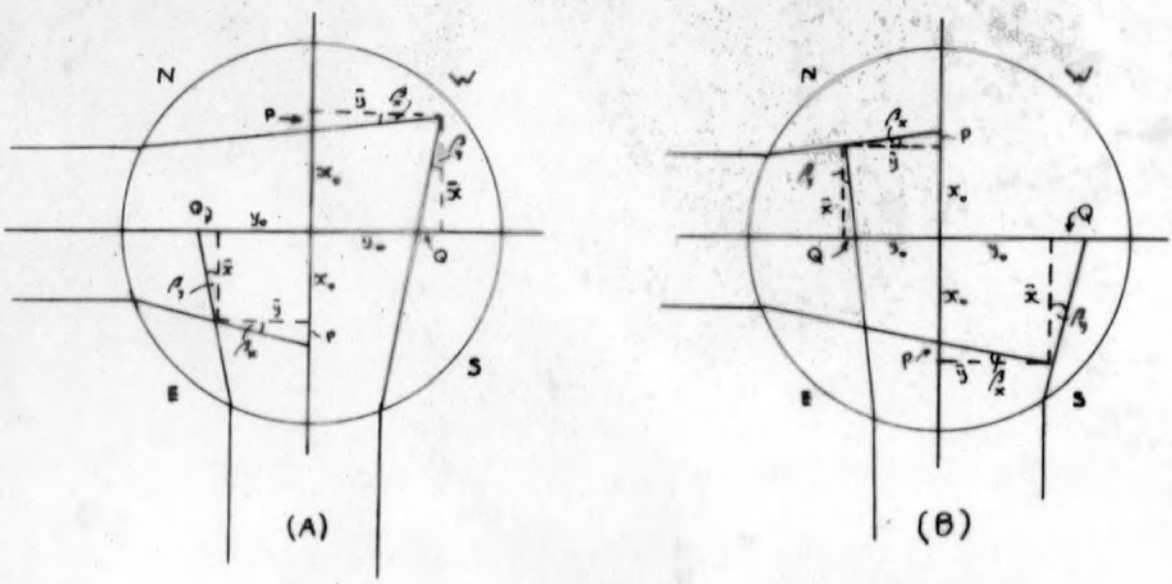

FIG. 4.7. GEOMETRICAL CONSTRUCTION FOR CORRECTIONS TO x_o, y_o FOR ALL QUADRANTS.

Thus,

$$\text{Sin } \theta' = \frac{x}{r}, \quad \theta' = \text{Sin}^{-1} \frac{x}{r}$$

and $$\text{Sin } \theta' = \mu . \text{Sin} \psi, \quad \psi = \text{Sin}^{-1} \left(\frac{x}{\mu . r} \right)$$

Now as OY is parallel to CP

$$\theta' + \beta = \theta + \alpha \quad (\text{and } \alpha = \psi - \phi)$$

$$\therefore \beta = (\theta - \theta') + \alpha \qquad \ldots\ldots\ldots\ldots\ldots\ldots\ldots\ldots\ldots\ldots (4.7)$$

Tables 4.1 and 4.2 give the values of θ, ϕ, ψ, θ' and α, β, $(\theta - \theta')$, $\text{Cos}\beta$, $\text{Tan}\beta$ respectively. Table 4.3 gives the values of $x/\text{Cos}\beta$ and $x_o - x$ for values of x from 0 to 0.6246 cm which was the estimated internal diameter of the flow tube.

It can be seen from table 4.2, that $\theta' > \theta + \alpha$ i.e. CD' in fig 4.6 is directed away from the horizontal in actual fact and not as indicated in the figure, so that the system F.E.C.H.D' is slightly divergent.

It is the exception for a droplet to lie on either of the axes OX or OY of fig 4.6 and so in very few cases are the values of x_o the real co-ordinates of the droplet. Consider the general case of droplets in the W and E quadrants, as labelled in fig 4.5, and with the angular and x_o y_o notation of fig 4.6. Fig. 4.7 A is a section of the pipe, drawn as a single line, containing a droplet in each of the W and E quadrants. The diagram is exaggerated. It should be noted that the distortions due to refraction in no case cause a droplet to appear in any quadrant other than the actual one. This follows from consideration of symmetry, or the principle

of least time; otherwise, the system would be both divergent and convergent. The true co-ordinates are called $\bar{x}$ and $\bar{y}$

W Quadrant

For a droplet in the W quadrant (Fig 4.7A).

$$\bar{x} = x_o + P$$

$$= x_o + \bar{y}.\text{Tan}\beta_x$$

$$= x_0 + \text{Tan}\beta_x.\ (y_o + \bar{x}.\text{Tan}\beta_y)$$

$$\therefore\ \bar{x} = \frac{x_o + y_o.\text{Tan}\beta_x}{1 - \text{Tan}\beta_x.\ \text{Tan}\beta_y} \qquad \ldots\ldots\ldots\ldots\ldots\ldots(4.8)$$

and by virtue of symmetry,

$$\bar{y} = \frac{y_o + x_o.\text{Tan}\beta_y}{1 - \text{Tan}\beta_x.\text{Tan}\beta_y} \qquad \ldots\ldots\ldots\ldots\ldots\ldots\ldots\ldots(4.9)$$

E Quadrant

Similarly for a droplet in the E quadrant (fig 4.7A)

$$\bar{x} = x_o - P$$

$$= x_o - \bar{y}.\text{Tan}\beta_x$$

$$= x_o - \text{Tan}\beta_x(y_o - \bar{x}.\text{Tan}\beta_y)$$

$$\therefore\ \bar{x} = \frac{x_o - y_o.\text{Tan}\beta_x}{1 - \text{Tan}\beta_x\text{Tan}\beta_y.} \qquad \ldots\ldots\ldots\ldots\ldots\ldots\ldots(4.10)$$

and by symmetry

$$\bar{y} = \frac{y_o - x_o.\text{Tan}\beta_y}{1 - \text{Tan}\beta_x.\text{Tan}\beta_y} \qquad \ldots\ldots\ldots\ldots\ldots\ldots\ldots\ldots(4.11)$$

N Quadrant

For a droplet in the N quadrant (Fig 4.7B)

$$\bar{x} = x_o - P$$

$$= x_o - \bar{y}.\text{Tan}\beta_x$$

$$= x_o - \text{Tan}\beta_x(y_o + \bar{x}.\text{Tan}\beta_y)$$

$$\therefore\ \bar{x} = \frac{x_o - y_o.\text{Tan}\beta_x}{1 + \text{Tan}\beta_x\text{Tan}\beta_y} \qquad \ldots\ldots\ldots\ldots\ldots\ldots\ldots(4.12)$$

and

$$\bar{y} = y_o + Q$$

$$= y_o + \bar{x}.\mathrm{Tan}\,\beta_y$$

$$= y_o + \mathrm{Tan}\,\beta_y(x_o - \bar{y}.\mathrm{Tan}\,\beta_x)$$

$$\therefore \quad \bar{y} = \frac{y_o + x_o.\mathrm{Tan}\,\beta_y}{1 + \mathrm{Tan}\beta_x.\mathrm{Tan}\beta_y} \qquad \ldots\ldots\ldots\ldots\ldots\ldots\ldots\ldots(4.13)$$

S Quadrant

Similarly for a droplet in the S quadrant (Fig.4.7B)

$$\bar{x} = x_o + P$$

$$= x_o + \bar{y}.\mathrm{Tan}\beta_x$$

$$= x_o + \mathrm{Tan}\beta_x.(y_o - \bar{x}.\mathrm{Tan}\beta_y)$$

$$\therefore \quad \bar{x} = \frac{x_o + y_o.\mathrm{Tan}\,\beta_x}{1 + \mathrm{Tan}\beta_x.\mathrm{Tan}\,\beta_y} \qquad \ldots\ldots\ldots\ldots\ldots\ldots\ldots\ldots(4.14)$$

and $\bar{y} = y_o - Q$

$$= y_o - \bar{x}.\mathrm{Tan}\,\beta_y$$

$$= y_o - \mathrm{Tan}\,\beta_y(x_o + \bar{y}.\mathrm{Tan}\,\beta_x)$$

$$\therefore \quad \bar{y} = \frac{y_o - x_o.\mathrm{Tan}\,\beta_y}{1 + \mathrm{Tan}\beta_x.\mathrm{Tan}\beta_y} \qquad \ldots\ldots\ldots\ldots\ldots\ldots\ldots\ldots(4.15)$$

As there is no real difference between x and y these can be written collectively as:

$$\bar{x} = \frac{x_o \pm y_o.\mathrm{Tan}\,\beta_x}{1 \pm \mathrm{Tan}\beta_x.\mathrm{Tan}\,\beta_y} \qquad \ldots\ldots\ldots\ldots\ldots\ldots\ldots\ldots(4.16)$$

19 Application of Corrections.

It was immaterial which of the co-ordinates was called x and which y, no hard and fast rule was adhered to except that a fixed method was used in tabulating the observations. A glance at the results was then sufficient to locate the position of the droplet from which the images originated and hence to assign the

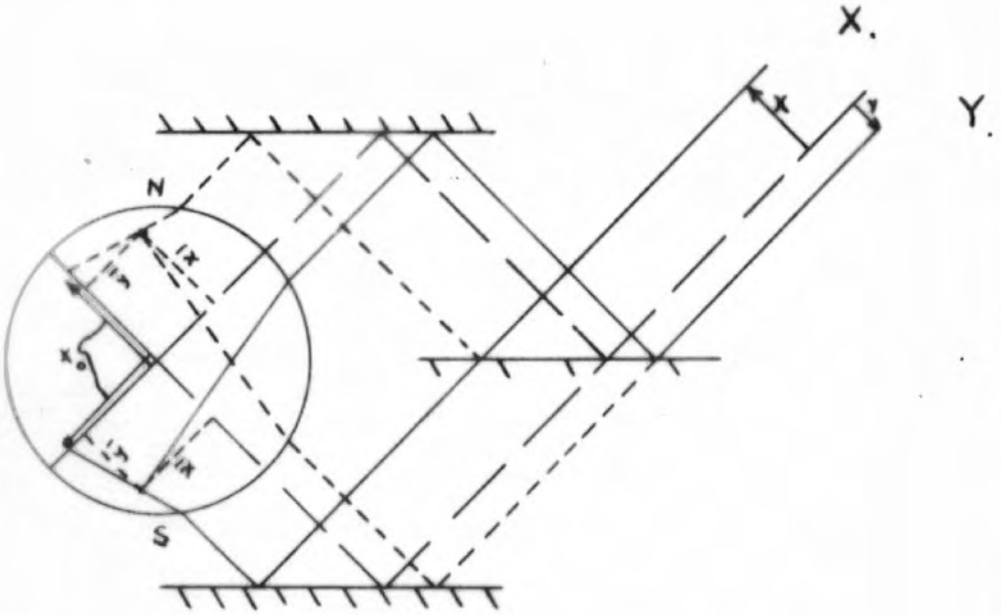

FIG. 4.8. LOCALISATION OF DROPLETS FOR AMBIGUOUS CASE OF N.S. QUADRANTS.

correction term to be used.

Referring to fig.4.5A, those parts of the image of the pipe above and below the photographic axis have been labelled X and Y respectively.

The identification of the relevant quadrants for droplets having both images on the same side of the flow tube axis is a simple matter, the X half corresponding to the W quadrant and the Y half to the east quadrant, and neglecting the sign in the denominator of the correction term the numerators take respectively the positive and negative sign.

When the images are situated one on either side of the centre of the tube image, fig.4.5 A,C, shows that the original drops could have been in either the N or S quadrant and a guess must be made as to which one, unless a differentiation of intensity of the images exists, when the quadrant can be identified exactly, as the brighter image will correspond to either the reflected or transmitted beam from the semi-reflecting mirror and a knowledge of whether it is greater or less than 50% reflecting gives the required information. Fig 4.8, however, shows that it is immaterial which quadrant is guessed. Here the full lines show the construction of the images for a droplet in the S quadrant and the dotted lines the position it would have to occupy in the N quadrant if it were to produce the same two images. The refraction is greatly exaggerated. It can be seen that the two positions are mirror images of each other about the partially aluminised

mirror and upon tracing back the x co-ordinate in the X section to both of the quadrants, the negative sign is required for the correction in both cases as x_o is greater than $\bar{x}$. In just the same way $\bar{x}$ requires the positive sign in both cases.

Hence an image in the Y region requires the positive sign while those in the X region require the negative sign unless both images occupy the same region and then the signs are opposite to those just quoted.

In tabulating observations, images in the Y half were given the symbol 'x' and those in the X half the symbol 'y' except when both occupied the same half when the first one measured, i.e. the one nearest the Y edge was called x. During tabulating, the letters Y or X, + or - were written next to the listed figures. The Y halves were those nearest to the beginning of the film record when viewed under the measuring microscope, the film running downward with regard to the figures of the mirror system.

The water jacket had here its greatest use as it greatly reduced the value of β and $\mathrm{Tan}\beta$ and increased $\mathrm{Cos}\beta$ and so limited the magnitude of the correction and eased the tedium of computing even when assisted with a calculating machine. Below x = 0.4 no correction was needed for x; $1 + \mathrm{Tan}\beta_x \cdot \mathrm{Tan}\beta_y$ could always be neglected, since when x = y maximum values of $\mathrm{Tan}\beta_x\ \mathrm{Tan}\beta_y$ occurred and the greatest possible error incurred by their neglect was not greater than 0.1% The correction $x_o \cdot \mathrm{Tan}\beta_y$, however, made itself felt even at small

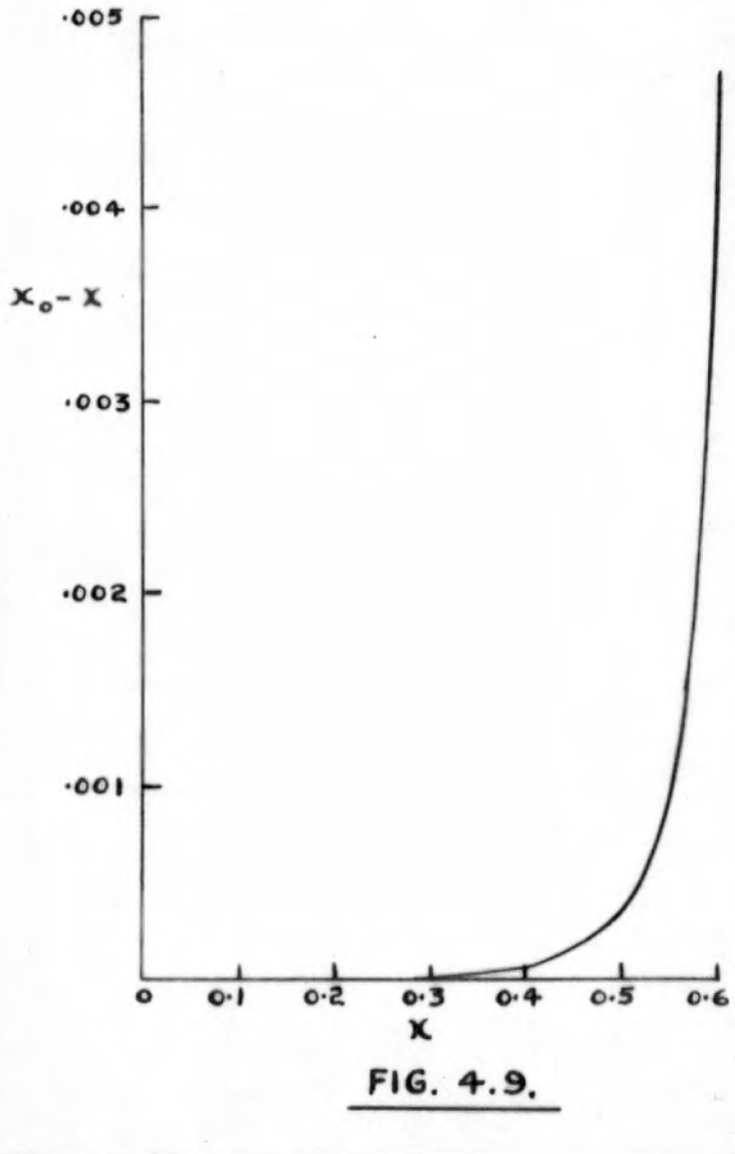

FIG. 4.9.

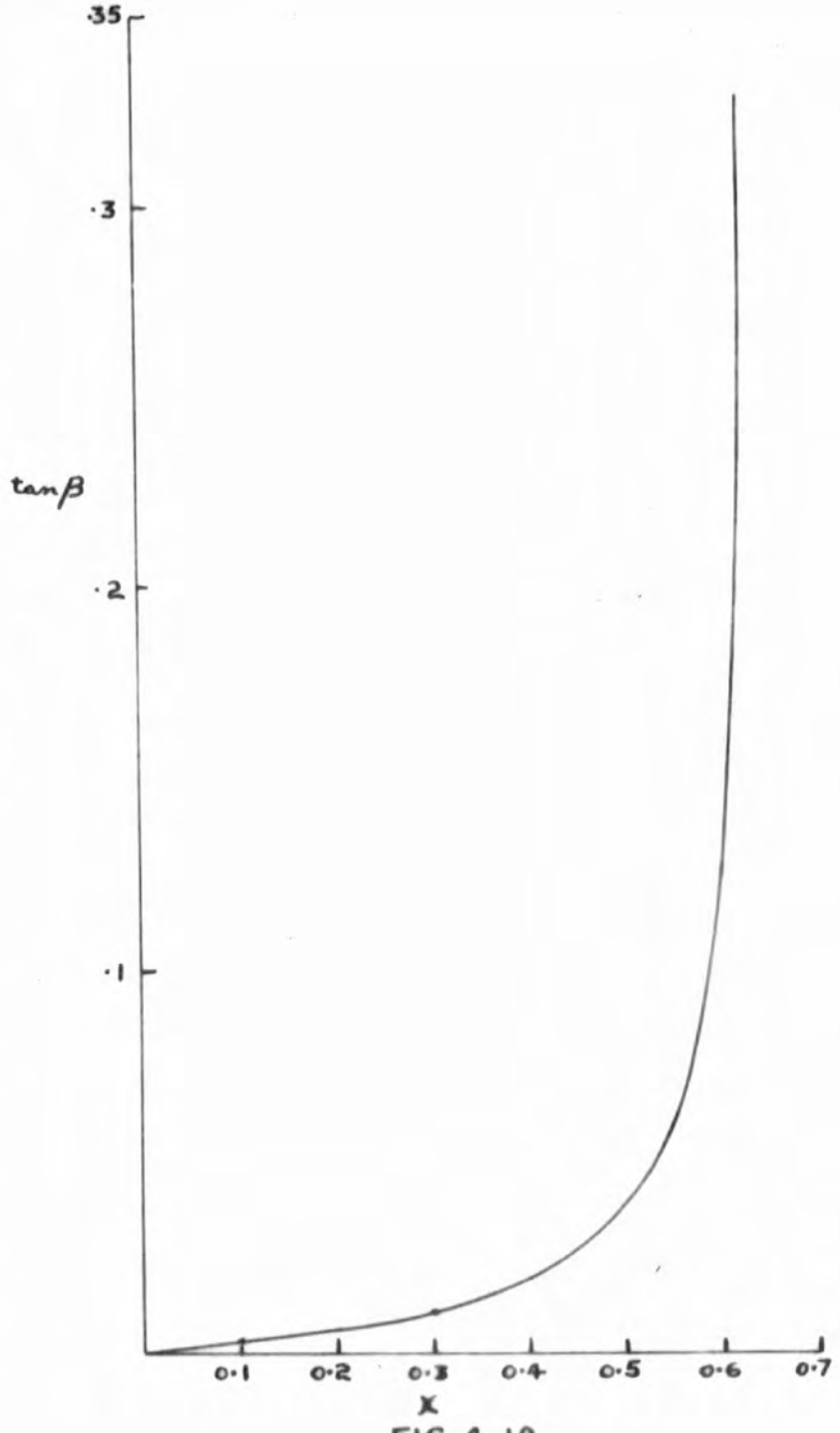

FIG. 4.10.

values of x as the corresponding value of y_o could be large with a resulting large $\text{Tan}\beta_y$.

The correction $x_o - x$ to be added to x was obtained from a graph of x against $x_o - x$, fig 4.9. Fig 4.10 is the graph of $\text{Tan}\beta_x$ against x from which $\text{Tan}\beta$ was read for each measured co-ordinate to give the multiplier for the corresponding y and vice versa. The true radial positions now readily follow. Sample tables of results are included later.

CHAPTER 5

THE STROBOSCOPE

20. Preliminary Considerations.

In view of the nature of the streamers employed as a means whereby the flow velocities in the flow tube could be ascertained, namely, small oil droplets and of the need for a continuous photographic record to be made of them it was necessary to have a form of stroboscopic illumination such that the streamers could be in effect "stopped" during each exposure of the recording cine camera.

Owing to the flared entry to the flow tube, the range of Reynolds' numbers of flow over which the flow remained laminar (with water) was 0 to about 12,000 (though, by allowing the reservoir to settle for a long time the flow was observed quite frequently to be laminar at Reynolds numbers of forty to fifty thousand); thus the associated maximum flow velocities varied within a range of about 1:10. To obtain a measure of the velocities of the droplets and hence the flow pattern, the distances travelled by them must be measured over a known time interval.

To obtain the necessary time exposure it was decided to investigate two methods, the first to give a relatively long known exposure time on each frame of the cine record with steady intense illumination, and the second to give two short duration flashes of illumination with a known time separation,

during each exposure, which must be intense enough to produce a photographic image of the droplets and at the same time short enough to produce a point image. In all events a stroboscope was required which would satisfy the following conditions:-

(a) It must be capable of producing either a single flash of illumination of known length or two very short duration flashes during each stationary period of the film.

(b) The duration of the single flash or the time interval between the two flashes 't', say, should be variable over a time range of not less than 1:20 millisecs, in order to cover the velocity range.

(c) The flash or flashes should be repeated with constant 't' every time the cine film was exposed and stationary, that is, they should be faithfully governed by the recording camera even should its speed alter.

21. Investigation of Stroboscopes.

General.

An intense beam of light of known width repeatedly passing over the flow tube, or a number of similar beams successively incident upon the tube, could give the required time exposure 't' and hence the exposure time could be altered by variation of the linear speed of the beams. Alternatively, beams passing over the flow tube at constant speed give variable exposure time if their widths are varied. Applications of these principles were employed in the following ways:-

22. Reed Stroboscopes.

A sprung reed, carrying a mirror, was maintained electrically in oscillation by current pulses generated through the action of an on/off switch which was in turn controlled by the recording cine camera. Light reflected from the mirror gave a beam whose speed at any instant could be considered to be sensibly constant and whose width was simply altered by obscuring various amounts of the mirror. The light incident on the mirror was produced by means of a "Pointolite". The frequency of vibration of the reed was maintained at half the camera exposure frequency by simple gearing of the camera switch and the centre points of the to and fro swings of the beam were utilised as light sources thus giving a stroboscopic illumination frequency equal to that of the camera exposure frequency. The light beams were split in two by inclined mirrors and after further reflections illuminated the flow tube in a manner similar to that shown in fig. 4.3.

This method necessitated that the reed should have a constant amplitude of vibration (and therefore frequency) but this was not properly achieved because of variations of camera speed and slight irregularities of the switch which caused varying phase differences between oscillation frequency and current impulse frequency; consequently accurate synchronisation of exposure and illumination was not assured.

Vibrating reeds carrying knife edges which could be arranged very simply to give variable widths of aperture produced unmoving fixed direction beams. Again, a half

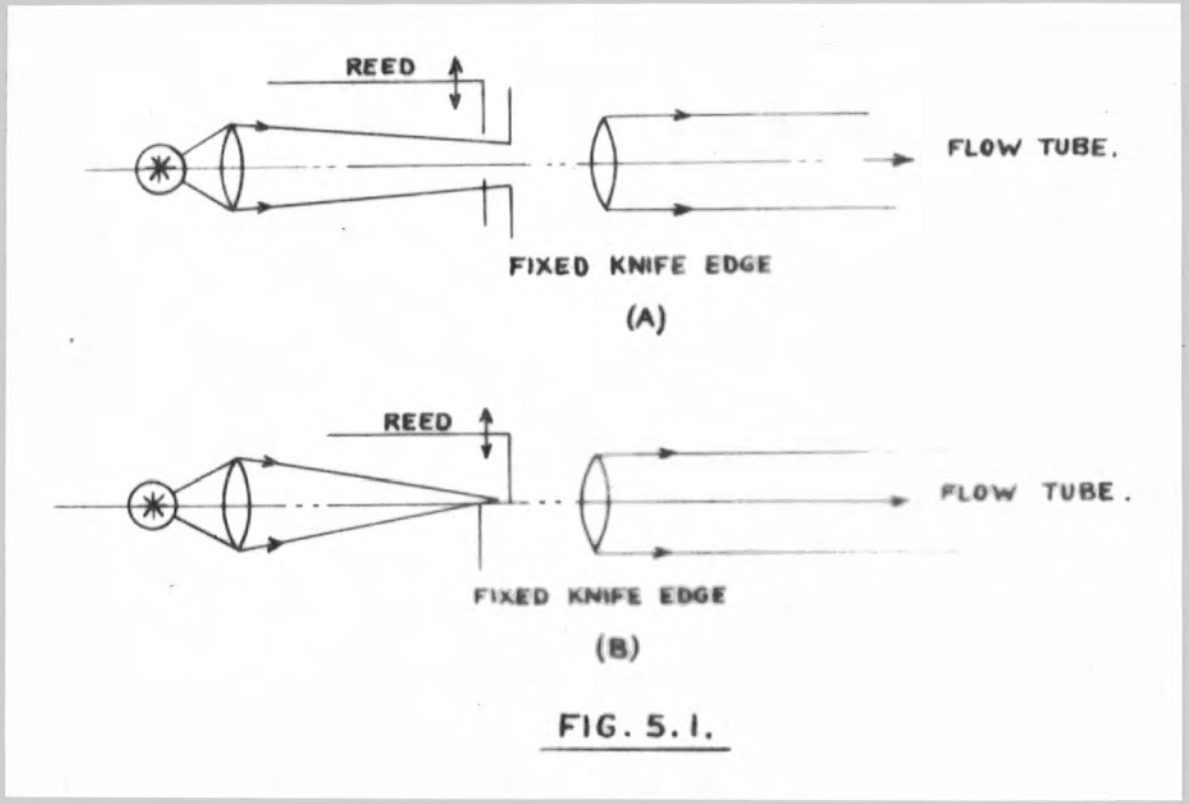
REED
FLOW TUBE.
FIXED KNIFE EDGE
(A)
REED
FLOW TUBE.
FIXED KNIFE EDGE
(B)

FIG. 5.1.

frequency could be used, or the full camera frequency if the peak amplitude in one direction was employed as the point of uncover of the light beam, fig.5.1.a.b. Phase differences could again occur here but the major difficulty was the variation of the light beam intensity caused by the change in aperture to the maximum as the reed uncovered the illuminated slot and then the reverse to the zero aperture. This produced the indeterminacy of the true end points of the line images of the oil droplets.

Errors in the actual time exposure occurred with such moving beam illumination in a similar way to that which will be indicated in what follows on apperture disc stroboscopes.

For the reasons indicated above reed stroboscopes proved unsuitable and were discarded.

23. Aperture disc stroboscopes.

The aperture disc was of the usual pattern having a rotating disc punctured with radial slots all at the same radial distance from the disc axis. The aperture disc was maintained in motion by magnetic impulses delivered to the teeth of a specially shaped cog wheel which rotated on the disc spindle on which it had only a friction grip. The maintaining pulses were derived once again from the switch which was controlled by the camera. The images of the slots, illuminated in turn by the "Pointolite", passed over an inclined mirror (as in fig.4.3) and thence on to the flow tube after reflection from one small region only of the inclined mirrors.

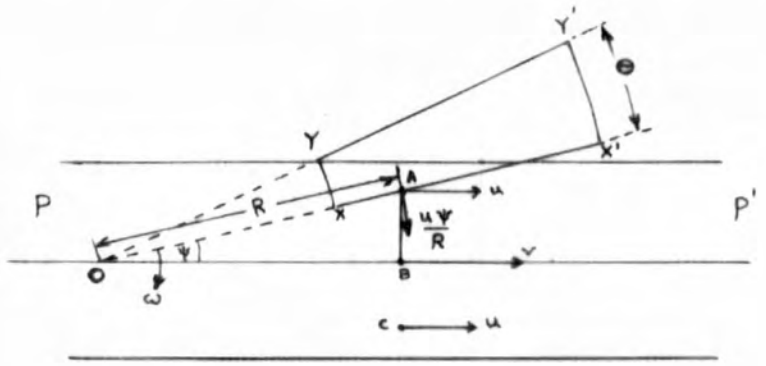

(A)

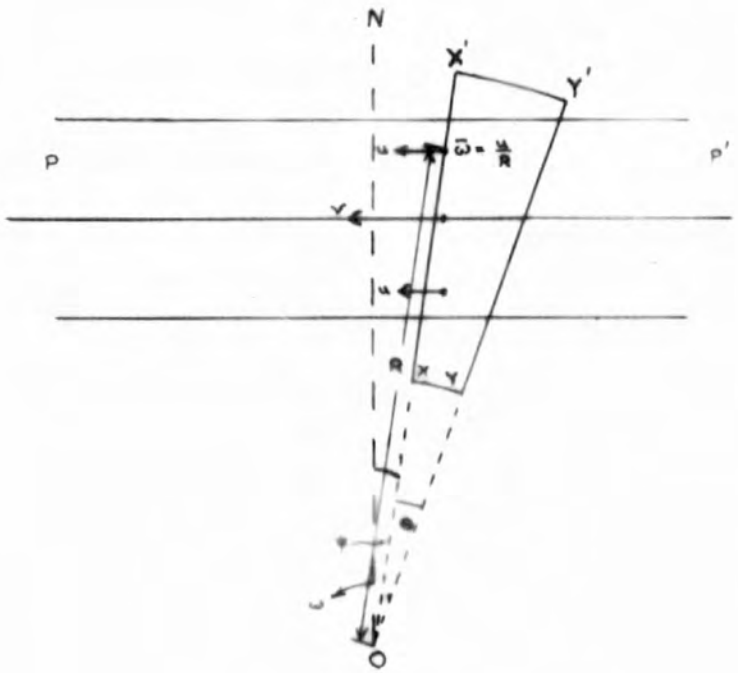

(B)

FIG. 5.2

24. Errors in Exposure Time.

The magnified wedges of light after reflections from the mirrors were rotating in a circle of radius R, about 30 cm, as they passed over the flow tube, and could be arranged to pass over the flow tube along a line parallel or perpendicular to it. In both cases errors of exposure time were involved though small in the latter case.

Consider fig.5.2 a,b, in which PP' is a section of the flow tube and A,B,C are three droplets which for convenience are considered to lie on the same diametral plane at right angles to O which is the axis of rotation of the wedges of light XYY'X' rotating with angular velocity ω radians per second. B is considered to be at the centre of the flow tube and A and C equally spaced on either side of it; the respective velocities of B, A and C are v,u and u cm. per second.

Case (A)

The droplet 'A' is first illuminated by the edge XX' of the light wedge and finally by the edge YY'. However by virtue of its linear motion down the tube, it has an angular velocity relative to the light wedge of $\bar{\omega} = \frac{u.\psi}{R}$ for the initial position shown, so that the net effective angular velocity of the light wedge is $\omega - \bar{\omega}$.

Throughout the time for which the droplet is illuminated this quantity $\bar{\omega}$ is not constant as ψ decreases as R increases. Because the period of illumination is small the droplets do not move more than a few millimetres during this time so that

the variations in R are only of the order of 1%. Ψ is $\mathrm{Sin}^{-1}\frac{r}{R}$ and because it is small it can be written $\Psi = \frac{r}{R}$ and again the variations are of order 1%. The total variations of ω then, are limited to within 2%. In the following analysis $\bar{\omega}$ is taken as constant.

Thus, the time of illumination of the droplet at 'A' will be:

$$T_a = \frac{\theta}{\omega - \bar{\omega}} \qquad \ldots\ldots\ldots\ldots\ldots\ldots\ldots\ldots\ldots\ldots (5.1)$$

where θ is the angle of the light wedge. Similarly, at 'C' the time will be

$$T_c = \frac{\theta}{\omega + \bar{\omega}} \qquad \ldots\ldots\ldots\ldots\ldots\ldots\ldots\ldots\ldots\ldots (5.2)$$

For droplets below the tube axis 00', the angular velocity of the light wedge is effectively increased. The difference $T_a - T_c$ is

$$T_a - T_c = \theta \left\{ \frac{1}{\omega - \bar{\omega}} - \frac{1}{\omega + \bar{\omega}} \right\}$$

$$= \theta \left(\frac{2\bar{\omega}}{\omega^2 - \bar{\omega}^2} \right) \qquad \ldots\ldots\ldots\ldots\ldots\ldots (5.3)$$

and the percentage difference with respect to T_c

$$100\left(\frac{T_a - T_c}{T_c}\right) = \frac{200.\bar{\omega}}{\omega - \bar{\omega}} \,\% \qquad \ldots\ldots\ldots\ldots\ldots\ldots (5.4)$$

When the flow is laminar $\frac{u.\Psi}{R}$ has a maximum value which is readily found by using the equation for the velocity at a distance 'r' from the axis of a pipe, by differentiation and equating to zero. Thus $\Psi = \frac{r}{R}$ and $\frac{u.\Psi}{R} = \frac{P.}{4.\eta\, L.R^2}\left(a^2 r - r^3\right)$ whence the maximum value occurs at $r = \frac{a}{\sqrt{3}}$

Using the equation of Poiseuille (1.5) and for Reynolds' number $(R_n)_{\bar{\omega}}$ can be written

$$\bar{\omega} = \frac{R_n.\eta.}{R^2}\left(\frac{r}{a} - \frac{r^3}{a^3}\right) \qquad \ldots\ldots\ldots\ldots\ldots\ldots (5.5)$$

As $\bar{\omega}$ is very much smaller than ω, which was 2.83 (there being 40 slots in the sector disc and the camera frequency being approximately 18 frames per second), the relative errors can from (5.4) be written as Error % = $\frac{200\bar{\omega}.\%}{\omega}$ which from (5.5) increases linearly with Reynolds' number.

The maximum value of Reynolds' number for which the flow was fully developed at the observation section was 2100 and this value yields a relative error percentage of 0.77%.

Thus for any particular geometrical arrangement the errors depend only on the Reynolds' number.

When the flow is not fully developed, i.e., at low values of $\frac{x}{a.R_n}$, and for a set value of Rn, the product u.r involved in $\bar{\omega}$ does not follow the same pattern as that for parabolic flow. From the curves of fig.3.1 chapter 3, it can be seen that for values of 'r' greater than $a/\sqrt{3}$. i.e. r/a greater than 0.577 all the curves will have a maximum value of u.r. at some value of 'r' greater than $a/\sqrt{3}$ and also that these maxima will be greater than the maxima for parabolic flow. Consequently the maximum errors involved in undeveloped flow will be greater than the errors which would be involved were the flow parabolic, the lower the value of $x/a.R_n$, whether this be due to a low 'x' or a large R_n.

At the axis of the flow tube $\Psi = 0$ as $r = 0$ and the period of illumination is the true value θ/ω.

Case (B)

For any droplet illuminated by the leading edge of the

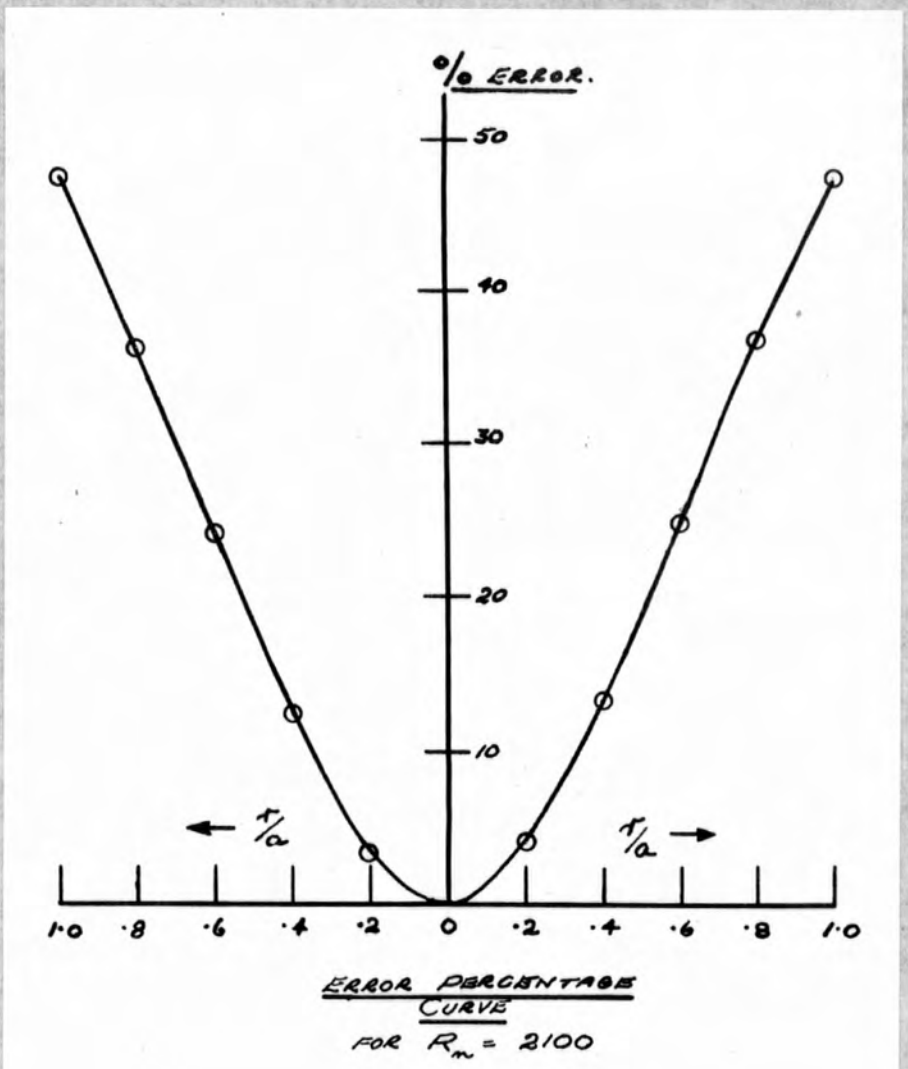

ERROR PERCENTAGE CURVE FOR $R_m = 2100$

FIG. 5.2 a

light wedge XX' the period of illumination will be

$$T = \frac{\theta}{\omega - V/R} \qquad \ldots\ldots\ldots\ldots\ldots\ldots\ldots\ldots\ldots\ldots (5.6)$$

where R is the distance of the droplet from O and V its velocity. This neglects a small relative radial velocity along R, due to the circular motion of the light wedge, which depends, as in case 'A' upon ψ (ON being perpendicular to the flow tube), and is small.

If the period of illumination for an axial droplet B is taken as the base from which errors are estimated, the difference in illumination times for this droplet and any other 'A', say is

$$T_b - T_a = \theta\left(\frac{1}{(\omega - v/R_b)} - \frac{1}{\omega - u/R_a}\right)$$

$$= \theta\left(\frac{R_a v - R_b . u}{(\omega . R_b - v)\ (\omega . R_a - u)}\right) \qquad \ldots\ldots\ldots\ldots\ldots\ldots (5.7)$$

and the percentage difference is

$$100.\left(\frac{T_b - T_a}{T_b}\right) = \frac{100.(R_a . v - R_b . u)}{(\omega . R_b - v)(\omega . R_a - u)} . \frac{(\omega . R_b - v)}{R_b} \%$$

$$= \frac{100.(R_a . v - R_b . u)}{R_b . (\omega . R_a - u)} \% \qquad \ldots\ldots\ldots\ldots\ldots\ldots (5.8)$$

This has a maximum value for droplets at extreme radii where u = 0. For the Reynolds' number of 2100, as in case 'A', it is 47.77%, and for the values of $r = \pm a/\sqrt{3}$ it is 23.8% and 22.8% respectively. The error curve is not quite symmetrical and it was drawn and is shown in fig.5.3a. Similar analysis applies if the aperture disc be considered to rotate in the opposite sense. In this case the minimum illumination time occurs at the axis of the pipe. A treatment somewhat

similar to the above has been given by A. Fage and J.H.Preston [31] for their fluid motion microscope.

Only this simple analysis is included as there existed greater disadvantages of the system which led to its failure, these were:-

1. The difficulty in arranging good definition of the slot images, which coupled with the scatter of light in the water jacket of the flow tube, resulted in the ends of the line images of the droplets being indeterminate.

2. Two difficulties were met with in disc stroboscopes similar to those in reed stroboscopes, namely, the synchronisation of the illumination with the exposure of the film and secondly, variations in camera speed were not faithfully followed by the aperture disc owing to its relatively large inertia. While the synchronisation difficulty could be overcome and slow speed variations of the camera followed, sudden speed changes, caused by variations in the camera voltage supply due to local changes of loading on the mains supply in the laboratory, resulted in large phase discrepancies between the arrival with respect to time of a magnetic driving pulse and the correct time of arrival of a tooth of the cog wheel in the neighbourhood of the pole of the electro-magnet. The toothed inertia wheel became out of step with the magnetic pulses which drove it and hence the rotation of the aperture disc ceased.

Because of these troubles a variable width slot aperture

disc was not constructed and work on this type of stroboscope was suspended. An investigation was then carried out on the possibility of using the double exposure method without using mechanical means.

25. Flash Tube Stroboscope.

High intensity light flashes capable of producing photographic images of the droplet streamers by scattered light could be produced by the use of inert gas discharge tubes, which, dependent upon the design and associated circuit elements have discharge times from about one to 1500 microseconds(32)(33). A suitable tube within this range could effectively "stop" the droplet motion. An investigation of various types of flash tubes and their modes of application was carried out and is discussed later in sections 14 and 15.

The published literature on stroboscopes was fraught with applications of triggered and untriggered flash tubes for photographic purposes which in general relied upon certain basic principles of circuitry(33)(34), (Section 35), and it was upon these principles that a flash tube stroboscope was designed though certain new techniques were applied because of the need for two flash tubes working slightly out of phase with respect to each other. To obtain the two exposures on each frame of the cine record it was considered necessary to have two flash tubes, rather than a single tube with a variable flashing frequency for the following reasons:-

(i) A single flash tube operating continually

with the required interval between flashes would be very wasteful because the majority of the flashes would not be utilised, i.e., when the cine film was not exposed. At the same time to comply with the maximum rating the intensity per flash would be low and the useful life of the tube would be greatly reduced.

(ii) Owing to the relatively large exposure time of the film (about 1/50 second) more than two images of the droplets could be produced on each frame of the record with a single constantly operating tube. This would result in confusion in sorting out the related images. This confusion would be greatly enhanced if there happened to be droplets flowing in the same stream line and near together. In this case the images of one could "catch up" those of the other.

These latter two considerations could be overcome by employing a double flash from a single tube during each exposure period. However:

(iii) About twice the light intensity would be available per flash with two tubes than would be produced with a single tube if the tubes were worked at full rating.

(iv) High rates of flow required flashing intervals of less than 10 milli-seconds which is the lowest that could be produced with full-wave rectification of 50 cycle A/C and a single flash tube.

These facts led to the desirability of two flash tubes working at the camera controlled frequency with one delayed relatively to the other.

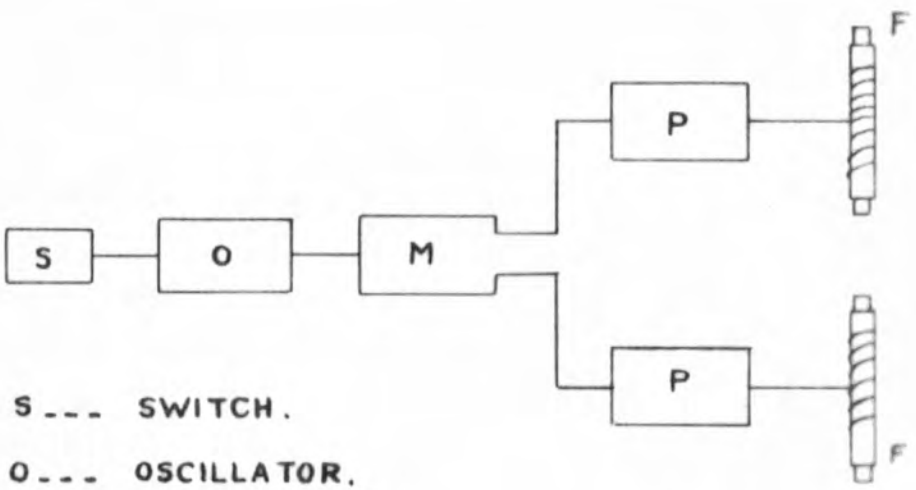

S --- SWITCH.

O --- OSCILLATOR.

M --- MULTIVIBRATOR.

P --- PULSE GENERATOR.

F --- FLASH TUBE.

FIG.5.3. STROBOSCOPE BLOCK DIAGRAM.

With two flash tubes two voltage pulses were required which could be suddenly applied to the flash tubes either as trigger pulses of the order of 5 - 10 Kv or as supply voltages greater than the hold off voltage of the tubes i.e., of the order of 3 Kv. The circuit which immediately suggested itself for the production of a double voltage pulse was the asymmetric multivibrator. Sudden voltage changes occur at the grids and anodes of the valves of a multivibrator and it is a simple matter to arrange any required repetition frequency. Further, the amount of asymmetry introduces a variable time interval between the sudden voltage changes occurring at the grids or anodes and in addition the multivibrator is comparatively simple to synchronise with the cine camera. These voltage pulses could then be fed to the control grids of two inductively loaded pentode valves which would thereby be suddenly backed off beyond cut-off, resulting in the production of high voltage oscillatory pulses at the anodes. It was hoped that these pulses, sharpened by means of spark gaps, would trigger the flash tubes. A circuit based upon these principles was constructed and a block diagram is shown in fig.5.3.

The switch was operated by the camera and closed every time the cine film was stationary. It consisted of a spring contact closed by a rotating cam on a shaft passing through the camera casing and driven by the camera mechanism at a rotational speed equal to the exposure frequency of the camera.

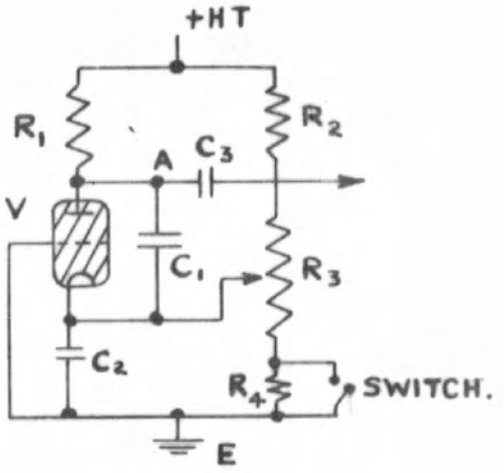

FIG. 5.4. THE OSCILLATOR.

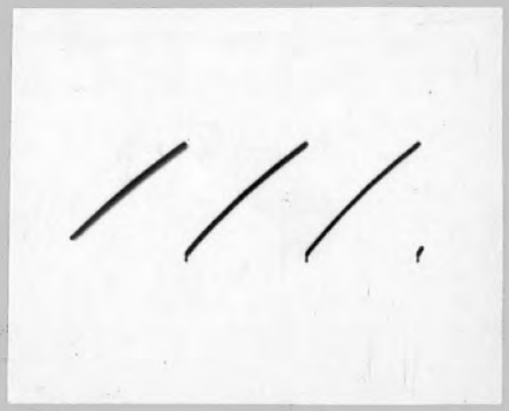

PLATE 5.1

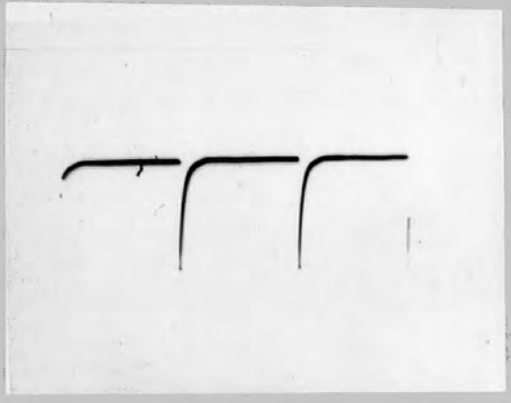

PLATE 5.2

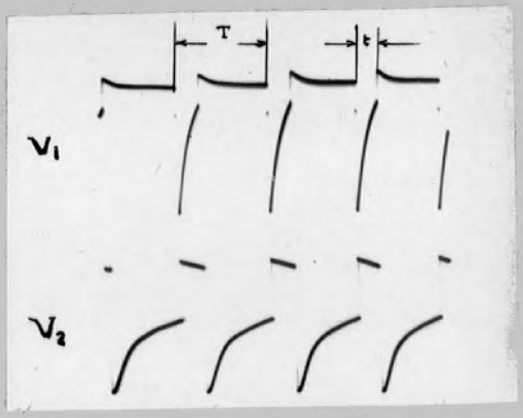

PLATE 5.3

In view of its simplicity a positive instantaneous closure was not assured and hence it was not used directly to produce a trigger pulse to control the multivibrator; its direct use resulted in one or other of the multivibrator valves having an uncertain action and consequently one of the pulse generating valves was ineffectively cut off.

Reich[35], Terman[36], Chance[37] give several ways of triggering a multivibrator into controlled oscillation and the method used here which offset the disadvantages of the switch was to introduce a thyratron relaxation oscillator between the switch and the multivibrator and to adapt the sharp negative going saw tooth oscillations to act as triggering pulses.

26. The Oscillator.

The thyratron oscillator fig 5.4 functioned in the usual manner, the closing of the switch S shorted out R_4 which constituted part of the biasing resistor and with this reduced bias the valve fired, in this way uncertainties in the switch did not matter as the grid ceased to have any control once the valve was conducting and reliable firing was assured.

In determining the values of R_1, R_2, R_3, R_4 certain conditions had to be fulfilled namely:-

(i) The time constant of the charging circuit C_1R_1 (R_3,R_4 could be neglected in comparison with R_1) to be such that C_1 be charged to a voltage between successive closures of the switch greater than the firing voltage of the thyratron as

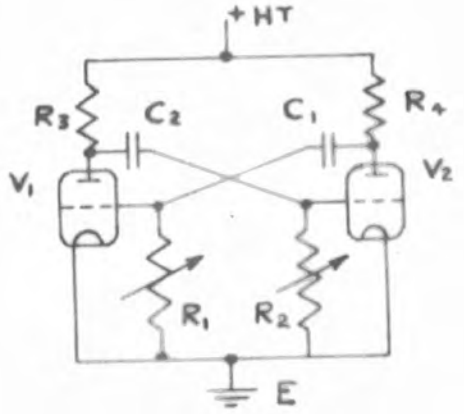

FIG. 5.5. THE MULTIVIBRATOR

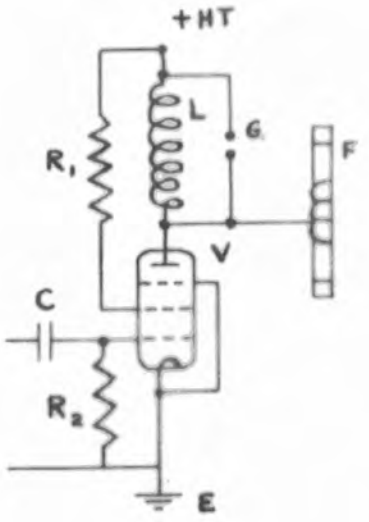

FIG. 5.6. THE PULSE GENERATOR

determined by the biasing voltage developed across the earthy side of R_3.

(ii) The bias voltage across R_3 and R_4 to be great enough to ensure that no firing occurred before R_4 was shorted.

(iii) The bias voltage across R_3 alone when R_4 shorted to be sufficient to prevent the thyratron from firing more than once while the switch was closed.

In terms of the circuit elements of the oscillator, if V_o is the supply voltage, 'i' the current in R_2, R_3, R_4: T_1 the period between successive switch closures, T_2 the time for which the switch remained closed and μ the slope of the grid voltage/firing voltage characteristic whose intercept on the grid voltage axis is V, then the conditions pertinent to i, ii, iii are :-

$$V_o.(1 - e^{\frac{-T_1}{C_1.R_1}}) > \mu.(i.R_3 + V) \quad \ldots\ldots\ldots\ldots\ldots(5.9)$$

$$V_o.(1 - e^{\frac{-T_1}{C_1R_1}}) < \mu.(i.(R_3 + R_4) + V) \quad \ldots\ldots\ldots(5.10)$$

$$V_o.(1 - e^{\frac{-T_2}{C_1R_1}}) < \mu.(i.R_3 + V) \quad \ldots\ldots\ldots\ldots\ldots(5.11)$$

and with these conditions satisfied, the oscillator frequency was controlled by the camera and by feeding its output through condenser coupling to one grid of the multivibrator its frequency was likewise controlled.

27. <u>The Multivibrator.</u>

The voltage wave form at A fig. 5.4 is shown in plate 5.1 and this was fed through C_3 to the grid of V_1 of the multivibrator fig. 5.5. The functions of C_3 were twofold, firstly it was a blocking condenser to prevent point A and hence the

grid of V_1 from being at a fixed positive potential due to the direct line to earth of the oscillator H.T. supply through R_1 fig. 5.4 and R_1 fig. 5.5 and secondly with the multivibrator grid leak it differentiated the wave form of plate 5.1 so that the voltage trigger which locked the multivibrator was of the form shown in plate 5.2. $C_3.R_1$ was small and V_1 maintained its normal grid working voltage while firing, i.e. effectively earth.

The natural frequency of the multivibrator, which under normal operating conditions was less than that of the oscillator and camera, was controllable through R_2 ($\gg R_1$) and C_2($\gg C_1$). Plate 5.3 shows the grid wave forms of V_1 and V_2. T was controlled by the recording camera and faithfully followed slow or sudden speed changes while t was variable by adjustment of R_1 and was sensibly constant for a fixed value of R_1 over a wide range of values of R_2. The t range was about 30 milliseconds at maximum R_1 to 0.1 milliseconds below which the negative grid swings had dropped to such a value as to be incapable of completely cutting off the pulse generator valves. Variations in t at any fixed set of conditions were estimated by means of a cathode ray oscilloscope to be not more than 2 or 3 micro-seconds and thus quite negligible for the normal values of t employed.

28. <u>The Pulse Generator.</u>

The grid wave forms of V_1 V_2 were fed by condenser resistance coupling to the control grids of two P.T.15 pentode

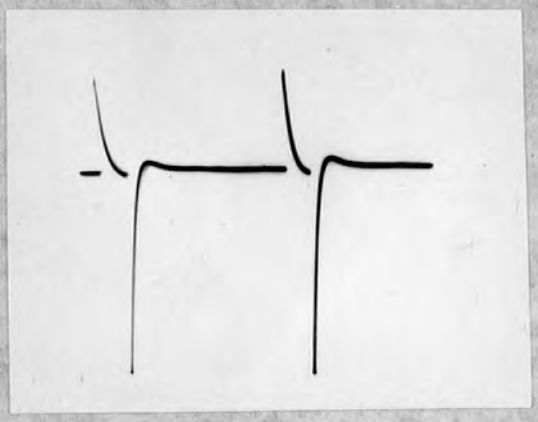

PLATE 5.4 a

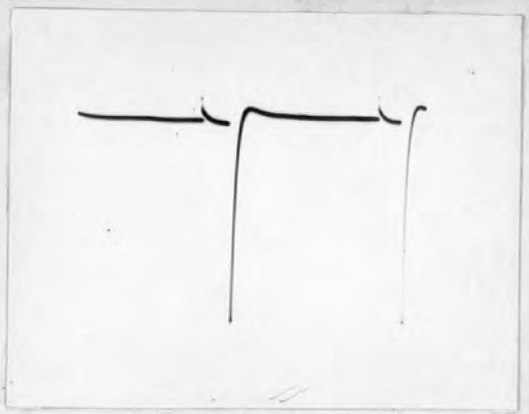

PLATE 5.4 b

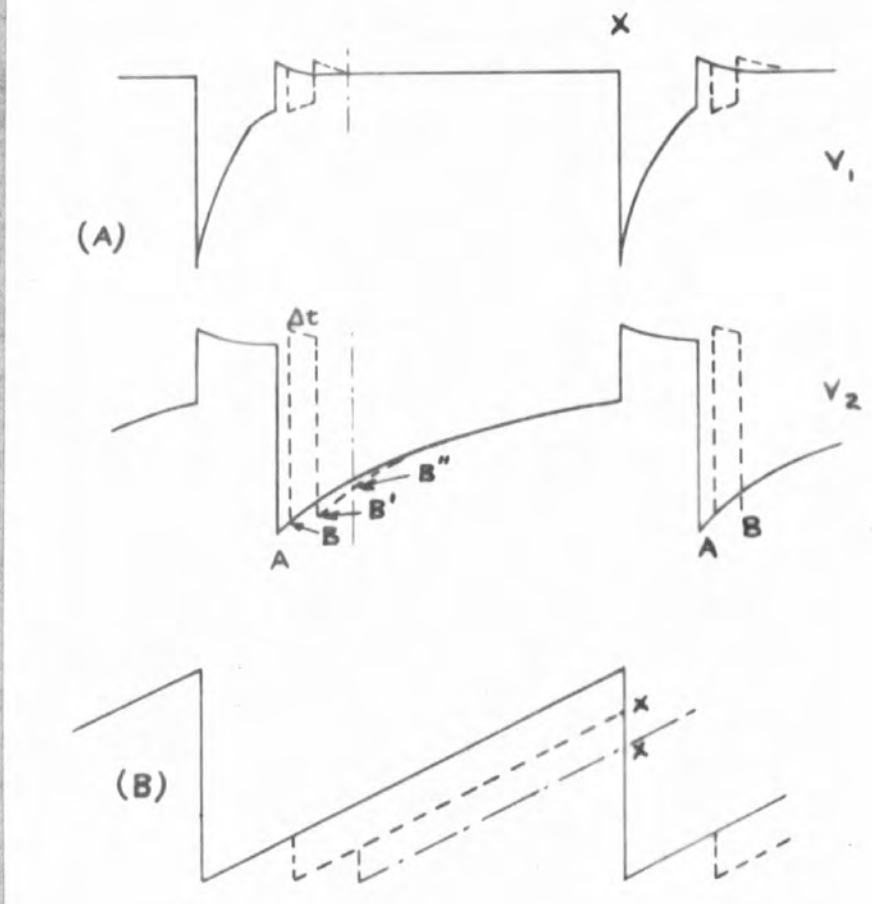

FIG. 5.7.

pulse generators fig 5.6 with inductive anode loads L. These negative going voltages of V_1 V_2 were large enough to completely and suddenly cut off the pentodes and in so doing the magnetic fields associated with the inductive loads collapsed and produced high voltage exponentially decaying oscillations at the anodes. These pulses were readily sharpened by the use of spark gaps across the loads (or to earth from the anodes) and they then formed effective triggers for the flash tubes.

The higher the anode current prior to cut off the greater was the resultant voltage: the more readily available high power valves were 807's (tetrodes) and P.T.15's (pentodes) and both were tried. The P.T.15's proved more acceptable, being able to withstand higher inter-electrode voltages without flash-over occurring and resultant softening, and were in consequence adopted in favour of the 807's.

In a later section the types of chokes which were tried as anode loads for the P.T.15's are discussed, and it was apparent that in certain cases the load time constants would be too large to allow a sufficient build up of current, during the interval 't', in the load of the valve fed direct from the grid of V_2 of the multivibrator (plate 5.3). The condenser resistance coupling of small time constant was therefore included and it converted the controlling input waveform from the normal multivibrator wave form to that shown in plate 5.4 a,b. 'a' and 'b' of the latter plate were effectively the same, the difference being due to the grid current in the pentode

in 'b' and thus the pulse generator control grids were then normally at earth potential and the valves fully conducting. The coupling also assisted in isolating the multivibrator from the pentodes as regards feed back of a positive pulse at cut-off. Diagramatically the effect of this feed back is shown in fig. 5.7a, the full line representing the correct operating wave form condition with cut-off at A and the dotted line the state of affairs upon the occurrence of feed back. The feed back was caused by the voltage change upon sparking across the spark gap of the inductive load and it occurred at a time corresponding to B in the diagram. When this occurred valve V_2 reconducted again and V_1 ceased to conduct and thus at B when V_1 refired there could occur in the pulse generator a second cut off and a further feed back provided Δt was sufficient time for a rebuild up of anode current. B' could then be repeated as B" and so on giving an uncontrolled condition. At the same time the effect was felt in the thyratron oscillator, the potential at A, fig. 5.4, being reduced by the occurrence of feed back so that the governing equations of the circuit were violated and closure of the switch did not necessarily produce a master controlling pulse for the multivibrator. The oscillator output waveform was in fact amended to that shown in fig. 5.7B, so that at X when the switch closed the potential at the thyratron anode could be insufficient to fire against the biasing voltage. The feed back was not very pronounced in V_1 owing to the large

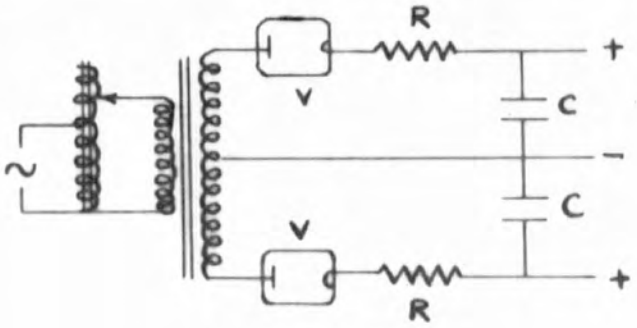

FIG. 5.8. FLASH TUBE POWER SUPPLY.

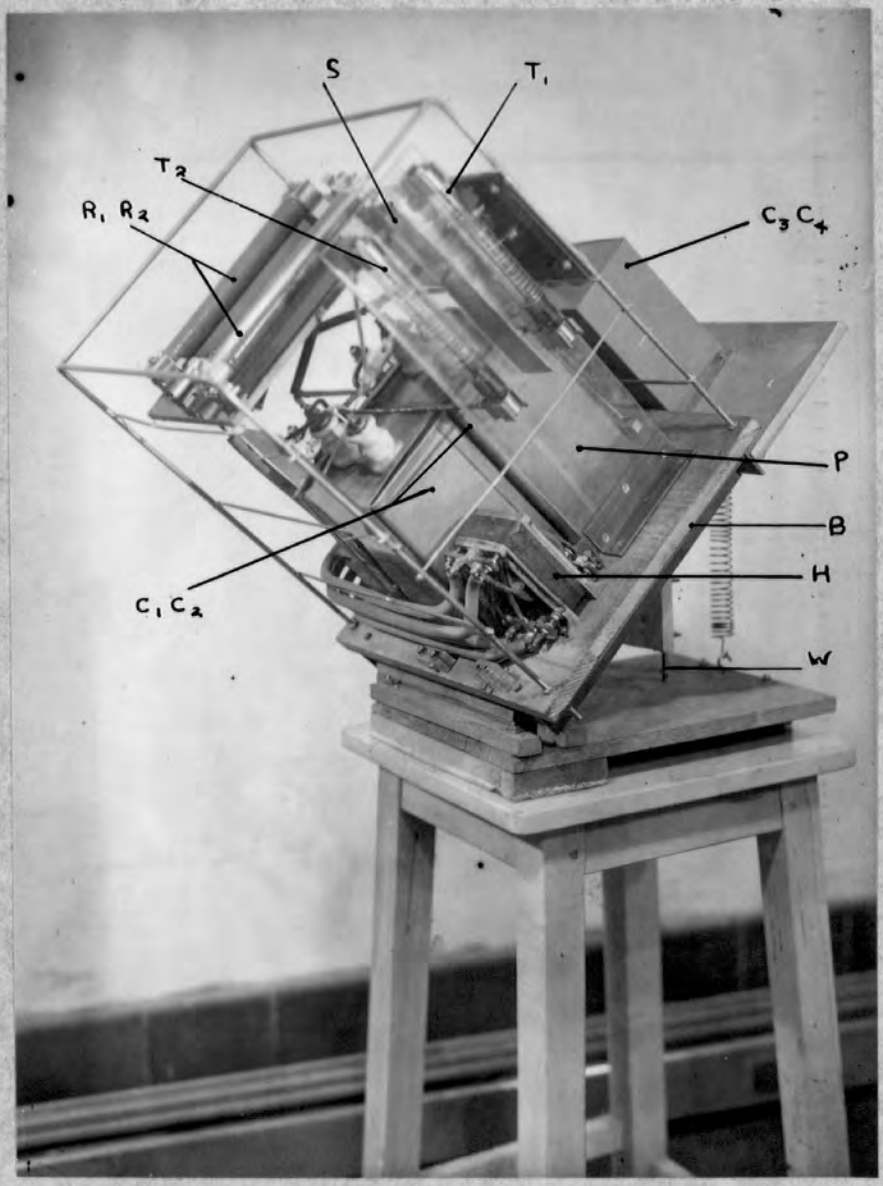

PLATE 5.5

slope of recovery line of the grid wave form. The sharpened voltage pulses developed at the anodes of the pentodes were used to trigger the Siemens' S.F.6 flash tubes* and were applied direct to a spiral of wire wrapped round the glass envelope of the tubes.

29. Flash Tube Supply Voltage.

A full account of the work carried out on the flash tubes with a view to ascertaining some of their properties, optimum operating voltages and mode of triggering is given later; it is sufficient here to say that the operating voltage was of order 2000 volts.

Two D.C. supplies, variable from 0 to 4000 volts, were made by half wave rectification of the two halves of a centre tapped 4000 volt transformer. The circuit diagram is shown in fig. 5.8.

The value of the time constant C.R. had to be such that the voltage could rise to the operating voltage of the flash tubes between flashes (about 1/20 second) and at the same time the wattage rating of the tubes 15 - 20 watts under stroboscopic conditions, limited the value of C to 1/2 μf. One hundred watt 25,000 ohm ceramic embedded wire wound resistors were to hand, their ohmic value was suitable and they were used, thus giving the C.R time of 0.0125 second. There exists a minimum

* We are indebted to Messrs. 'Siemens Lamp Supplies Ltd.' who kindly provided us with modified S.F.6 flash tubes. These were Xenon filled and contained a specially activated electrode.

value of R to prevent sudden application of the voltage to the flash tubes after discharge which could cause spontaneous discharge and also to prevent a continuous conduction through the flash tube which could occur if the charging of the storage condenser was rapid enough to maintain current flow in the flash tubes.

Since the rectifier heaters were at H.T. potential, a special filament transformer was wound to withstand the high voltage between primary and secondary. It was constructed on a perspex former and had two secondary windings of four volts; the step down ratio was 3:1 and it was built into the power pack and supplied from a twelve volt galvanometer lantern supply. Plate 5.5 is a photograph of the power pack without the main transformer supply. The flash tubes T_1 T_2 were mounted on a perspex sheet P and screened from each other by the earthed tin sheet S which served to prevent the flashing of one tube from initiating the discharge in the other. This effect was thought to be due to optical or ultraviolet excitation and perhaps also electrostatic strains though it was not investigated further since the inclusion of the screen obviated the trouble. The condensers C_1 C_2 resistors R_1 R_2 and heater transformer H can also be seen. The whole was mounted upon a hinged base B the angle of tilt of which could be adjusted by means of the screw W to give the 45° inclination to the horizontal of the tubes in which position they were used as previously pointed out. C_3 C_4

were additional 1/2 μf condensers mounted externally to the power pack which could be connected in series or parallel with C_1 C_2 to reduce or increase the flash intensity if necessary. As an additional capacity they were only used with old tubes, which had become blackened with cathode deposition, when the apparatus was being aligned.

30. Pulse Generating Chokes.

As inductive loads for the pulse generators there were available:-

(a) The secondary windings of high voltage transformers.

(b_1) and (b_2) Secondary windings of large and small Rhumkorff coils respectively with partial iron cores.

(c) Smoothing chokes.

(d_1) and (d_2) Stack wound and layer wound air or partial iron cored coils.

It was desired to investigate these types to find suitable coils rather than turn to pulse transformers of which none were immediately available and which would have required severe modifications to the design decided upon, requiring as they do a high current density primary pulse as from for example a triggertron or power thyratron.

The coils d_1 d_2 were quite unsuitable for the purpose as their inductances were very low but they were examined for completeness sake. Rhumkorff coils used required normally a large primary current to produce a large secondary pulse and so only the secondary windings were employed.

PLATE 5.6

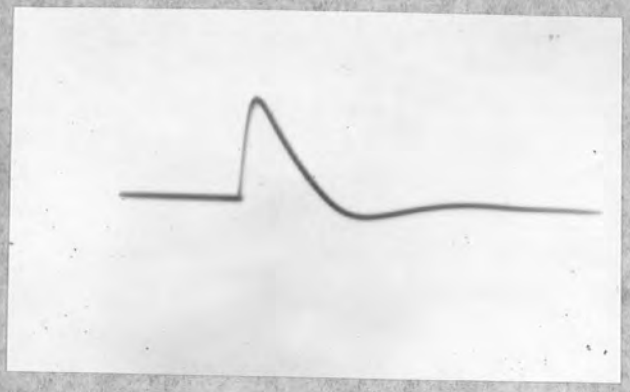

a. (11 KV)

b_1. (11 KV)

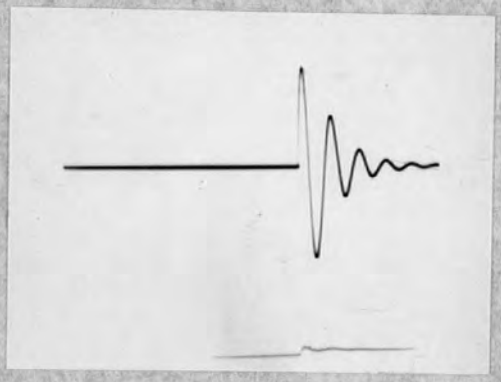

b_2. (8 KV)

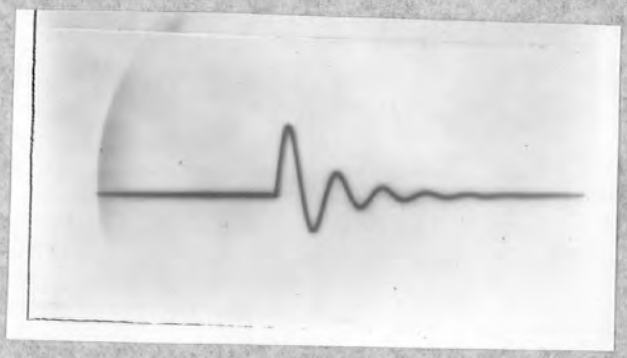

c. (7 KV)

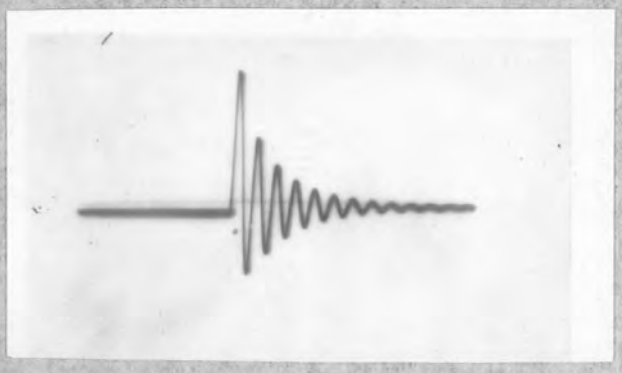

d_1. (2 KV)

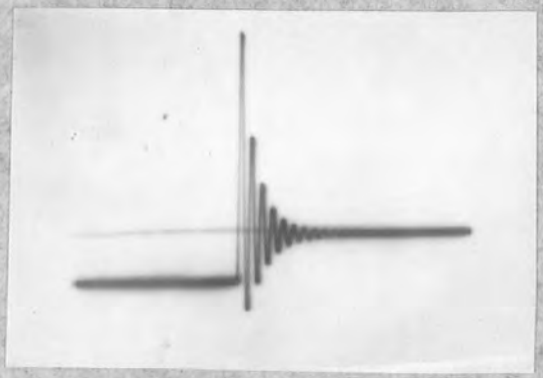

d_2 (1.2 KV)

Horizontal time axis = 5 m.secs

The various coils were tested successively by connecting them individually as anode load to the pentode whose grid was fed from the grid of V_2 of the multivibrator and the wave forms produced by the coils were displayed on a double beam cathode-ray tube which had for its time base trigger the grid wave form of valve V_1 of the multivibrator. The rapid decay of the oscillatory voltages produced at the pentode anodes at cut off required that the total time of X - sweep should be small in order to spread the wave forms, so that the asymmetry of the multivibrator had correspondingly to be increased to ensure that the pulses should be displayed, i.e., 't' (plate 5.3) was made considerably less than the period of sweep.

It was possible to pick up the wave forms for display on the C.R.O. in two ways, either by means of a direct connection to a potential divider connected between pentode anode and earth or, by merely suspending a lead from the C.R.O. near the coils which then acted as an aerial. One disadvantage of the latter method was that no indication of the actual or relative values of the high voltages produced could be obtained. There were other disadvantages which are discussed later.

Plate 5.6 a, b_1, b_2, c, d_1, d , shows the oscillatory wave forms generated by the four types of coils, the supply voltages for the pulse generators being 250v. The magnitudes of the respective voltage peaks and the time scale are indicated. The wave forms depicted were the same whether direct or aerial pick up was used provided the potential divider was large enough

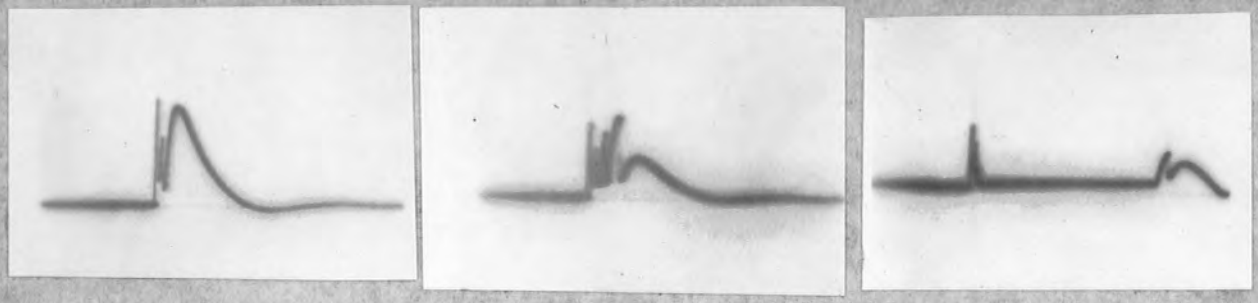

a. b. c.

PLATE 5.7

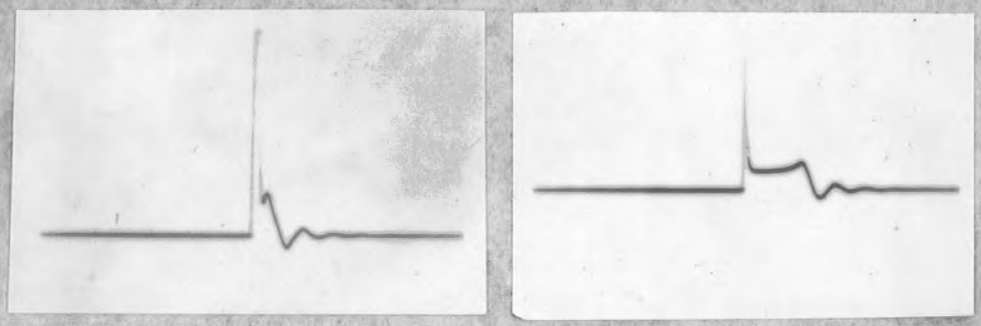

a. b.

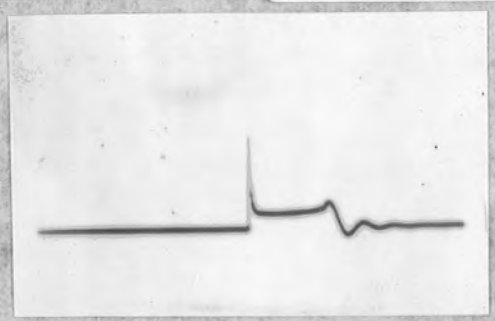

c.

PLATE 5.8

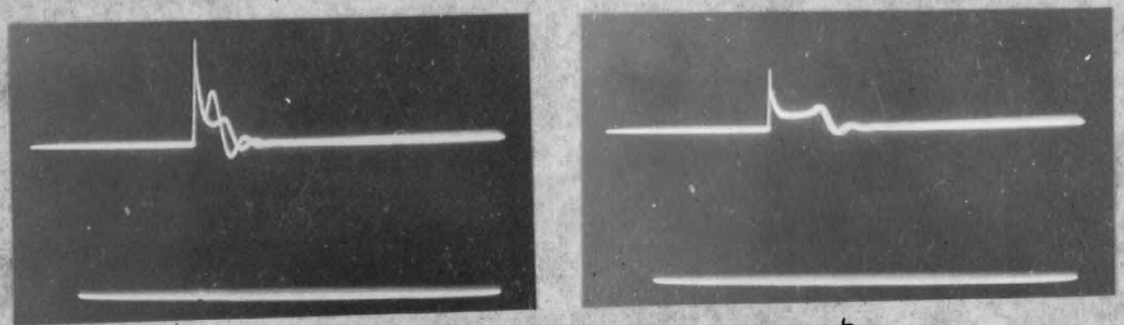

a. b.

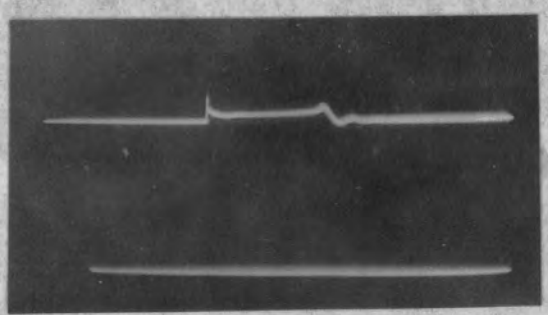

c.

PLATE 5.9

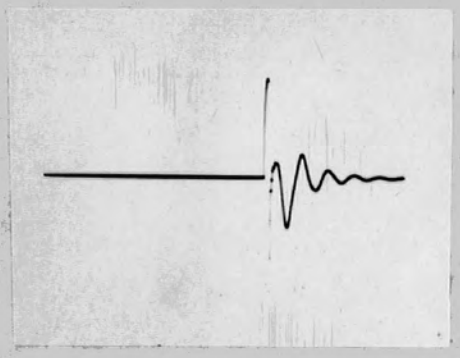

a.

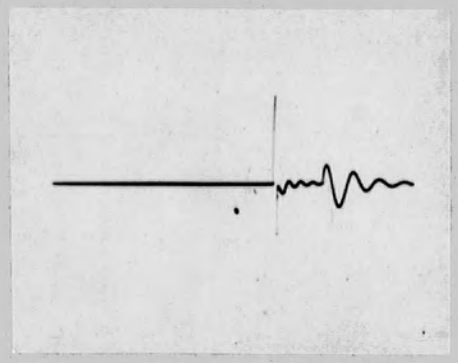

b.

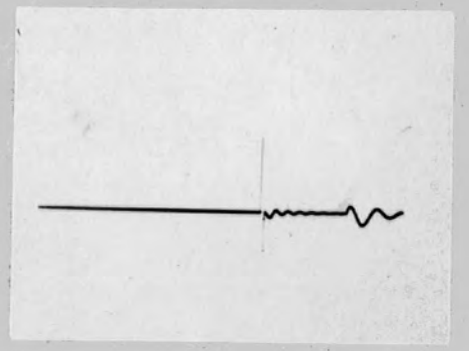

c.

PLATE 5.10

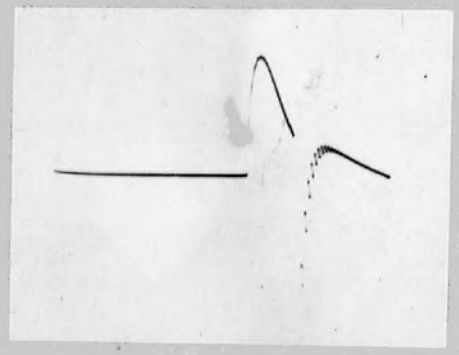

a.

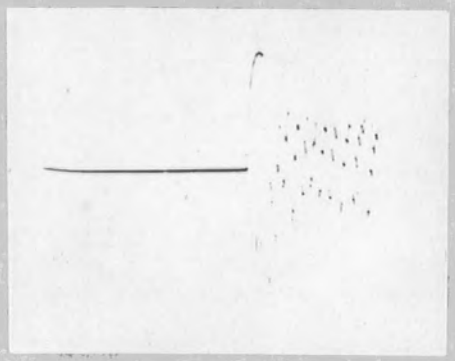

b.

PLATE 5.11

not to cause a more rapid decay of the oscillations by bleeding energy to earth and at the same time forming a resistance path to earth so that there was not a current break effectively to zero at cut-off. In this respect the aerial pick up gave a check as to whether or not the potential divider was large enough.

The effect upon the oscillatory wave forms of damping the oscillations by the introduction of a spark gap across the coils or to earth from the anode can be seen from plates 5.7, 5.8, 5.9 (a.b.c) which apply respectively to the high voltage transformer secondary winding, the Rhumkorff coil and the 20 henry chokes. The supply voltage was again 250 volts and the three plates for each apply to a large, medium and small gap respectively. The coils d_1 and d_2 were tested only with a 500 volt supply and the voltage peaks were not large enough to allow for a range of spark gap sizes. Plates for these two coils are not shown as with such a small spark gap reproducible wave forms could not be produced; the wave forms were similar to that of plate 5.8a allowing for the lateral discontinuity of the horizontal axis (plate 5.6 d_1 d_2).

Further to the remarks already made about the aerial method of pick up for displaying the voltage wave forms, plate 5.10 (a.b.c) and 5.11 (a.b) show the traces displayed on the C.R.O. using the small Rhumkorff coil and high voltage transformer respectively with aerial pick up. For the Rhumkorff coil there was the usual three spark gap sizes

(approximately 5,3 and 2 millimetres) and a large and medium gap for the transformer coil. The direct pick up connection for the two cases showed wave forms similar to those of plates 5.8 (a.b.c) 5.7 (a.b). A distinct difference can be seen in the two methods of pick up, though displaying the two methods simultaneously using both beams of the C.R.O. showed that either method indicated the same point for the occurrence of the spark on the wave forms. Further disadvantages in the use of the aerial method of pick up are now immediately apparent. The true relative voltages at the pentode anodes are not shown due to the fact that the input condenser to the C.R.O. amplifier has one side floating and large magnetically induced voltages indicate a large though false negative voltage occurring immediately after the passage of the spark. What was estimated to be the exponential decay of this voltage is well shown on plate 5.11(a) and to a much less extent on the three parts of plate 5.10. Plate 5.11 (b) is just discernible as a tenfold spark. The high frequency oscillation on the return trace from the negative kick was also due to the C.R.O. coupled with the aerial lead which had a certain amount of self inductance and capacity to earth via its mesh screening. These oscillations made the wave forms difficult to decipher and were absent in the instances where direct pick up was used.

Further discussion of the above photographs is delayed until sections 33 and 34.

31. Analysis of Coil Behaviour.

Glasoe and Lebacqz[38] quote the result

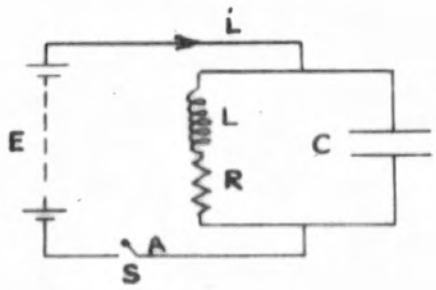

S--- SWITCH

C--- DISTRIBUTED CAPACITANCE OF CHOKE

L.R--- INDUCTANCE, RESISTANCE OF CHOKE

E--- POTENTIAL ACROSS CHOKE

FIG. 5.9. INDUCTIVE KICKER.

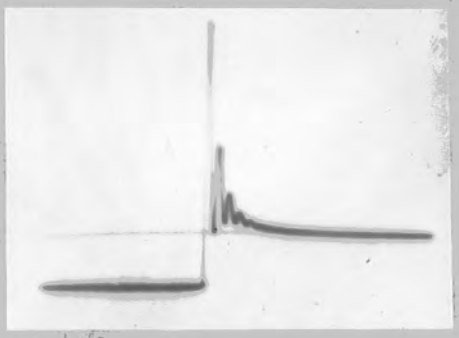

PLATE 5.12

$$V = I.\sqrt{\frac{L}{C}}.\ \mathrm{Sin}\ \frac{t}{\sqrt{L/C}} \qquad \ldots\ldots\ldots\ldots\ldots\ldots\ldots\ldots\ldots\ldots (5.12)$$

for the voltage appearing across the condenser C of the 'inductive kicker', fig. 5.9. at a time 't' seconds after the switch S is opened. This is an approximation to the complete solution of the differential equation which governs the flow of charge in the circuit after breaking the switch and is operative in the case when the inductance L has a negligibly small resistance, i.e. the damping term of the governing equation is neglected. If C is taken as the distributed capacitance of the inductive anode load of the pentode pulser and E the steady state potential across the inductance L then the figure can be taken as the equivalent circuit diagram of the pulse generator.

The equation to be solved applicable to the circuit is:-

$$V - L\ \frac{di}{dt} - R\ i = 0 \qquad \ldots\ldots\ldots\ldots\ldots\ldots\ldots\ldots\ldots\ldots (5.13)$$

$$\text{or}\quad \frac{q}{c} + L.\frac{d^2q}{dt^2} + R.\frac{dq}{dt} = 0 \qquad \ldots\ldots\ldots\ldots\ldots\ldots\ldots\ldots (5.14)$$

and must satisfy the initial conditions which are:-

$$i = I = \frac{E}{R} \text{ at } t = 0 \text{ and } q = Q = CE \text{ at } t = 0$$

The general solution is

$$q = e^{-bt}\ (A.\mathrm{Cos}\ \alpha t + B.\mathrm{Sin}\ \alpha t) \qquad \ldots\ldots\ldots\ldots\ldots\ldots (5.15)$$

where A and B are constants to be determined and $2b = \frac{R}{L}$ and $\alpha = \sqrt{a^2 - b^2}$ where $a^2 = \frac{1}{LC}$.

Evaluating the constants by use of the initial conditions, the complete solution becomes:-

$$q = CEe^{\frac{-Rt}{2L}}\left\{\mathrm{Cos}\sqrt{\frac{1}{LC} - \frac{R^2}{4L^2}}.t + \frac{1}{\sqrt{\frac{1}{LC} - \frac{R^2}{4L^2}}}.\left(\frac{R}{LC} - \frac{1}{RC}\right)\mathrm{Sin}\sqrt{\frac{1}{LC} - \frac{R^2}{4L^2}}.t\right\} \ldots (5.16)$$

This equation can more conveniently be written in the form:-

$$q = CEe^{\frac{-Rt}{2L}} \cdot \left\{ 1 + \frac{\left(\frac{R}{2L} - \frac{1}{RC}\right)^2}{\frac{1}{LC} - \frac{R^2}{4L^2}} \right\}^{1/2} \cos\left\{ \left(\frac{1}{LC} - \frac{R^2}{4L^2}\right)^{1/2} . t - \beta \right\}$$

$$= \frac{Ee^{\frac{-Rt}{2L}}}{R.\left(\frac{1}{LC} - \frac{R^2}{4L^2}\right)^{1/2}} . \cos(\alpha.t - \beta) \quad \ldots\ldots\ldots\ldots\ldots\ldots\ldots\ldots (5.17)$$

where $\beta = \tan^{-1}\left\{ \frac{\frac{R}{2L} - \frac{1}{RC}}{\left(\frac{1}{LC} - \frac{R^2}{4L^2}\right)^{1/2}} \right\}$ ..... (5.18)

In this form it can readily be seen that:-

(a) The magnitude of the voltage maxima are directly proportional to the steady state voltage across the inductance.

(b) The period of oscillation is given by:-

$$\frac{2\pi}{\left(\frac{1}{LC} - \frac{R^2}{4L^2}\right)^{1/2}} \quad \ldots\ldots\ldots\ldots\ldots\ldots\ldots\ldots\ldots\ldots\ldots\ldots (5.19)$$

(c) In the absence of the damping term the amplitude of sustained oscillations is:-

$$\frac{E}{RC.\left(\frac{1}{LC} - \frac{R^2}{4L^2}\right)^{1/2}} \quad \ldots\ldots\ldots\ldots\ldots\ldots\ldots\ldots\ldots\ldots\ldots\ldots (5.20)$$

(d) The rate of damping is increased with increasing R and decreases with increasing L.

The effect of introducing an iron core into a normally air cored coil is twofold; there results an increase in both the inductance and the eddy current losses. Plate 5.12 shows the increased damping caused by introducing a partial iron core into coil d_2 (layer wound) and there would appear also to be a slight increase in period.

The theoretical first voltage maximum is given by eq. (5.17)

upon substituting the principal value of $(\alpha t - \beta)$ obtained by equating to zero the first derivative of q with respect to time. Thus, as $q = CV$

$$\dot{V} = \frac{E}{RC\alpha}\left\{-\frac{R}{2L}e^{\frac{-Rt}{2L}}\cos(\alpha t - \beta) - e^{\frac{-Rt}{2L}}\sin(\alpha t - \beta)\right\} = 0 \quad \ldots(5.21)$$

which yields $\tan(\alpha t - \beta) = -\frac{R}{2L\alpha}$ .....(5.22)

$$\therefore \cos(\alpha t - \beta) = \frac{2L\alpha}{(4L^2\alpha^2 + R^2)^{1/2}} \quad \ldots(5.23)$$

$$\therefore V_{max} = \frac{E}{RC\alpha} \cdot e^{\frac{-Rt}{2L}} \cdot \frac{2L\alpha}{(4L^2\alpha^2 + R^2)^{1/2}} \quad \ldots(5.24)$$

and as $e^{\frac{-Rt}{2L}}$ is very nearly unity for the first maximum $V = \frac{E}{R}\sqrt{\frac{L}{C}}$ which is the approximation given at the beginning of the section.

Using a C.R.O. the inductance and capacitance of the Rhumkorff coil were found by measuring the ringing periods with and without an additional parallel capacitance.

In eq.(5.19) neglecting $R^2/4L^2$ in comparison with $1/LC$, with C' as the value of the additional capacitance, the two periods of oscillation T' and T'' are given by

$$T'^2 = 4\pi^2 . LC \quad \text{and} \quad T''^2 = 4\pi^2 L(C + C') \quad \ldots(5.25),(5.26)$$

from which

$$C = \frac{T'^2 C'}{T''^2 - T'^2} \quad \text{and} \quad L = \frac{T''^2 - T'^2}{4\pi^2 C'} \quad \ldots(5.27),(5.28)$$

and if $T'' = 2T'$, then $C = \frac{C'}{3}$ and $L = \frac{3T'^2}{4\pi C'}$. The values of C and L calculated in this way were:-

C = 147.4 μf and L = 23.6 henry, which upon substitution into the equation $V = \frac{E}{R}\sqrt{\frac{L}{C}}$ give V = 9.3 kv., and compares

favourably with the value of 10 - 11 kv measured with a C.R.O. and a potential divider.

32. Mechanism of the Spark Gap.

The mechanism whereby the flash tube discharge is initiated is the distortion of the electrostatic field between the flash tube electrodes, by the application of a sudden high voltage triggering pulse (in the case of triggered flash tubes), to such an extent that any free electrons in the contained gas become accelerated sufficiently to start an electron avalanche whereupon the main discharge takes place. The normal unsparked pulses had little effect in general in triggering the discharge, as is shewn later, in other words the rate of rise of voltage as given by eq. 1 had not ordinarily a sufficiently great accelerating effect upon such electrons. The irregularly spaced discharges which did occur when regularly spaced unsparked pulses were applied no doubt occurred quite statistically and were dependent upon the availability and distribution of electrons. In these respects it was difficult to see why a reduction of voltage brought about by the passage of a spark across the spark gap could bring about the incipient stages of the avalanche.

It was thought at first that the discharge in the flash tubes could be initiated by a differentiating effect of the spark gap upon the high oscillatory voltage. The lead to the triggering electrode has a certain amount of capacitance to earth and a large leakage resistance to earth or H.T., fig 5.10,

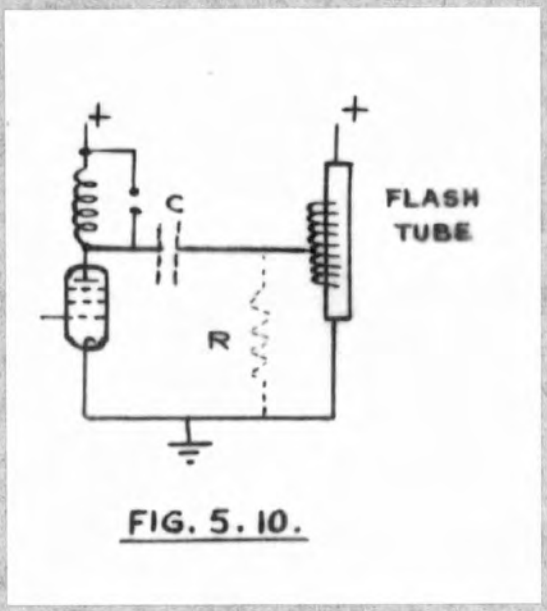

FIG. 5.10.

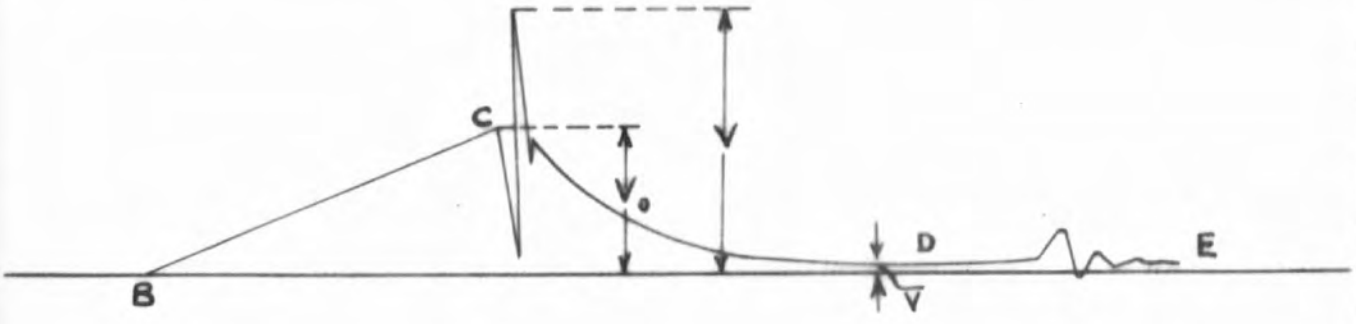

FIG. 5.11. ANODE PULSE WAVE FORM WITH HIGH FREQUENCY SPARK GAP OSCILLATION.

a differentiating action could occur, and thus augment the sharpness and magnitude of the sudden voltage change upon the passage of a spark. However, the magnitude of a pulse transmitted by such a condenser resistance network is less than that of the input pulse and thus, unless the triggering electrode be effectively locked to earth by virtue of this leakage resistance then the effect of the stray elements is merely to alter the rate of change of voltage and not to reduce the triggering electrode to a negative potential which could start an electron avalanche. The potential of the triggering electrode throughout a series of sparks and that of the anode side of the spark gap were observed by means of direct connections to the Y-plates of a double beam C.R.O., to reduce unwanted effects of the C.R.O. amplifier, and the initial voltage rise of the pulse coil acted as beam trigger. The spark gap was made small so that a fifty μ sec time base sweep could be used, and while in consequence of maximum brilliance the background intensity was so great as to vitiate photography, it was noted as was expected that at no time was there any indications of a voltage negative with respect to earth on the triggering electrode and also that the voltage fluctuations as shewn by both beams were, as far as could be seen, precisely the same.

The period during the passage of a spark was now further investigated. If a very high frequency oscillation occurred at A, fig. 5.9 upon the passage of a spark across the gap, then,

though the first quarter cycle would merely have the effect of reducing the potential of A to a point near earth (i.e H.T) relative to the potential across the flash tube and have no effect upon it, the next half cycle would very rapidly raise the potential of A, and hence the triggering electrode to something in the region of twice that across the gap just prior to sparking and just such a voltage rise would have the desired triggering effect. Using the same C.R.O. displaying technique as before but with a 50 μ-sec X-sweep and again full brilliance a very highly damped high frequency oscillation was just discernible though it was not found possible to photograph it. A very small spark gap was used, and diagramatically the trace was as indicated in fig.5.11. BC represents the initial drawn out rise in voltage of the anode, and the start of the decay CD appeared to be exponential. V was about twice V_o and $\bar{V}$ was about the supply voltage to the pulse generators. The portion DE was identifiable as similar to the end sections of previously shewn photographs of sparked pulses. This high frequency oscillation appeared to have a frequency of about 10 megacycles/sec. or more. The Rhumkorff coil was used throughout this experiment.

The leads from the choke to the spark gap enclose a certain area and hence have a limited inductance and a certain amount of ohmic resistance so that the high frequency oscillation was considered due to the L.C.R. of the spark gap circuit, where, the capacitance was the distributed capacitance of the choke;

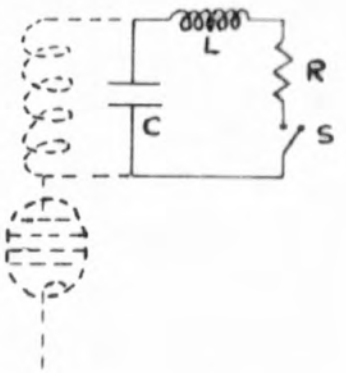

C --- DISTRIBUTED CAPACITY OF CHOKE

L, R --- INDUCTANCE AND RESISTANCE OF LEADS.

S --- SPARK GAP.

FIG. 5.12. EQUIVALENT CIRCUIT OF SPARK GAP.

the equivalent circuit was therefore that of fig 5.12. The spark gap acted as a switch which closed upon the passage of a spark. The analysis of the circuit is similar to that given previously, the difference lying in the initial conditions which are here v = Vo, i = Io at t = 0. Assuming the capacitance of the gap to be zero, i.e., negligible in comparison to the capacitance of the choke and hence unaffecting the initial conditions (q = Q = (C+c)V), and to consist of only a small resistance (that of a conducting gap) the solution with similar notation is:-

$$v = Ve^{-bt}(\cos\alpha t + b\sin\alpha t) \quad \ldots\ldots\ldots\ldots\ldots\ldots\ldots (5.29)$$

The value of $b = \frac{R}{2L}$ is very large, the inductance of the connecting loop being very small while R is relatively large, consisting of the sum of the lead resistance (small) and the resistance of the conducting gap which can be according to Morecroft [39] as high as $\frac{1}{2}$ ohm, hence, as observed the damping was very great, the period very small and so normally this oscillation was quite unnoticable.

33. Multiple Sparking and Spark Gap Conduction.

It can be seen from the plates showing the effect on the pulse shape of varying the spark gap size that the length CD, fig 5.11. of the voltage wave form increased as the spark gap size decreased, though the initial drop remained very sharp being the exponential discharge of the capacitance of the choke through the conducting gap. The effect was shewn to be variable at a fixed gap size by blowing a stream of air across

the gap which reduced the length CD and conversely, smoke or the presence of a radio-active material increased it. At the same time the maximum amplitude of the final burst of oscillations was seen to decrease with increase of this 'quiescent" state. It was thus concluded that a current flow was maintained across the gap for a time whose variations about a mean, for a particular gap size, were thought to be quite random, then, conduction ceased whereupon, to a smaller degree, the whole process was repeated as for the original steady current cut off, hence the continued oscillations DE, fig.511. An explanation was herein found for the phenomenon of multiple sparking which was very obvious with the high voltage transformer, particularly with the large gap sizes. The mean free path in air at atmospheric pressure being very small ($2{\cdot}1 \times 10^{-5}$ cm) there was little likelihood of persistent residual ionisation in a large gap and only a small part of the available energy of collapse of the coils' magnetic field was dissipated by the passage of a spark and the second effective current break was sufficient to produce a further high voltage oscillation which only in the case of extremes of gap sizes was insufficient to cause the passage of a second spark. The process could then be repeated several times.

This brief investigation of the phonomenon associated with the spark gap was carried out in the course of the work and the conclusions reached were in agreement with the work of J.P. Molnar(40) on Townsend discharges in argon following that of

R.W.Engstrom and W.S. Huxford[41], which showed the existence of 'metastables' in the interelectrode interspace. There appears, however, to be no published work concerning the existence of a continued conduction with spark gaps in air at atmospheric pressure.

34. Choice of Inductive Load.

The smoothing chokes 'c' were immediately discarded because they could not withstand the high voltages for any length of time before breakdown of the insulation occurred. Breakdown either across the interelectrode space of the pentodes or in the coil insulation was manifest by discontinuities in the voltage wave forms of the same type as were produced by the passage of a spark, though in general smaller in nature.

Large almost critical damping was seen to occur with the high voltage transformer coil (resistance 8000 ohm) though the available energy was large and the dissipation of this energy was by no means completed by the passage of a single spark across the gap. In virtue of this, multiple sparking occurred, as shewn above, at all but the largest and smallest of gap sizes and with the latter the resulting pulse was insufficient to trigger the flash tubes. A single spark could be produced with this coil but only with difficulty and constant adjustment to the gap and even then the position at which the spark occurred on the voltage rise showed considerable variation (see particularly the single spark of plate 5.11 a

using aerial pick up). It will be shown later that the flash tube discharge occurred ideally very shortly after the sudden drop in voltage associated with the spark. The multiple sparking was apt to occur with both the transformer coils and the Rhumkorff coils with large gaps with both of the pentode supply voltages of 500v and 250v, particularly at the former, and it will be apparent under the discussion on flash tubes, that was highly undesirable. It could be eliminated by the use of coils with not too high an inductance, the stored energy being thus limited and largely dissipated by the passage of a single spark across the gap, and having an appreciable energy dissipation due to eddy current losses in the core, and ohmic losses. In these respects the Rhumkorff coils were best suited for the purpose, provided the supply voltage was limited to 250 v, and were in consequence adopted as a final choice of inductive load for the pentode pulsers.

From the point of view of knowing when the flash tubes fired it was highly desirable that the discharge took place at the time of sparking. It was necessary then to ensure that the spark occurred at the same point of the voltage pulse curve to within negligibly small limits. The statistical lag in the discharge across a spark gap supplied with the theoretical break down voltage can be of the order of $\frac{1}{2}$ second but this uncertainty can be reduced to a very small amount if the applied voltage is increased from below the breakdown voltage to a value in excess of it. If the rate of rise is rapid

enough and the same on successive occasions then the spark will occur at effectively the same point on the voltage curve. The maximum pulse voltage that could be produced by the Rhumkorff coils was very much in excess of that necessary to trigger the flash tubes, so the spark gaps were set to fire early in the first quarter cycle of the high voltage oscillations, but at the same time late enough to be capable of producing a sufficiently high triggering pulse. Set in this position a C.R.O. showed that the sparks took place across the gap to within a few micro-seconds of the same position on the voltage curve. Two similar Rhumkorff coils were available and they showed almost identical responses to current cut-off.

A distinct delay existed between the arrival of the multivibrator cut-off pulse at the control grid of the pentode pulser and the occurrence of a spark, due to the oscillatory frequency of the anode load, transit time etc., but the delay incurred was, however, the same for both pulse generators and so the interval between the two flash tube triggering pulses could be taken as the conducting time 't' of the valve V_2 of the multivibrator.

35. <u>The Flash Tubes.</u>

A flash discharge tube in general consists of a straight or spiral tube of hard glass or quartz into the ends of which are sealed electrodes, the tube being filled with a rare gas at high or low pressure. Essential to the operation of such

tubes is a high current density during the discharge and this is obtained by discharging through the tube a condenser charged to a relatively high potential. A single flash of light of luminous energy that is a function of the charge on the condenser and condenser voltage is thus produced upon discharge. Such tubes, by suitable design and filling, may be used to give single light flashes or as a stroboscopic source at rates well over 1000 flashes a second.

The instantaneous wattage dissipated is of a high order and can be calculated from the formula $\frac{CV^2 . 10^{-6}}{2}$ = energy in joules (watt-seconds), where C is the condenser capacity in micro-farads and V is the voltage to which the condenser is charged. The average power in watts can be obtained by dividing this quantity by the time of discharge in seconds. The whole of the energy is not dissipated per flash, a residual voltage of order 100 volts remaining on the condenser after the discharge has passed, also, there are ohmic losses but these can be made negligible by careful circuit design.

The important characteristics of the tubes are the rate of rise of light intensity, its duration and nature. These are determined by the capacity of the condenser and the potential to which it is charged, by the inductance and resistance of the circuit and by the gas used and the pressure to which the tube is filled. The duration of the flash increases proportionately with the capacity of the condenser but little with the voltage so for a given energy a high voltage and small

capacity gives a shorter more intense flash. Low pressure filling increases the flash duration as also does the resistance and inductance of the circuit. Thus, spiral flash tubes have a longer flash duration than straight tubes while leads to the flash tubes should be made to enclose as small a loop as possible. Argon filling gives a spectrum rich in the blue violet and is thus photographically very suitable while Xenon and Krypton approximate better to sunlight[32][33]. (The spectrum is a continuum with a super-posed spark spectrum). Impurities and high pressure make the initiation of the discharge more difficult and hydrogen increases the breakdown voltage and at the same time affects the triggering of the tube in an adverse manner. For stroboscopic flashing rapid de-ionisation is assisted by the proximity of the tube walls, resulting in tubes with narrow conducting channels, alone or inside a main outer glass tube. A disadvantage to the narrow conducting channel is the tendency for the discharge to take place along the tube walls with possible local overheating with subsequent crazing and liberation of gases which mar the triggering characteristics of the tube and increase the breakdown voltage.

Basically the triggering mechanisms for the flash tubes fall into two groups.

1. Tubes fed with a potential supply below the hold off voltage which rely, for discharge initiation, upon the application of a triggering pulse to a third electrode near

very small; both types however can be given good triggering characteristics by the use of activated cathodes. The nature and shape of the electrodes has very little effect upon the operation of the tubes except that a pointed trigger electrode may cause erratic behaviour[32][33].

Ageing of the tubes became apparent by an increase in their erratic behaviour, control becoming difficult, no doubt due to the liberation of gas from the crazed tube walls, and by a black deposit on the walls of the tube near the cathode which greatly reduced the light intensity.

The blackening was due to metallic sputtering from the cathode under the extreme pulverisation it received during discharge. Laporte[44] eliminated this blackening by the use of bent tubes or an internal shield; with the tubes used here it was reduced to a minimum by connecting the tubes with the cathode as that electrode nearest the seal to the outer wall of the inner narrow channel, when the blackening was restricted to the region near the cathode and did not spread over the outer glass envelope.

36. Flash Tube Triggering.

Having assembled the stroboscope it was very soon obvious by watching the camera controlled switch in the light from the flash tubes that the time interval between the two flashes was not constant.

Using a cathode ray oscillograph it was soon established that the interval between the negative going grid swings of the

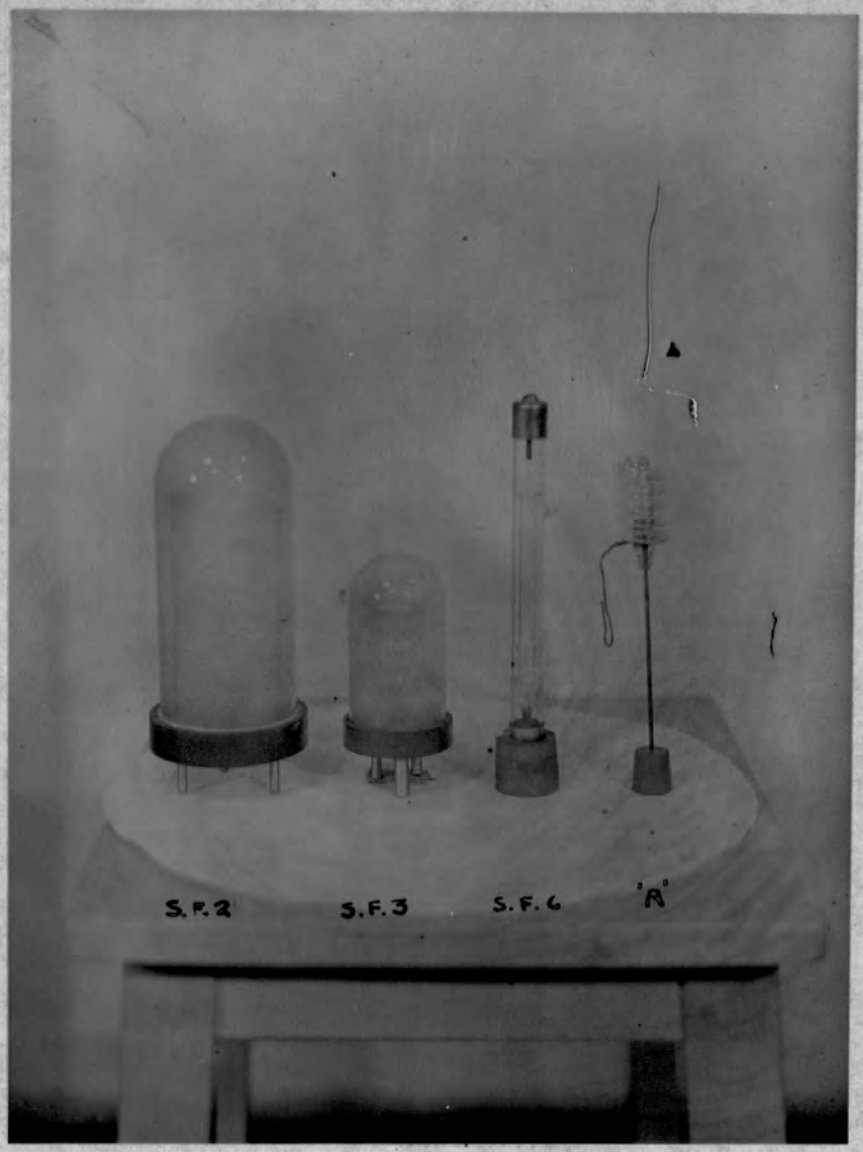

PLATE 5.13

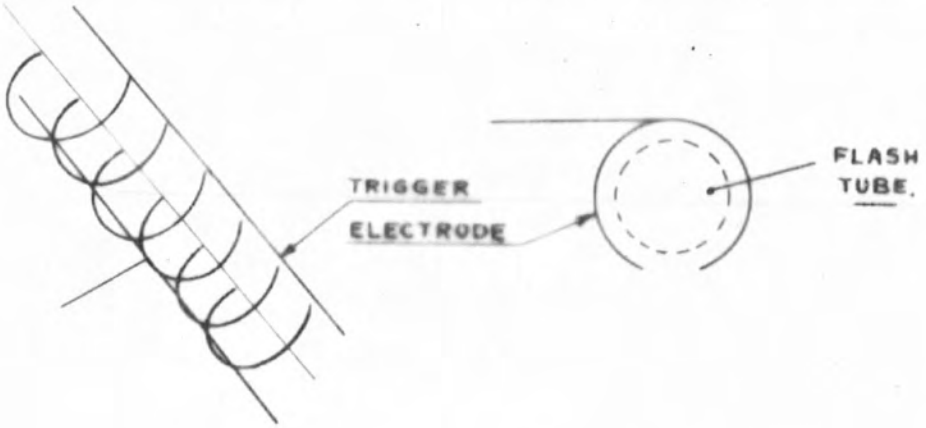

FIG. 5.14.

multivibrator were sensibly constant and so it was necessary to carry out an investigation into the discharge and triggering of the flash tubes with a view to determining the cause and magnitude of these variations and a means of eliminating them.

A double beam cathode-ray tube was employed so that the flash tube triggering pulse and a response from a vacuum photo-cell to the light flashes could be viewed simultaneously. The time base was triggered by the first of the two cut off voltages from the multivibrator and the time interval between the grid swings reduced so that a 5 or 1.5 milli-second time base sweep could be used. The width of the photo-cell response on the upper beam of the C.R.O. was not indicative of the response time of the flash tube but was a function of the resistance of the photo-cell circuit and input capacitance of the C.R.O. amplifier. The leading edge of the trace was an indication of the initiation of the discharge.

A triggering electrode for a flash tube is shewn in perspective in fig 5.14.

At a later stage there became available three other types of flash tubes, S.F.2, S.F.3, and a special activated cathode tube which is here called tube 'A', and these with an S.F.6. are shewn in plate 5.13.* These tubes were tested also to determine if they could be substituted for the S.F.6's and whether any of their features could be incorporated with

* We were indebted to Messrs. Siemens Lamp Supplies Ltd., who put these flash tubes at our disposal.

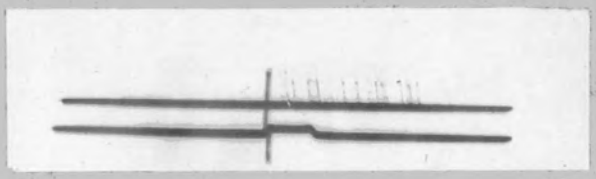

a.

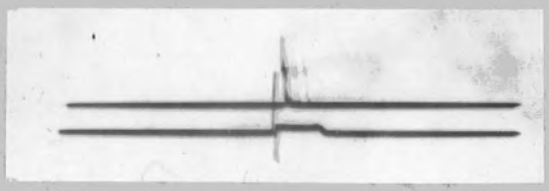

b.

PLATE 5.14

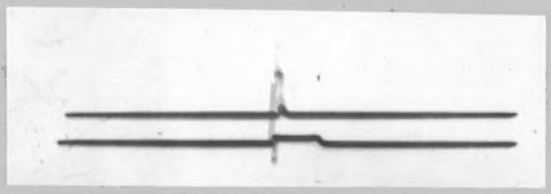

c.

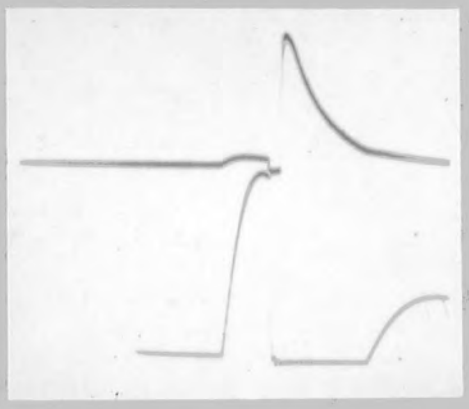

a.

b.

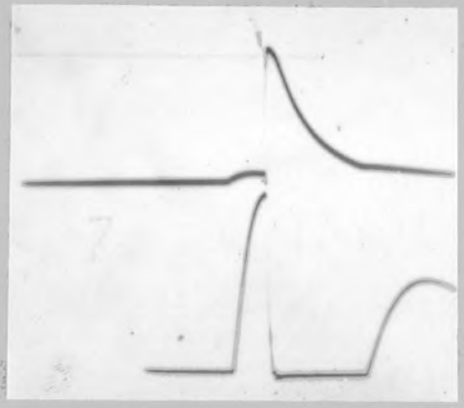

c.

PLATE 5.15

advantage in a modified S.F.6. Inside the pearl envelopes of tubes S.F.2 and S.F.3 the assembly was similar to that of tube 'A'.

Plate 5.14(a) shows a time exposure of the two C.R.O. traces with a five milli-second time base sweep. The upper trace was the photo-cell response to the S.F.6.flash tube which was operated at 2100 volts; the pentode pulser supply was 250 volts and the anode load used was a Rhumkorff coil. The lower trace was the trigger pulse. Plate 5.14 b,c, shows similar results with a flash tube supply of 2400 volts and 2700 volts respectively. The triggering response was much better at the higher voltages but there was the decided disadvantage that the tube was overloaded. The order of voltage at the spark gap on firing was 7000 volts.

It was not possible to take time exposures of the photo-cell response and triggering pulse when the transformer coil was being used as pulse coil owing to the large scatter in the position of the sparking point and the multiple sparking. With a pulser supply of 250 volts and a supply to the flash tubes of 2100 volts, single exposures were taken of the two C.R.O. beams of which three are shewn in plate 5.15 a,b,c. The spark gap was adjusted to its maximum to give generally single sparks. A delay of about .15 milli-second between sparking and flash tube discharge is shewn in 'a', a double spark in 'b' and a 'quiescent' state of about one milli-second is shewn in 'a' and 'c'. These two times were by no means the

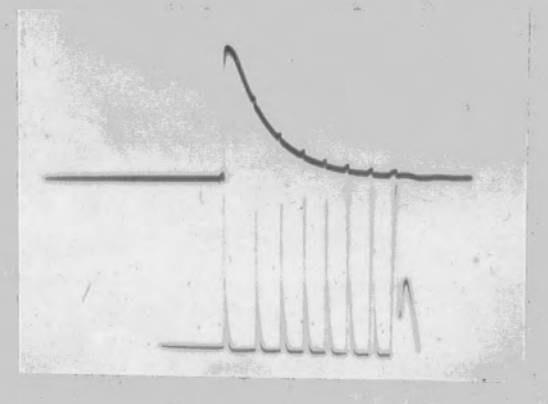

a.

PLATE 5.16

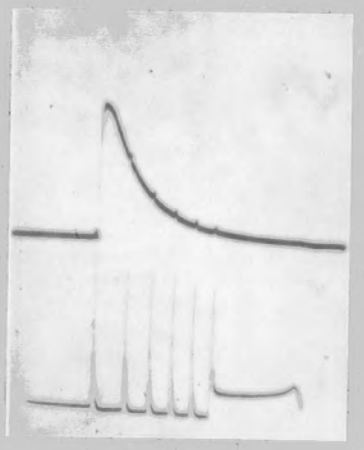

b.

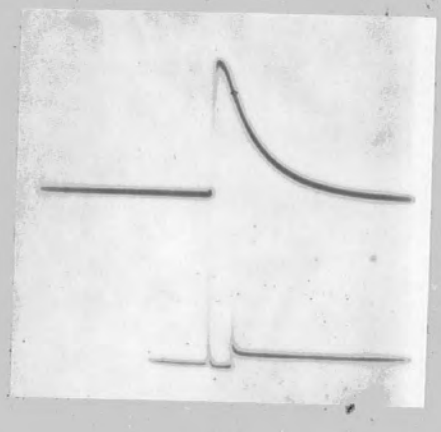

c.

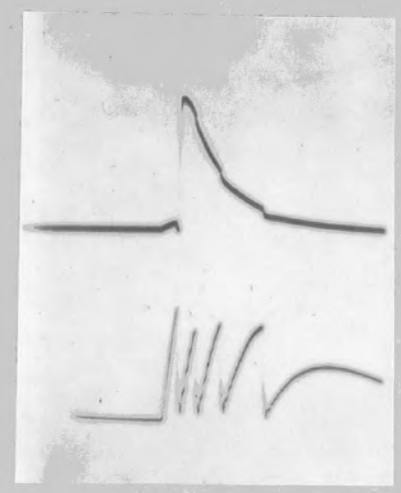

a.

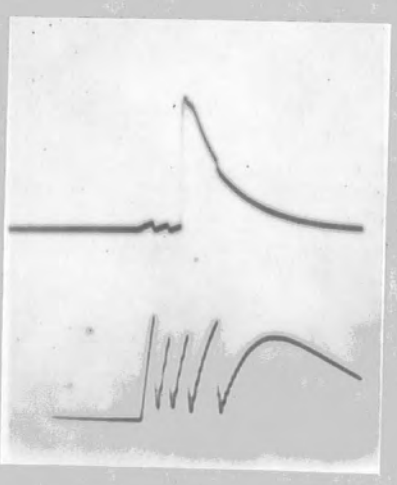

b.

PLATE 5.17

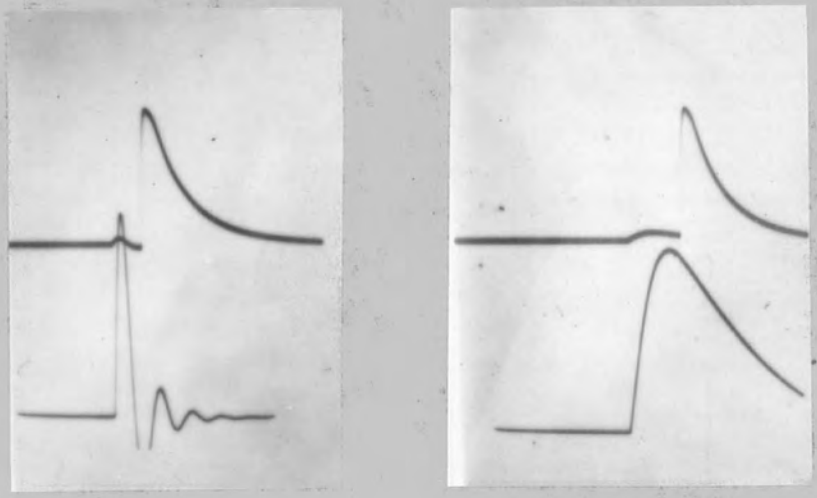

a. b

PLATE 5.18

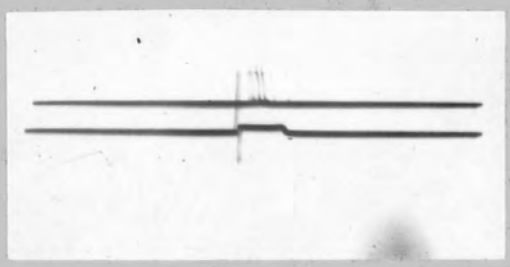

PLATE 5.19

maximum which were encountered when using the transformer coil pulser.

The pulser supply voltage was now increased to 500 volts in order to increase the triggering voltage (the flash tube supply remaining at 2100 volts). Multiple sparking was immediately detectable by ear and some results obtained by photography of the traces are shewn in plate 5.16 a,b,c, for large, medium and small spark gaps respectively, (approximately 7,5 and 2 mm). The voltage at sparking was estimated to be about 12 - 14 kv for the largest gap. The traces are a good example of multiple sparking and in 'c' can be seen a quiescant state of more than two milli-seconds. The discharge of the flash tube on all of these three occurred correctly upon the passage of the spark; in contrast, plate 5.17 a,b, obtained under similar conditions with the transformer coil and as few multiple sparks as possible, shews a slight delay in 'a' but flashing between the second and third pulses in 'b'. A delay could be detected by the fortuitous interference between the two beams of the C.R.O., as could be seen on inspection of the photographed traces. With a 500 volt supply to the pulser and with the Rhumkorff coil and transformer coil, in the absence of a spark gap, the triggering responses were as shewn in plate 5.18 a,b respectively. These plates were typical but do not shew the maximum delays which were obtained under such conditions.

Changing the trigger electrode to the form of intimately

wound turns of wire round the flash tube over about two thirds of its length between electrodes, produced a better triggering response as is indicated in plate 5.19 which was obtained in a similar manner to the plates above, with a sparking potential of about 7000 volts, 2100 volts on the flash tube supply condensers and a 250 volt supply to the pulser and a Rhumkorff coil. Delays still existed but very much reduced when compared with the responses of plate 5.14 a,b,c.

The examination so far indicated that better triggering on the whole was obtained by the use of higher voltage triggering pulses and higher supply voltages to the flash tubes, neglecting the obvious improvement by the altered trigger electrode. Both of these remedies however suffered from distinct disadvantages. The higher the triggering pulses the greater was the tendency for feed back to occur to the multivibrator and oscillator, (section 28), and over-running the flash tubes was occasioned by their increased operating voltages. Added to this there were no two balanced tubes, and whereas the operation of one was temporarily improved by the increased voltage the other suffered adversely, tending to become self-triggering with the overheating, in all events both tubes soon reached this state.

The photographs clearly shewed that the delays were quite random and in some cases as high as 2 milli-seconds and more. With the best triggering responses obtained there still existed delays which could be as high as .3 milli-seconds, and

though quite small when compared with flashing intervals of 25 milli-seconds or so, constituted appreciable uncertainties with the smaller flashing intervals of two or three milli-seconds for a flow at a Reynolds' number of 6000 or so. When known profiles were being measured actual velocities could not be deduced if the flashing intervals were erratic, though it was possible to find a multiplying factor for the measured velocities from each frame of the cine-film record so that the results formed a smooth curve. This process could not obviously be applied to the case of unknown profiles when anomalies were being sought. It was then essential to obtain tubes with reliable triggering characteristics to within negligible limits. Even with the increased voltage trigger pulses delays still existed and there was no certainty that the discharge would occur upon the passage of the first spark of a multiple spark.

Tubes S.F.2, S.F.3 and tube 'A' were now available for testing. The triggering electrodes of S.F.2 and S.F.3 had the form of a conducting strip interwoven round the turns of the spiral conducting glass channel while tube 'A' was triggered by applying the trigger pulse to a piece of gauze round the central portion of the spiral tube which contained the activated cathode.

S.F.2 was found rather difficult to trigger with this type of pulse when operated at 2100 volts, and required the largest pulse obtainable using a Rhumkorff coil with a 250 volt

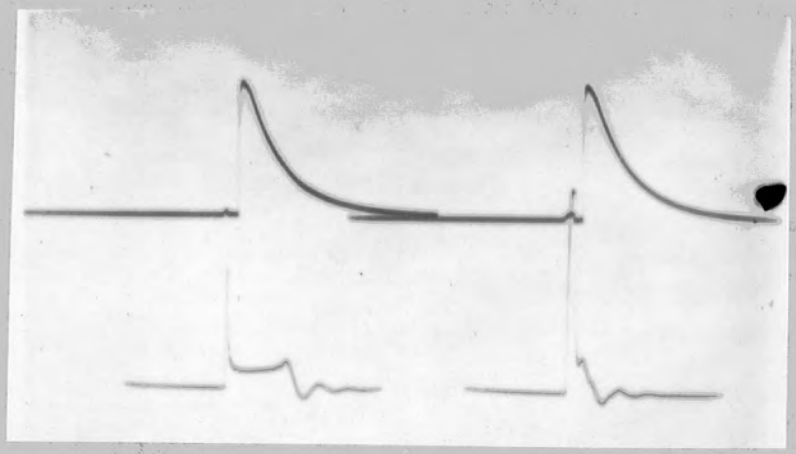

a. b.

PLATE 5.20

a. b.

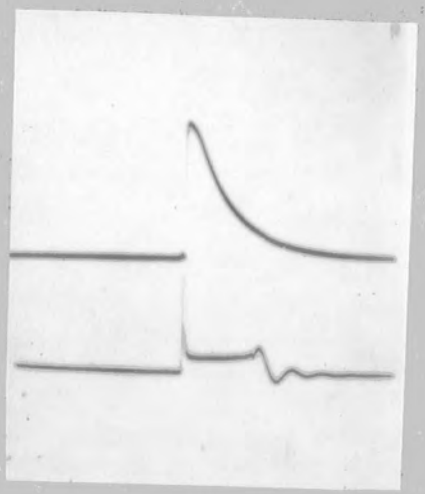

c.

PLATE 5.21

supply to do so, with consequent uncertainty in the position of the spark. It was found that the tube became more easily triggered after operating the tube for a little while until it became heated. A simple triggertron pulser was set up which gave 7 kv or 14 kv pulses and while the triggering was improved slightly by this means, the delays were not removed completely. It was not considered worth while carrying on with the triggertron pulser as it did not accomplish any great improvement, as was soon shewn by a few tests, and in any case it would have necessitated a large measure of rebuilding and amending of the equipment. With the supply arrangements etc. the same as for the S.F.6 tests above (250,2100 volts), two typical photographs obtained in the usual manner are shewn in plate 5.20 a,b with a large and medium spark gap. The time base sweep was five milli-seconds and the delays in firing can be seen to be about .1 - .15 milliseconds.

In a precisely similar manner the three plates 5.21 a,b,c, were obtained with tube S.F.3 and the Rhumkorff coil for three different sizes of spark gap.*

Tube 'A' gave excellent response to triggering at voltages well below the optimum operating voltage of 2000 volts with

* Little was done with tubes S.F.2 and S.F.3 as there appeared to be no better triggering response with them and further, their size and shape, considering the form of the apparatus, made them hardly suitable for substitutes for the straight type S.F.6 tube without severe modifications being carried out.

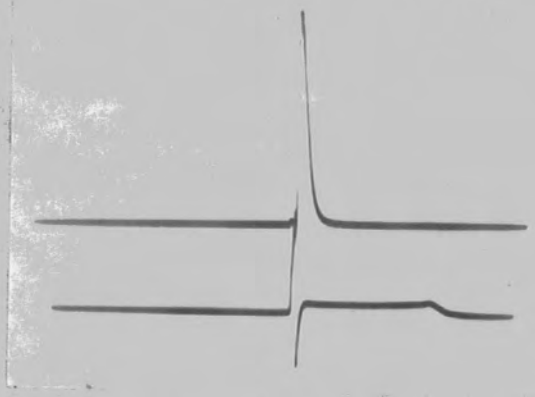

PLATE 5. 22

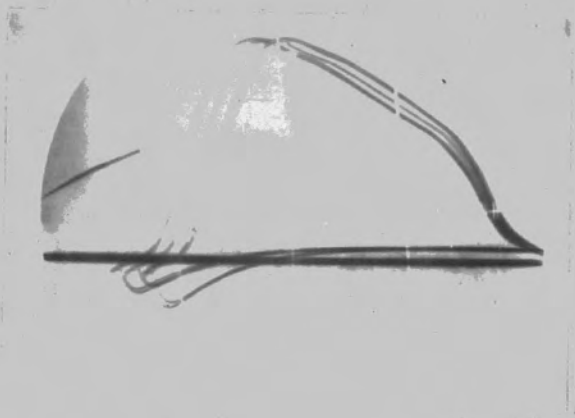

PLATE 5. 23.

delays barely discernible. So easily was the tube triggered that the discharge occurred well down the voltage rise to the sparking potential of the spark gap, and moreover, though the tube fired on the rise of the voltage curve, it fired at the same point on each occasion to within a few micro-seconds. By reducing the size of the gap drastically the sparking point could be reduced to below this critical point and then the flash tube became correctly triggered. In this triggering condition the only variations were in the jitter of the multivibrator and in the fluctuations of the sparking point of the gap which, as far as could be made out by means of the C.R.O. were only of the order of two or three micro-seconds. Plate 5.22 is a time exposure obtained in the usual manner though the conditions were somewhat altered. A resistance was connected in series with the pulser coil to reduce the steady state current and hence the magnitude of the pulse and the gap was reduced to $\frac{1}{2}$ millimeter so that the trigger was of the order of 1000 - 1500 volts. The time base sweep was 6 milliseconds and three or four exposures occurred. The plate shews that the triggering characteristics were excellent and for all practical purposes there was no triggering delay.

The obvious step now was to obtain S.F.6 tubes with activated cathodes. These were received through the kind co-operation of Siemens' Lamp Supplies Ltd., and their triggering response was of the highest order. Plate 5.23 shews a quintuple time exposure with a fifty micro-second time

base sweep and 2000 volts on the flash tube. The sweep was triggered by the actual triggering pulse which was of order 1000 volts. The only variations can be seen to lie in the position of the triggering spark.

In consequence of these investigations activated cathode tubes were obtained for the stroboscope.

CHAPTER 6.

PROFILE DETERMINATION

37. Experimental.

In carrying out the profile determinations set out below, the general procedure, as indicated in the previous chapters, was carried out.

From the investigations of the flashing delays of the flash tubes it was apparent that the flashing intervals could be repeated to within a few microseconds by using activated cathode flash tubes, and that the major errors met with would result from the human element, defects and limitations of the recording camera and measuring travelling microscope. It was unfortunate, however, that almost immediate upon the completion of the work on the stroboscope, there came about the failure of all save one of the activated cathode tubes. During the subsequent profile determinations therefore, the interval between the flashing of the two tubes underwent random fluctuations which were reduced however to a certain extent by operating the tubes at a voltage a few hundred volts in excess of the rated operating voltage. *

Variations of the flashing interval were manifest by observing the camera controlled switch during the course of a run and also by examining under a microscope the spacing

* These experimental activated cathode flash tubes were provided quickly for this work by Siemens Lamp Supplies Ltd., and the failure occurred due to insufficient annealing of the glass envelope. Such failures could not be expected to occur in

normal production tubes.

between dual images of the same droplet on consecutive frames. Following the same droplets from frame to frame of the cine camera record, where possible, provided a means of ascertaining the magnitudes of the interval variations and thus, multiplying factors could be obtained for the results from successive frames (neglecting other sources of error), so that they could be made to lie upon a common profile curve where such existed. This procedure however needed careful handling if only those droplets with low values of U/U_m could be followed. With the combination of human errors, limiting accuracy of the vernier and the engraving of its scale, and definition of the images, errors of a few hundredths of a milli-meter could occur and these represented, for very slow moving droplets near the tube wall and for cases of low flow rates, some 10-20% perhaps of the measured droplet spacing. In such instances as these it was preferable to plot the results as obtained and by inspection and trial and error choose factors until such time as it was estimated the best curve had been achieved.

Fortuitously the flared entry to the flow pipe, which was made of perspex, was of a good shape and very large Reynolds No's could be obtained with water, the flow remaining rectilinear. As indicated by a dye streamer, Reynolds No's as high as 50,000 or more were obtainable with the flow still laminar. Such high Reynolds No's were not attainable when there were dispersed oil droplets born by the water, though turbulence even so did not

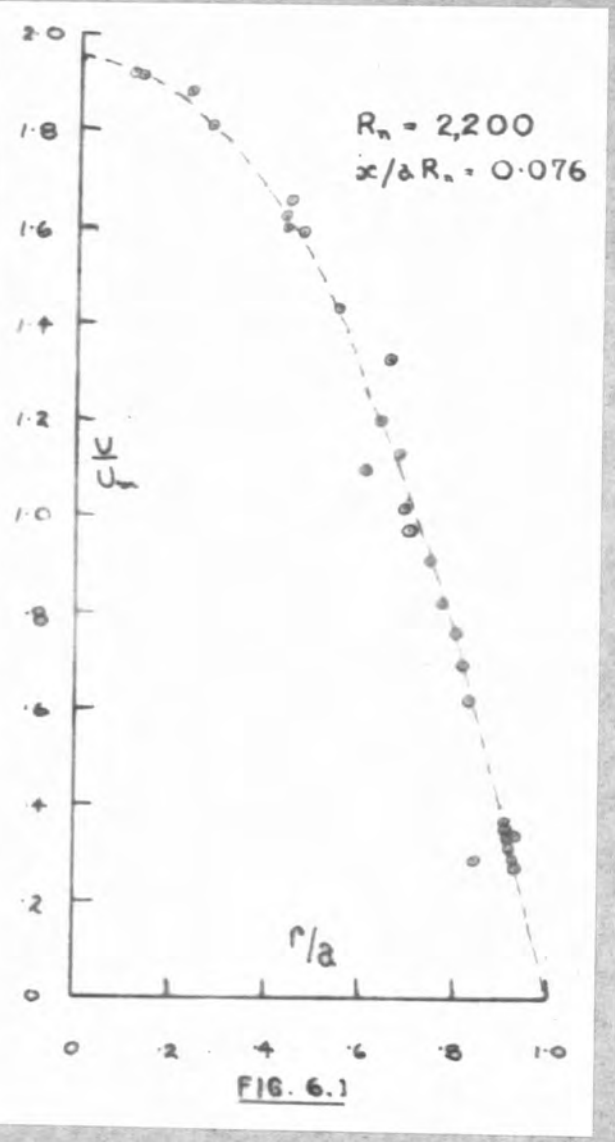

FIG. 6.1

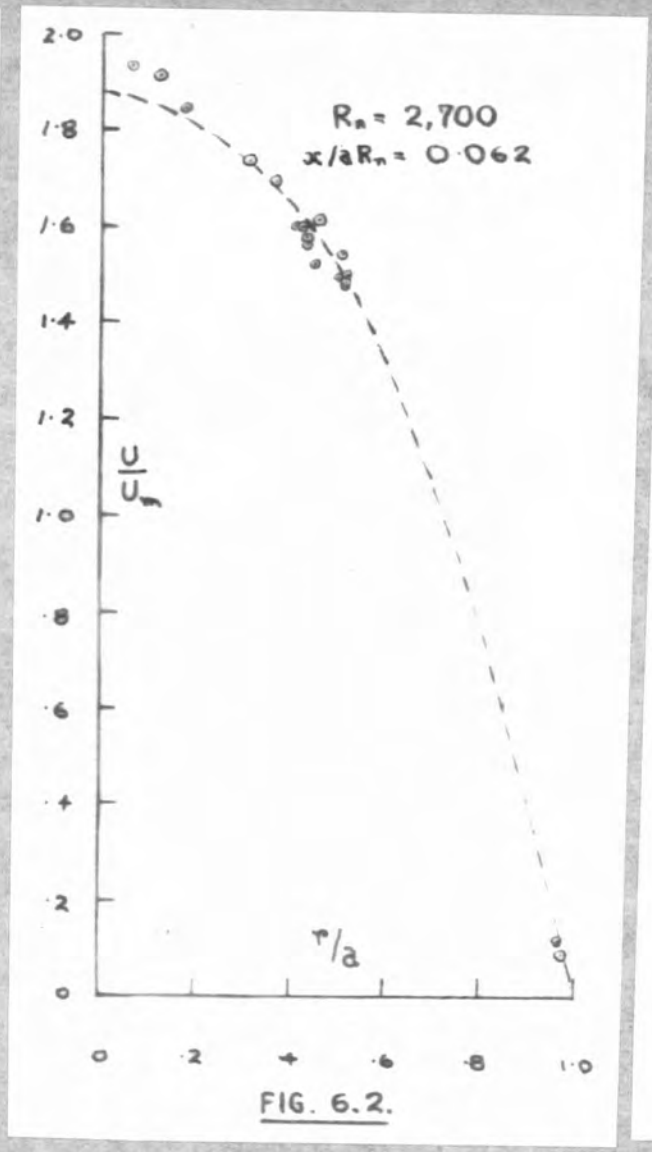

FIG. 6.2.

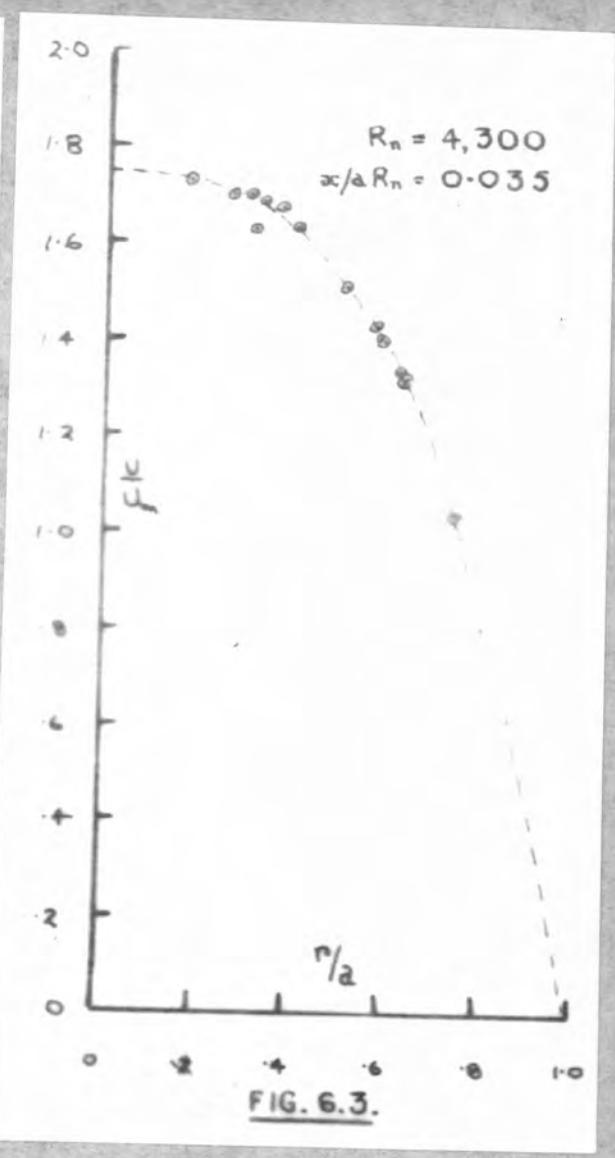

FIG. 6.3.

set in until unusually high values of the Reynolds No's were reached.

The following table gives the values of the flow rate and Reynolds No's. for the profiles determined and also the conditions under which they were obtained.

Tap water. Flared entry.		Tap water. Flared entry removed.		Ammonia Soap. Flared entry.
x/aR_n	R_n	x/aR_n	R_n	Rate of flow 'Q' (ccs/sec)
0.076	2,200	0.106	1560	4.0
0.062	2,700	0.089	1880	8.25
0.039	4,300			11.3
				13.5
				17.0
				19.0

The three normal profiles which were determined using water (1st and 2nd columns of table) showed, by comparison with the experimental results of Schiller and Nikuradze[22] that the method and technique were satisfactory. The profiles obtained are shown in figs. 6.1; 6.2; 6.3.

The flow conditions existing at the entrance to a pipe depend upon the nature of the entrance to the pipe, and the experimental profile curves of Schiller and Nikuradze were obtained with the tube fitted with a flared entry. Without the flare there is effectively a reduced throat area[45] and it was considered worth while determining the shape of the velocity

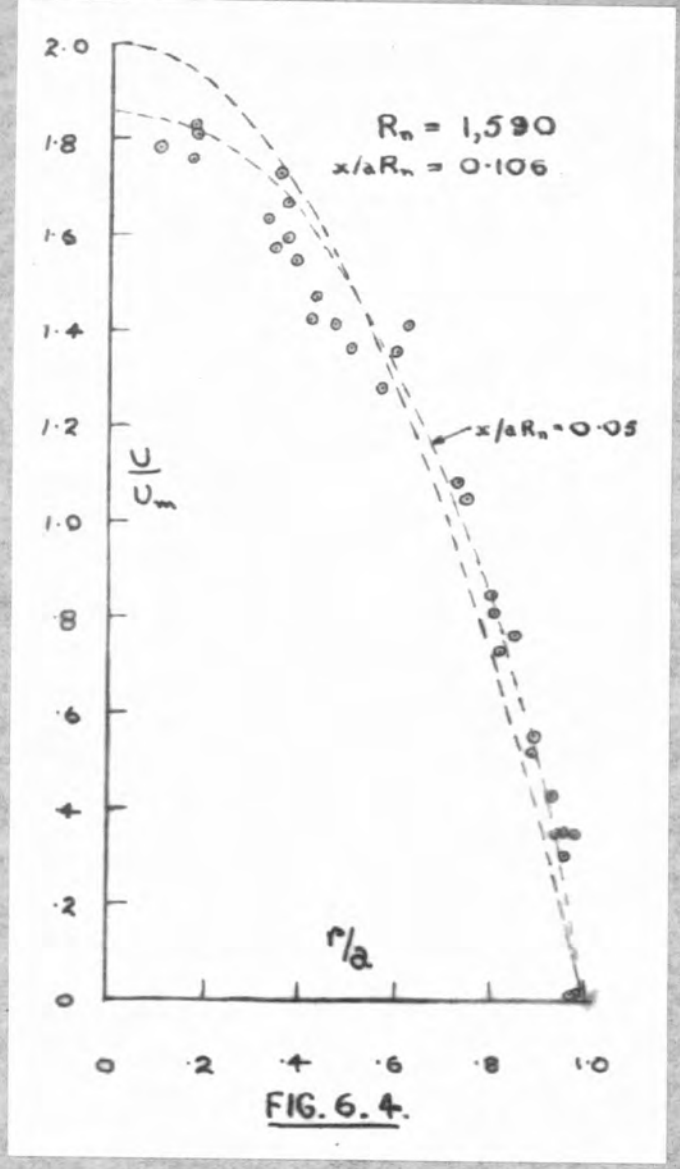
2·0
1·8
1·6
1·4
1·2
1·0
·8
·6
·4
·2
0
R_n = 1,590
x/aR_n = 0·106
x/aR_n = 0·05
C/U
U_m
r/a
0
·2
·4
·6
·8
1·0

FIG. 6.4.

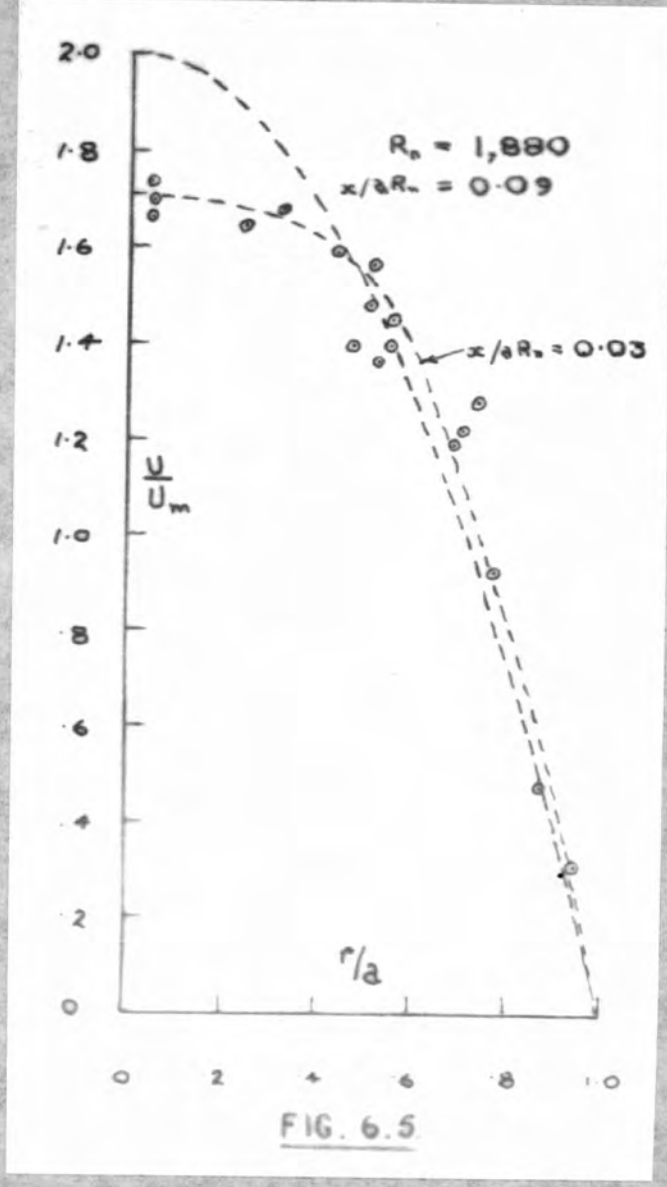
2·0
1·8
1·6
1·4
1·2
1·0
·8
·6
·4
·2
0
R_n = 1,880
x/aR_n = 0·09
x/aR_n = 0·03
C/U
U_m
r/a
0
2
4
6
8
1·0

FIG. 6.5

profile for water in the flow tube with the flared entry removed. The maximum obtainable Reynolds No. for laminar flow was now very much reduced and agreed with the accepted values obtained by many experimenters, Reynolds[46], Stanton and Pannel[47], Barnes and Coker[48], Ruckes[49], and was very nearly 2000. Columns 3 and 4 of the table give the conditions of the experiments and figs. 6.4 and 6.5 show the profiles obtained. For comparison the theoretical velocity profiles (parabolic for such low values of x / aR_n) and also the particular profiles from Schiller and Nikuradze's results which appear best to fit the experimental plotted points are also shown. The values of x/aR_n for these curves are those in column 5 of the table.

The last column of the table gives the values of the rates of flow at which the velocity profiles were measured for an ammonia soap solution. The soap was prepared in distilled water by mixing known strength solutions of ammonia and an oleic acid suspension. The final strength of the soap solution was 80 gms oleate in 35 litres of solution. In the first instance a solution of sodium oleate and potassium chloride was prepared as the visco-elastic medium but had to be discarded owing to the fact that it was opaque. This was thought to be due to the impurity of the oleic acid, which was used nevertheless as no other was immediately available, and both the sodium and ammonia soaps produced by its use showed the characteristic thread pulling and oscillatory properties of

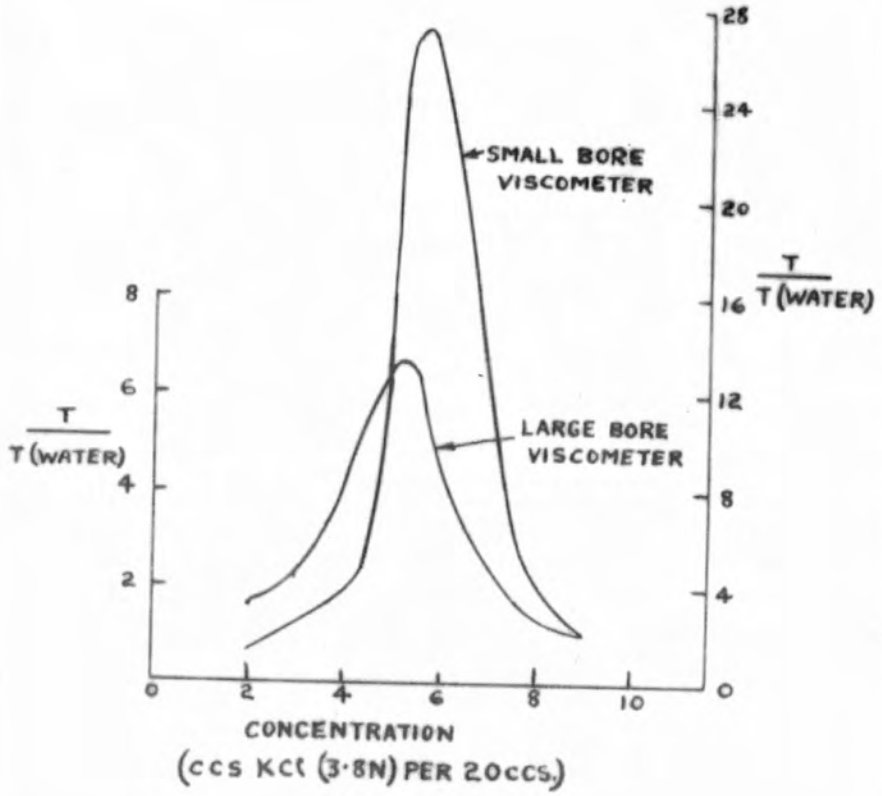
SMALL BORE VISCOMETER
LARGE BORE VISCOMETER
T / T (WATER)
T / T (WATER)
0
2
4
6
8
10
CONCENTRATION
(ccs KCl (3·8N) PER 20ccs.)

FIG. 6.6.

visco-elastic solutions, (28). An absolute measure of the viscosity of the solution could not be obtained as its value depended upon the rate of shear. The flow times, relative to that of water, in two capillary tube viscometers of different bore are shown plotted in fig.6.6 for the sodium soap with various KCl concentrations. The narrower the bore the greater was the apparent viscosity, and ultimately for tubes of bore comparable with that of the flow tube the viscosity appeared very little different from that of water. The curves were very similar to those of Van der Jong. Because of the doubt as to the value of the viscosity, rates of flow only are given in the table and not Reynolds' numbers.

The ammonia soap solution could be kept quite clear by maintaining a slight excess of ammonia and appeared to be quite unaffected by the presence of small quantities of benzine and carbontetrachloride and could thus be re-used several times. The solution was eventually discarded upon the appearance of a blue opalescence due to the chemical attack of the ammonia on the metal of the reservoir and resultant opacity. Though the oleic acid was impure no special precautions had to be observed in making the soap, and a simple capillary tube viscometer showed the viscosity of the various samples to be very nearly identical.

On the assumption that the kinematic viscosity of the soap was the same as that for water the maximum value of the Reynolds' number which was obtainable was, while maintaining

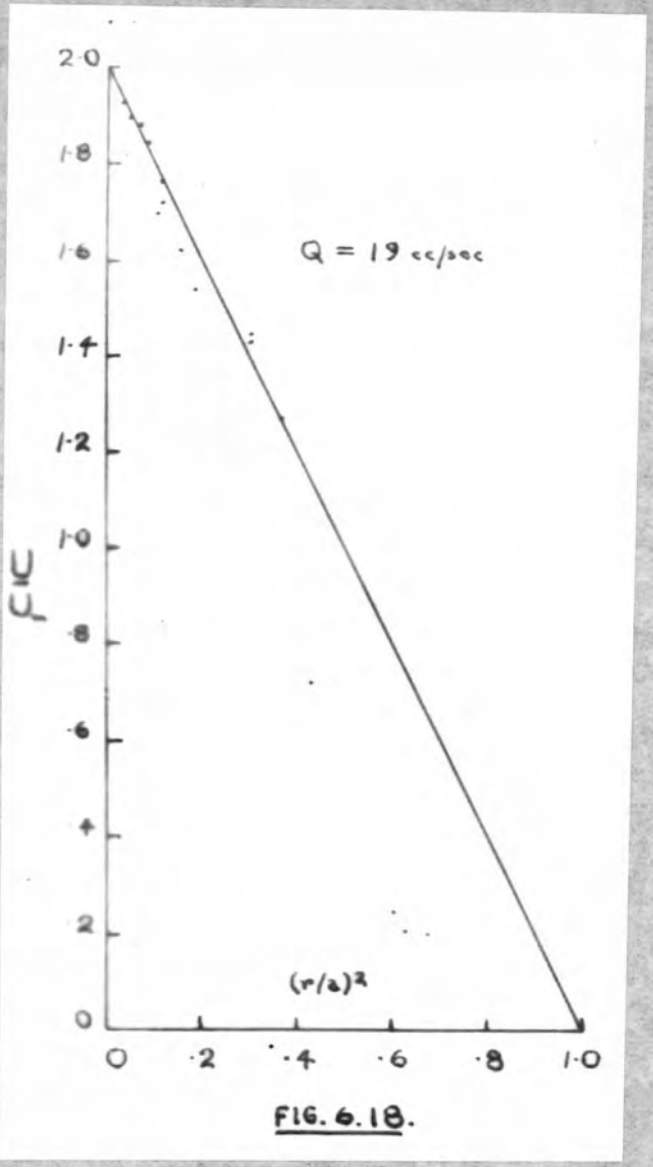

FIG. 6.18.

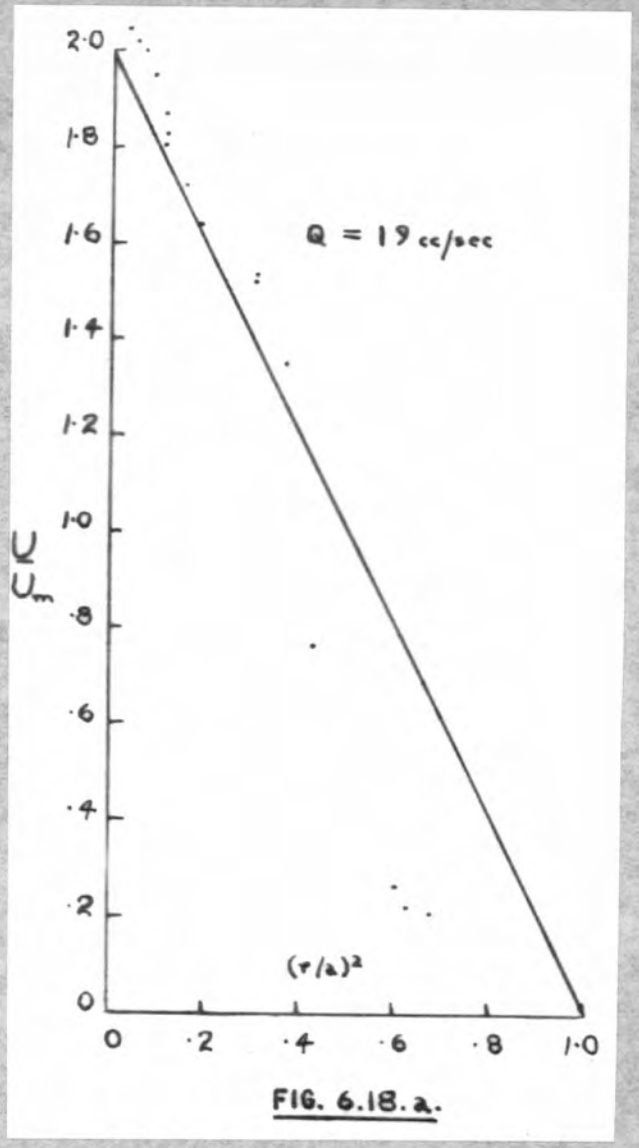

FIG. 6.18. a.

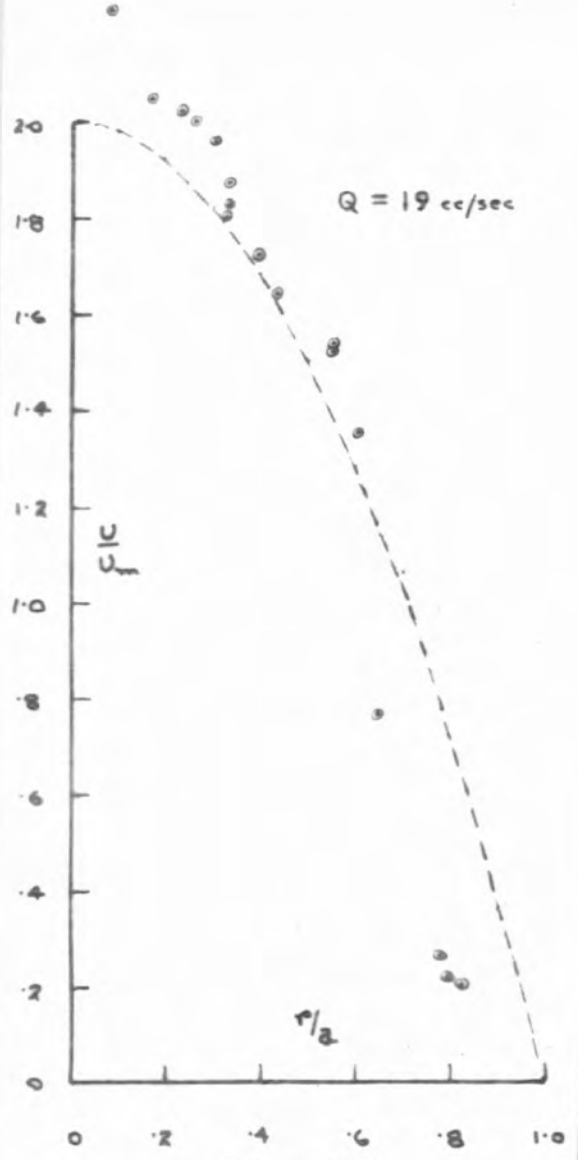

FIG. 6.12.a.

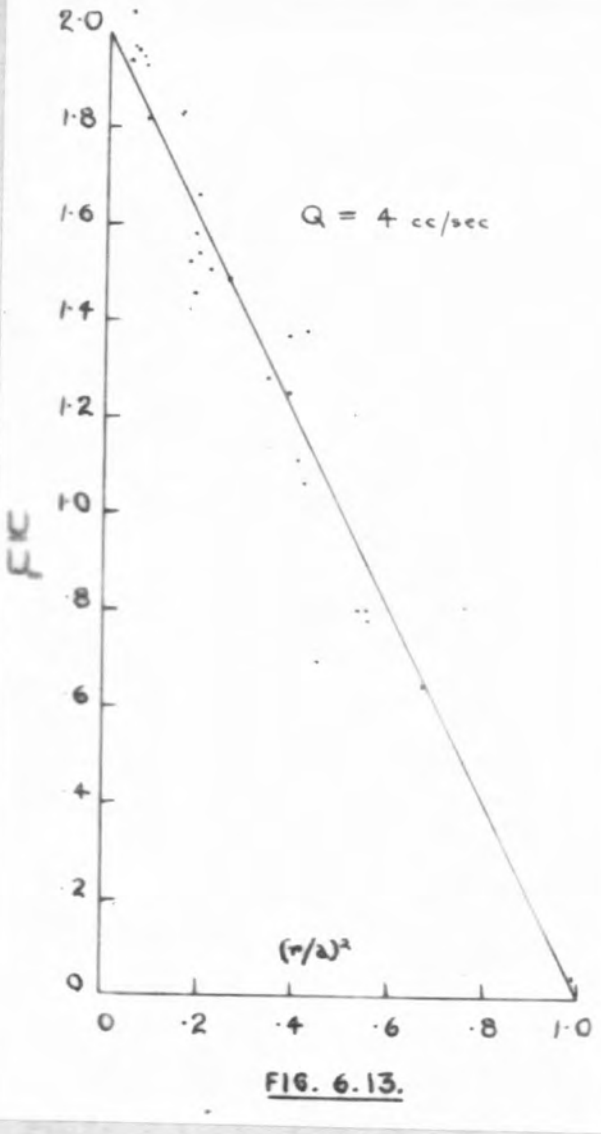

FIG. 6.13.

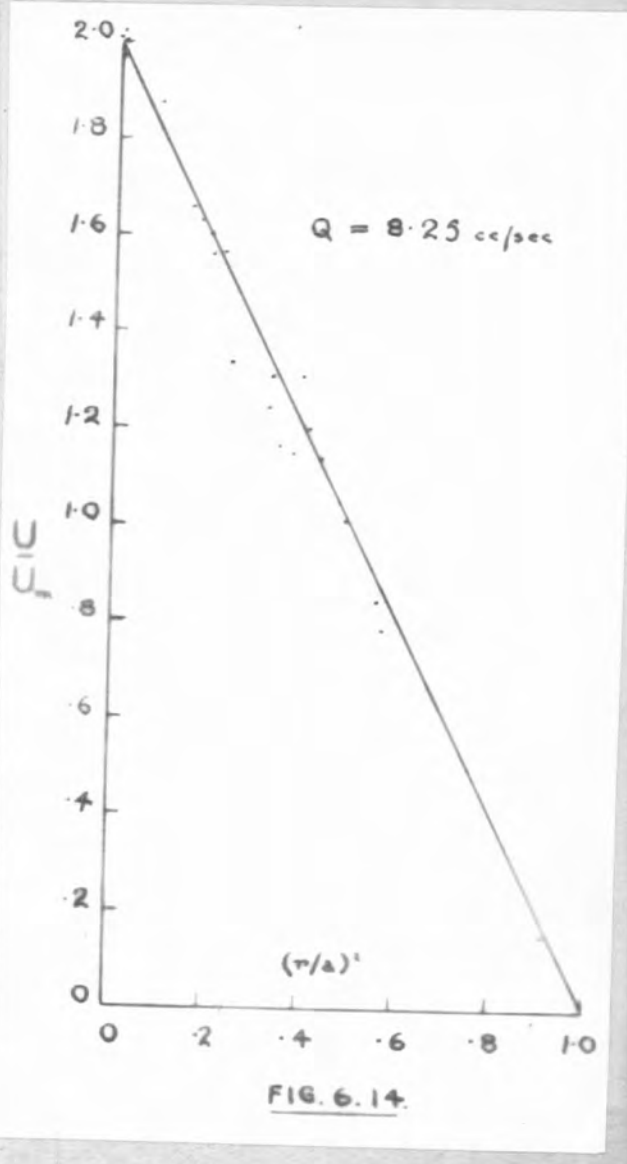

FIG. 6.14.

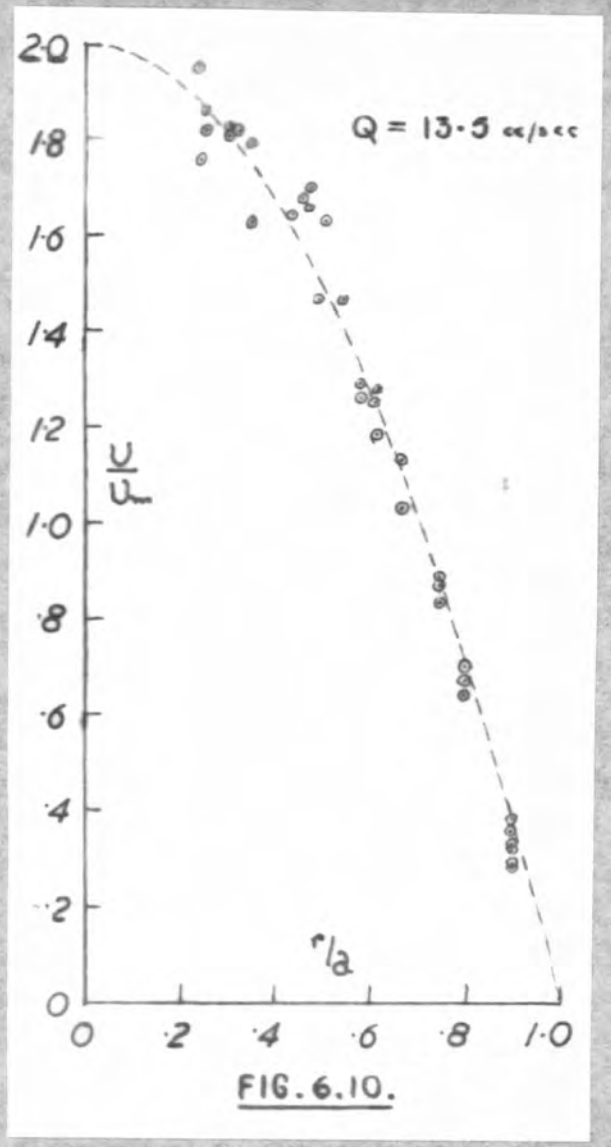

FIG. 6.10.

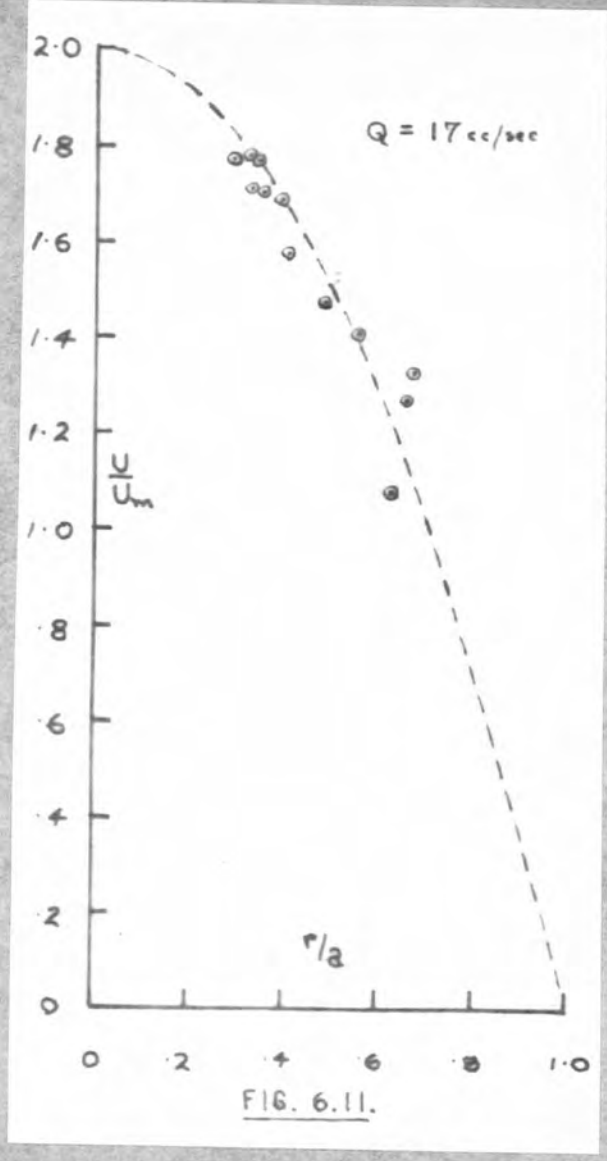

FIG. 6.11.

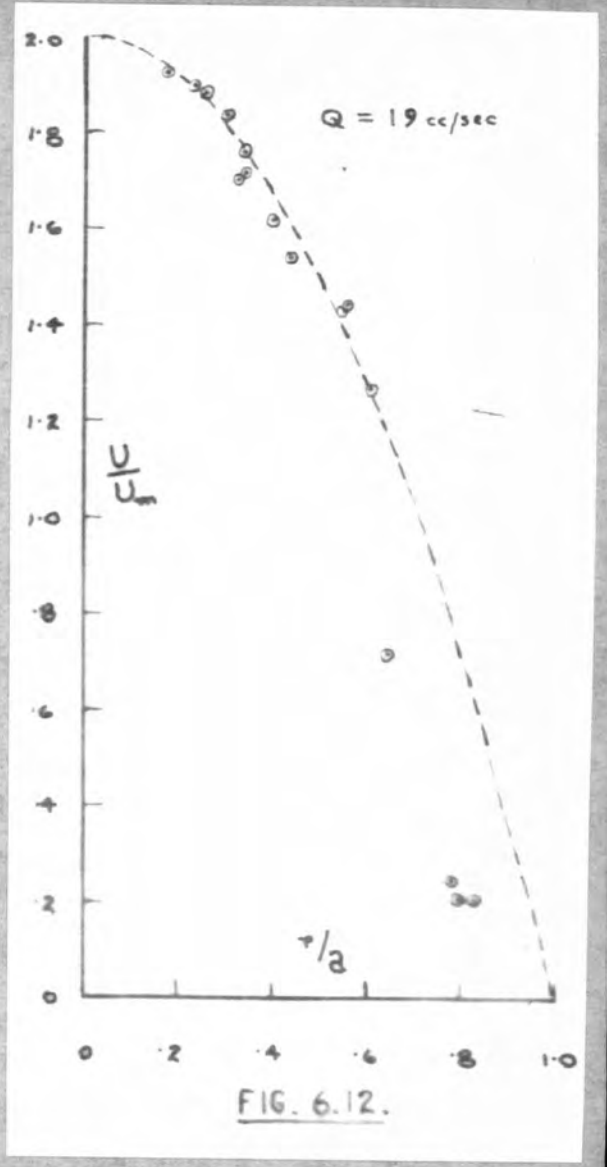

FIG. 6.12.

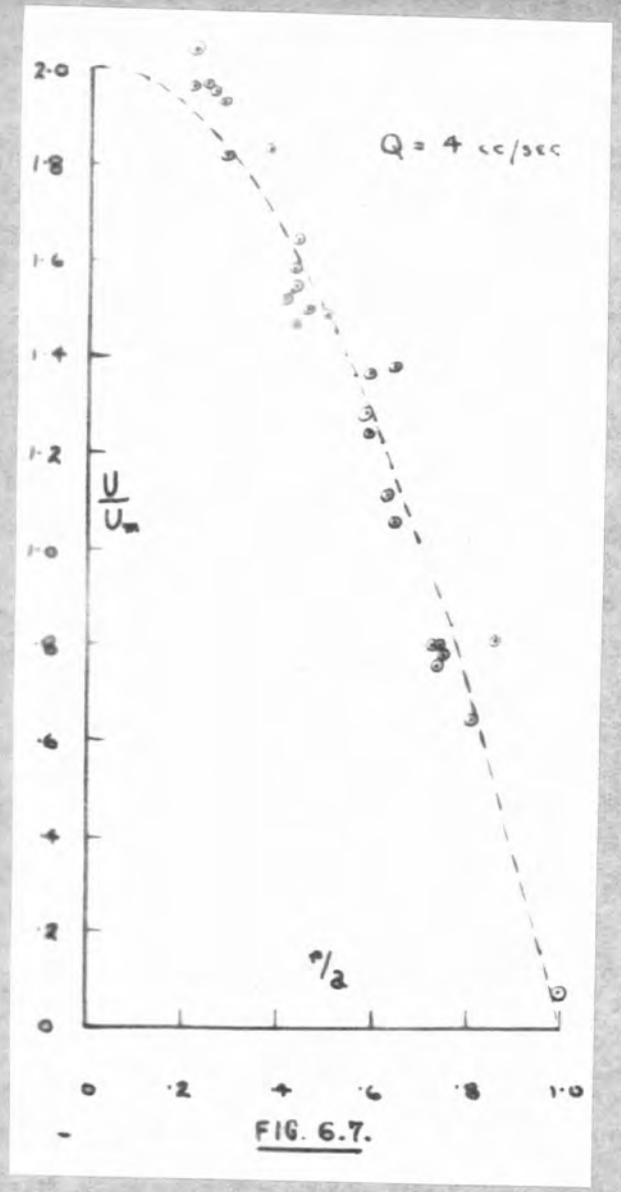

FIG. 6.7.

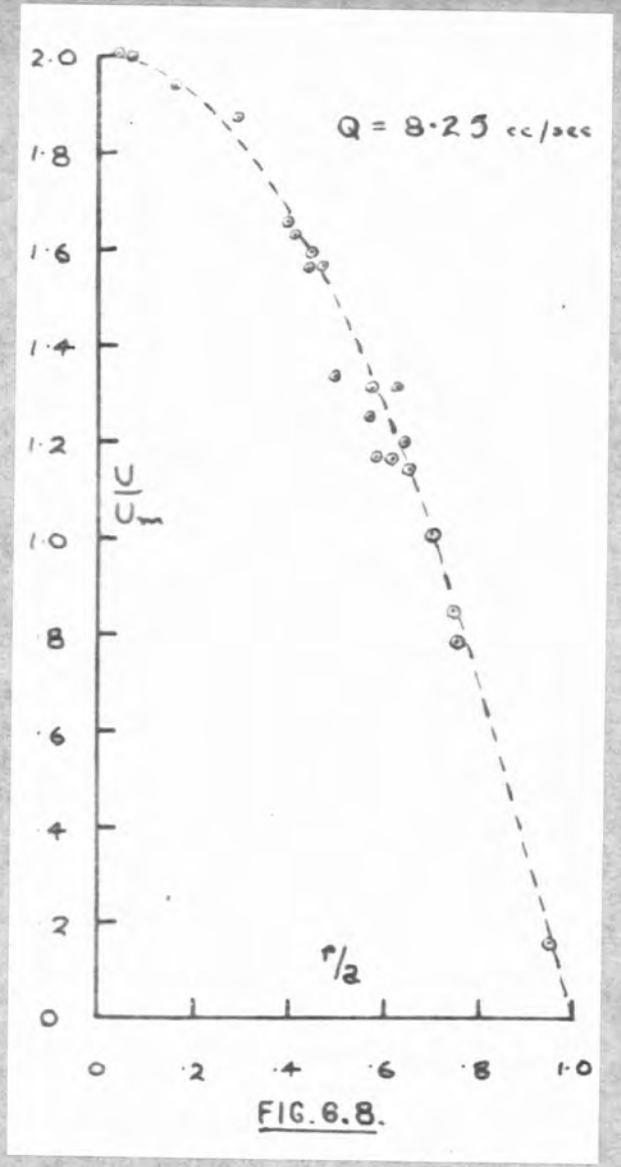

FIG. 6.8.

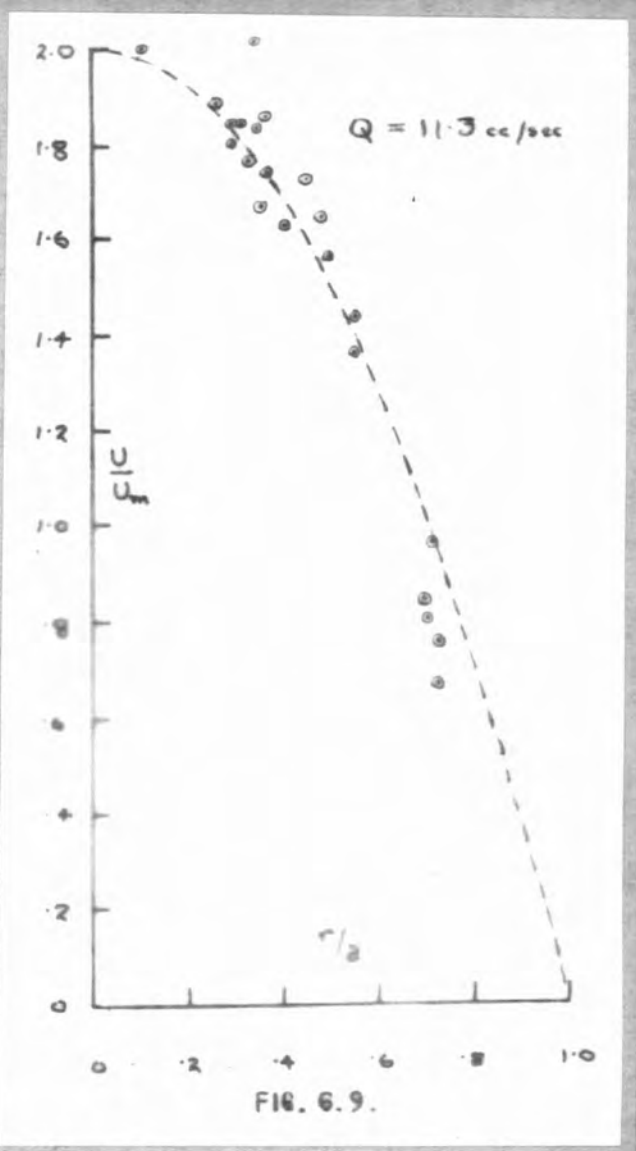

FIG. 6.9.

rectilinear motion, a little under 2000. Figs 6.7 - 6.12a show the plots of the velocity profiles obtained; the dotted curves are theoretical Poiseuille parabolas.

38. Discussion of profiles obtained.

The three profiles obtained using tap water showed good agreement with Schiller and Nikuradze's experimental results and indicated that the technique was satisfactory and that multiplying factors could be obtained successfully for the results from different frames of any particular run.

There were no theoretical or practical grounds for endeavouring to fit to the profiles obtained using tap water and the flow tube without a flared entry, curves corresponding to values of x/aR_n different from the actual experimental values. From the two results obtained it appeared possible to assign values of x/aR_n to the curves much lower than the actual values, though it was not possible to deduce any empirical or theoretical relationship between the x/aR_n values owing to the fact that restrictions imposed by the time available prevented other such profiles from being determined.

In general the curves obtained for the ammonia soap solution showed agreement with the theoretically deduced parabolic velocity profiles (1)(3) for visco-elastic fluids. At the maximum flow rate of 19 ccs per second, however, there is an apparent anomaly in the regions near the flow tube walls. For this reason the curve is plotted in two ways. In fig.6.12 the points with large values of r/a are ignored in the fitting of the curve to the parabola, while in fig.12a all the points

are plotted about the parabola in a manner in which it was estimated that the curve through the points would correspond to a flow rate equal to that for the parabola through U/Um =2. When the points at the higher values of r/a are ignored the curve approximates very well to a parabola. Though the points at high r/a were obtained from successive frames of the record it is thought very probable that the oil droplet was in fact an abnormally large one, very near to or actually in contact with the wall. In either case a value of U/Um would result, which would be lower than the theoretical value for a parabolic profile. In the same way, other abnormally low values of U/Um at large values of r/a, it was believed, would also be due to unusually large drops; a few such points can be seen in the various plots.

That the 'wall' effect was to be felt more upon oil droplets borne by the soap solution was only to be expected. In such cases, high rates of shear would be developed in the very small interspace between the droplet and the wall, particularly if the drop happened to be large, and here the local value of the viscosity would be greater than the normal value and thus produce an increased drag upon the droplet.

The profiles obtained seemed to indicate quite definitely that the parabolic law, as predicted by theoretical considerations, held for visco-elastic fluids. The figures, 6.13 - 6.18a, show the results of figures 6.7 - 6.12a plotted in the form U/Um. v. $(r/a)^2$ respectively.

39. Limitations of Technique.

The accuracy of the electronic side of the apparatus has been discussed above and was shewn to be certainly as good as .1%.

A critical factor in the technique was the size of the oil droplets. Obviously if they are large then the general flow pattern will be altered and the velocity of the droplets as measured will not be an indication of fluid velocity corresponding to the position of the droplet centre. The oil droplets produced by the .006 in. diameter jets were considered to be small enough to give a representative picture of the flow pattern, and the profiles obtained using water confirmed this. There was a danger of producing occasionally large drops however, as pointed out earlier and such did apparently occur and great care had to be exercised in producing and dispersing the droplets in order to keep their number down to a minimum, a steady regular movement of the jet was essential. Even so a few large drops were produced and in order to effect there removal, the benzine-carbon tetrachloride mixture was a fraction more or less dense than the fluid so that the larger droplets sank or rose to the surface of the liquid. Methods are now available for the production of very small fluid droplets, notably Walton and Prewett[50], though these small droplets could not be used with the present apparatus without improvements being made upon the focussing of the stroboscopic light and its intensity in order to make photographic recording

possible and also, at the same time, the background scattering due to slightly irregular flow tube walls and water jacket would have to be eliminated by careful polishing, cleanliness and choice of flow tube.

With buoyant drops in a flow field with a velocity gradient in the direction of the drops diameter, there exists a velocity difference between the flow of the fluid at extremes of the diameter athwart the mean flow direction. A dynamic pressure difference[51] then exists across the diameter and the drop thus experiences a force tending to move it into the region of higher velocity of flow. This is particularly so for the larger size droplets where an appreciable velocity difference can exist across the drops and hence also a relatively large pressure difference. The tendency is therefore to bring about a state of congestion in the centre regions of the pipe and a dearth of droplets near the walls. This occurred frequently in the earlier experiments when a large number of results were vitiated as a technique for producing the droplets had not been developed and a too large and indecipherable number of droplet images appeared in the centre regions of the photographic record. The radial movement could be discerned often quite clearly. Nevertheless, the profiles which were measured show a preponderence of droplets in the regions of low r/a though small drops were employed. This migration to the centre was thought to be due to the earlier stages of flow in the entrance of the flow tube where large velocity gradients

exist in the regions outside the central plug of undeveloped flow.

The two-directional stroboscopic lighting made for a more accurate localisation of the droplet but again the accuracy of the localisation depended upon the size of the droplet, being greater the smaller the droplet.

One of the greatest sources of error in the recording of the droplet images was inherent in the quality of the photographic equipment and the vernier of the travelling microscope used to examine the records. A long focus 16mm. camera was adapted by means of simple lenses to focus at about 4 or 5 inches and consequently the focussing of the droplet images was not very sharp nor were the images of the individual frame edges. A further difficulty, was the determination of the size and positioning of the flow tube image relative to the frame edges, due to the poor focussing. For the 6 runs using the soap solution with identical camera positioning, the flow tube image sizes were as follows:-

0.536	0.538	0.538
0.534	0.538	0.538

Similar magnitude errors could arise in the positioning of the tube centre relative to the datum frame wall. With correct values of U/Um, these errors would not materially alter the shape of a profile curve, though in measuring small values of U/Um such errors could amount to up to20% or so of the value of U/U_m As already pointed out, this fact needed considering when the curve fitting was being carried out.

SUMMARY

The velocity distributions existing in anomalous fluids, flowing in pipes of circular cross section, has been determined theoretically by several investigators to be parabolic, provided that the motion is rectilinear.

It was decided to construct an apparatus with which velocity distributions for any type of transparent fluid flowing in a pipe of circular section could be measured accurately. The apparatus was such as to yield a three dimensional view of the fluid at the observation section of the pipe. Thus all components of velocity could be measured.

The actual flow velocities were measured by a streamer method which was an adaption of the methods of Relf and Birkhoff and Cagwood. Small oil droplets dispersed in the fluid, whose density was equal to that of the fluid under investigation, were illuminated stroboscopically and viewed from two directions mutually at right angles using the principle of the ultra-microscope.

The stroboscopic illumination consisted of a double repetitive flash; the short time interval between the dual flashes was controllable and the overall repetitive frequency was governed by the recording cine camera. By measurements of the droplet images a complete three-dimensional picture of the flow at the observation section of the flow tube could be obtained.

The optical system whereby the orthogonal viewing was achieved consisted of two plane mirrors parallel to and on either side of the flow tube with a semi-aluminised mirror between and parallel to them. The geometry and optics of the system readily showed that the images of the pipe as seen by observation at 45° to the semi-aluminised mirror were, when the system was correctly adjusted for symmetry and parallelism, of equal size and superimposed.

The stroboscope comprised an asymmetrical multivibrator, frequency controlled by means of the recording cine camera through the agency of a thyratron relaxation oscillator, whose rapidly going negative grid voltages backed beyond cut-off two inductively loaded pentodes. High voltage oscillatory pulses were thus produced at the valve anodes, due to the collapse of the loads' magnetic fields, and after pulse sharpening with spark gaps these pulses initiated the discharges in two Siemens' S.F.6 flash tubes.

Theoretical and practical considerations were given to the choice of inductive loads for the pentode pulsers and various types of Siemens' flash tubes were investigated as regards their triggering characteristics and delay in flashing after triggering.

The very near instantaneous mean flow of the fluid through the flow tube was measured using a hot wire anemometer technique, the working substance being air displaced from a thirty litre

bottle by the fluid issuing from the flow tube. A constant or varying flow rate could thus be used.

A series of profiles was obtained using water at known flow rates and the results showed that the technique was sound. Profiles were then obtained for water and the flow tube without its flared entry. Finally a series was obtained with a visco-elastic ammonia soap solution.

REFERENCES.

1. Reiner M. Twelve Lectures on Theoretical Rheology Amsterdam,(1949).

2. Scott-Blair G.W. A Survey of General and Applied Rheology, Pitmans 2nd Ed.(1949).

3. Oldroyd J.G. Proc.Roy.Soc. A.200 p.523. (1950).

4. Lawrence A.S.C. Proc.Roy.Soc. A.148 p.59.(1935).

5. Eirich F.R. Proc. 1st Int.Congr. Rheol.Scheveningen.(1949

6. Goldstein S. Modern Developments in Fluid Dynamics. Oxford. Chap.VI, Section 2. (1938).

7. Richardson, E.G. Dynamics of Real Fluids. Arnold.(1950).

8. Richardson E.G. and Tyler. Phys.Rev. 32 509. (1931).

9. Bramwell, Relf and Fage, A.R.C. Reports & Memoranda, No.71.(1912). Ower and Johansen, A.R.C. Reports & Memoranda, No. 1437. (1932).

10. Miss Barker, Proc.Roy.Soc. A.101 435-445. (1922).

11. Townend,Phil.Mag.(7) 14 (700-712; (1932). Journ.Aero. Sciences, (3) (1936). Proc.Roy.Soc. A.145 180-211.(1934

12. Relf, Adv.Comm.for Aeronautics, Reports & Memoranda, No.76 (1913).

13. Jones, Farren and Lockyer, A.R.C. Reports & Memoranda, No.1065 (1927).

14. Pichot and Dupin Comptes Rendus, 192 1079 (1931).

15. Andrade and Tsein, Proc.Phys.Soc. London 49 381-391.(1939).

16. Favre, A. Pub.Scient. et.tech. du Min de l'air No.137 (1938).

17. Birchoff and Cagwood, J. App.Phys. 20 646 (1949).

18. Kolin, A. Proc.Soc. Exp.Biol & Med. 35 p.53 (1936); 46 p.235 (1941).

19. Kolin, A. J. Appl.Phys. 15 p.2. (1944).

20. Kolin, A. Rev.Sci.Instr. 16, p.109, (1945).

21. Alcock and Sadron, Physics (U.S.A.), 6 92-95. (1935).

22. Schiller, Nikuradze, from Goldstein, Vol.1 Chap.Vll pp. 299-308. (1938).

23. Hagenbach, from Goldstein, Vol. 1 Chap.Vll pp.300. (1938).

24. Couette, Ann.de Chimie et de Physique (6) 21 433-510 (1890)

25. Hindley, J. Sci.Instr. 24 295-6. Nov.(1940).

26. Matheson and Eden, Rev.Sci. Instr. 19 502-6. Aug.(1948).

27. Keenan and Macintosh, Rev.Sci.Instr. 19 336-9. May (1948).

28. Bungenberg de Jong H. and Van der Berg. H.J., Kon. Med. Akad. W et. 51 1197 (1948).

29. Laub, J.H. Elect.Engng. N.Y. 66 12116-10 Dec. (1947).

30. King L.V. Philos. Trans, A.214 (1914).

31. Fage and Preston, J. Roy.Aero.Soc. pp.124-140. April (1941).

32. Mitchell, Trans. I.E.S. 24, 4 (1949).

33. Edgerton, H.E. J. Appl.Phys. 8 p.1. (1937).

34. Quinn and Bourque, Rev.Sci.Instrum. 22 No.2 (1951).

35. Reich, Theory and Application of Electron Tubes (New York) McGraw-Hill) Chap.10 (1944).

36. Terman, Radio Engineers' Handbook, Section 6, (New York McGraw-Hill) (1943).

37. Chance B. et.al. Waveforms p.171 (New York,McGraw-Hill) (1949).

38. Glasoe and Lebacqz. Pulse Generators. p.305 (New York, McGraw-Hill) (1948).

39. Morecroft, Principles of Wireless. (1921).

40. Molnar, Phys.Rev. 83 No.5 p.940. Sept.(1951).

41. Engstrom and Huxford, Phys.Rev. 58. 67 (1940).

42. Stigel R. Elektrische Stossfertigkeit, J Epsenger (1939).

43. Chesterman, W.D., et.al. Inst.Electrical Eng. __ 1127 (1951

44. Laporte M. Nature 168 p.552 Sept.29 (1951).

45. Schiller, Proc. 3rd Internat. Congress for Applied Mechanics, Stockholm (1930); Goldstein, Mod.Dev. in Fluid Dynamics, Oxford, Chapter Vll pp.149-150 (1938).

46. Reynolds, Phil. Trans. 174 935-982; (1883); Scientific Papers, 2, 51-105.

47. Stanton and Pannel, Phil.Trans. A. 214 199-224 (1914).

48. Barnes and Coker, Proc.Roy.Soc. A.74 341-356 (1905).

49. Ruckes, Ann.d.Phys. (4) 25 983-1021. (1908)

50. Walton W.H. and Prewett W.C. Proc.Phys.Soc.Lond. B.62 p.341 (1949).

51. Goldstein, Mod.Dev.in Fluid Dynamics, Oxford Chap.1. pp.31-32. (1938).

ACKNOWLEDGEMENTS

Grateful thanks are due to Professor J.E.P. Wagstaff for the provision of facilities which made possible the execution of this work; J.E. Caffyn B.Sc., F.Inst.P. for invaluable guidance throughout the course of the work; Dr. W.A. Prowse for valuable discussion particularly in connection with the behaviour of spark gap; the laboratory staff for construction of various equipment, and Siemens Electric Lamp Supplies Ltd., who kindly assisted in providing flash tubes with activated cathodes, and to the late H.W. Cummings of Siemens Electric Lamp Supplies Ltd., for discussion of statistical lag in firing of the flash tubes.

The Council of the Durham Colleges provided a maintenance grant which made possible the course of the work, and thanks are due also to the Research Fund of the Durham Colleges for the provision of a grant towards equipment.

RESULTS TABLE FOR FIG. 6.8

Q = 8.25 cc/sec. U_m = 6.73 cm/sec. Δt = 22 m. sec
Scale factor = 2.768
Vernier reading for frame edge:- 10.981; 10.982; 10.982; 10.982; 10.981
" " " pipe " :- 11.038; 11.038; 11.038
" " " " " :- 11.572; 11.572; 11.572; 11.572; 11.572
Centre of pipe image = 0.534/2 + 0.054 cm from reference edge of frame.
= 0.3234 cm.

drop No	Vernier readings for droplet images			Image distances from edge	Unscaled x's & y's x	Unscaled x's & y's y	Scaled x's & y's x	Scaled x's & y's y	x_o	y_o	$\bar{x}$
Vernier reading for datum edge = 11.004											
1	11.200	11.200	Y	0.1960	0.1274	-	0.3532		0.3523		0.3512
2	11.255	11.255	Y	0.2510	0.0724	+	0.2003		0.2003		0.2017
1	11.300	11.300	Y	0.2960	-	0.0247		0.0758		0.0758	
3	11.341	11.341	X	0.3370	0.0136	+	0.0376		0.0376		0.0377
3	11.360	11.360	X	0.3560	+	0.0326		0.0902		0.0902	
2	11.409	11.409	X	0.4050	-	0.0816		0.2258		0.2258	
4	11.440	11.440	X	0.4360	0.1126	+	0.3115		0.3115		0.3154
4	11.452	11.452	X	0.4480	+	0.1246		0.3448		0.3448	
Vernier reading for datum edge = 9.589											
1	9.795	9.795	Y	0.206	0.1174	+	0.325		0.325		0.3271
2	9.838	9.838	Y	0.249	0.0744	+	0.207		0.207		0.2084
3	9.942	9.942	X	0.353	0.0296	+	0.0819		0.082		0.0831
1	9.972	9.972	X	0.383	-	0.0596		0.165		0.165	
2	9.979	9.979	X	0.390	-	0.0766		0.212		0.212	
3	10.122	10.122	X	0.533	+	0.2096		0.5789		0.582	
Vernier reading for datum edge = 10.8325											
1	11.008	11.008	Y	0.1755	0.1749	+	0.4093		0.4094		0.4096
2	11.027	11.027	Y	0.1945	0.1289	+	0.3567		0.3567		0.3587
3	11.129	11.129	Y	0.2965	0.0269	+	0.0744		0.0744		0.0748
1	11.159	11.159	X	0.3265	-	0.0031		0.0086		0.0086	
4	11.165	11.165	X	0.3325	0.0091	+	0.0252		0.0252		0.0252
4	11.169	11.169	X	0.3365	+	0.0131		0.0362		0.0362	
2	11.204	11.204	X	0.3715	-	0.0481		0.1332		0.1332	
3	11.246	11.246	X	0.4135	-	0.0901		0.2493		0.2493	
Vernier Reading for datum edge = 11.3742											
1	11.562	11.562	Y	0.1918	0.1316	+	0.369		0.369		0.3711
2	11.567	11.567	Y	0.1968	0.1266	+	0.3502		0.3502		0.354
3	11.646	11.646	Y	0.2758	0.0476	+	0.1317		0.1317		0.1326
4	11.699	11.699	X	0.3288	0.0054	+	0.01495		0.01495		0.01495
4	11.701	11.701	X	0.3308	+	0.0074		0.0205		0.0205	
1	11.741	11.741	X	0.3708	-	0.0474		0.1312		0.1312	
3	11.782	11.782	X	0.4118	-	0.0884		0.2445		0.2445	
2	11.788	11.788	X	0.4178	-	0.0944		0.2614		0.2612	
Vernier reading for datum edge = 11.301											
1	11.497	11.497	Y	0.196	0.1247	-	0.3523		0.3523		0.3475
2	11.499	11.499	Y	0.198	0.1254	+	0.2470		0.3470		0.3480
3	11.502	11.502	Y	0.201	0.1224	-	0.3387		0.3387		0.3357
1	11.511	11.511	Y	0.210	-	0.1134		0.3138		0.3138	
3	11.544	11.544	Y	0.243	-	0.0804		0.2225		0.2225	
4	11.546	11.546	Y	0.245	0.0784	-	0.2169		0.2169		0.2161
5	11.550	11.550	Y	0.249	0.0744	+	0.2058		0.2058		0.2070
4	11.581	11.581	Y	0.280	0.0434	-	0.1201		0.1201		0.1194
6	11.618	11.618	Y	0.317	0.0064	+	0.0177		0.0177		0.1780
7	11.630	11.630	X	0.329	+	0.0056		0.0155		0.0155	
7	11.639	11.639	X	0.338	+	0.0146		0.0404		0.0404	
2	11.650	11.650	X	0.349	-	0.0256		0.0708		0.0708	
6	11.691	11.691	X	0.390	-	0.0666		0.1843		0.1843	
5	11.693	11.693	X	0.392	-	0.0688		0.1898		0.1898	

$\bar{y}$	r^2	$\frac{r}{a}$	$\left(\frac{r}{a}\right)^2$	Theoretical $\frac{U}{U_m} = 2\left[1 - \frac{r^2}{a^2}\right]$	(cms) dual image spacing	(cm/sec) drop velocity	$\frac{U}{U_m}$	$\frac{\overline{U/U_m}}{U/U_m}$	Plotted points
	0.12902	0.5751	0.3308	1.2385	0.055	6.915	1.027	1.206	1.314
	0.09104	0.4973	0.2473	1.4054	0.056	7.04	1.046	1.343	1.338
0.0753									
	0.00958	0.1568	0.0246	1.9508	0.081	10.18	1.515	1.288	1.937
0.0903									
0.2244									
	0.22142	0.753	0.5670	0.866	0.033	4. 15	0.6168	1.405	0.7885
0.3492							Mean =	1.279	
	0.13370	0.5852	0.3426	1.3151	0.052	6.54	0.972	1.217	1.167
	0.08779	0.4745	0.2252	1.5497	0.070	8.8	1.308	1.185	1.57
	0.35442	0.9530	0.9082	0.1836	0.007	0.88	0.13081	1.403	0.157
0.1643							Mean =	1.201	
0.2106									
0.5895									
	0.16784	0.656	0.4303	1.1393	0.049	6.16	0.91551	1.244	1.143
	0.14606	0.612	0.3745	1.2509	0.050	6.29	0.93451	1.338	1.168
	0.06754	0.4164	0.1734	1.6532	0.070	8.8	1.308	1.238	1.634
0.0086									
	0.00195	0.0706	0.0050	1.99	0.086	10.81	1.607	1.264	2.007
0.0362							Mean =	1.249	
0.1319									
0.2487									
	0.15462	0.63	0.3969	1.2062	0.053	6.665	0.99031	1.218	1.313
	0.19188	0.701	0.4914	1.0172	0.041	5.155	0.76601	1.328	1.014
	0.07688	0.444	0.1971	1.6057	0.065	8.17	1.214	1.323	1.608
	0.00064	0.0406	0.0017	1.997	0.085	10.69	1.59	1.265	2.106
0.0205							Mean =	1.325	
0.1300									
0.2435									
0.2580									
	0.21673	0.745	0.5550	0.8899	0.036	4.53	0.673	1.323	0.853
	0.12603	0.568	0.3226	1.3548	0.052	6.54	0.972	1.393	1.251
	0.16115	0.643	0.4135	1.1731	0.050	6.29	0.9345	1.255	1.203
0.3089									
0.2201									
	0.06095	0.3955	0.1564	1.6871	0.069	8.685	1.29	1.308	1.66
	0.07842	0.4485	0.2012	1.5977	0.065	8.175	1.215	1.315	1.564
	0.03392	0.2946	0.0868	1.8265	0.078	9.805	1.458	1.252	1.876
0.0552	0.00190	0.0697	0.0049	1.9900	0.084	10.56	1.570	1.268	2.02
0.0406							Mean =	1.287	
0.0702									
0.1833									
0.1886									